

New Zealand Aquatic
Environment and Biodiversity
Report No. 76
2011
ISSN 1176-9440

Trends in relative mesopelagic biomass using time series of
acoustic backscatter data from trawl surveys

R.L. O'Driscoll
R.J. Hurst
M.R. Dunn
S. Gauthier
S.L. Ballara

Trends in relative mesopelagic biomass using time series of acoustic backscatter data from trawl surveys

R.L. O'Driscoll
R.J. Hurst
M.R. Dunn
S. Gauthier
S.L. Ballara

NIWA
PO Box 14 901
Wellington

**New Zealand Aquatic Environment and Biodiversity Report No. 76
2011**

**Published by Ministry of Fisheries
Wellington
2011**

ISSN 1176-9440

©
**Ministry of Fisheries
2011**

O'Driscoll, R.L.; Hurst, R.J.; Dunn, M.R.; Gauthier, S.; Ballara, S.L. (2011).
Trends in relative mesopelagic biomass using time series of acoustic backscatter data from trawl surveys.
New Zealand Aquatic Environment and Biodiversity Report No. 76.

This series continues the
Marine Biodiversity Biosecurity Report series
which ceased with No. 7 in February 2005.

EXECUTIVE SUMMARY

O’Driscoll, R.L.; Hurst, R.J.; Dunn, M.R.; Gauthier, S.; Ballara, S.L. (2011). Trends in relative mesopelagic biomass using time series of acoustic backscatter data from trawl surveys.

New Zealand Aquatic Environment and Biodiversity Report 2011/76.

Time series of acoustic indices of mesopelagic fish abundance were developed for the Chatham Rise and Sub-Antarctic from data collected during trawl surveys from 2001 to 2009. Common mesopelagic groups include myctophids (*Lampanyctodes hectoris*, *Symbolophorus* spp.) and pearlside (*Maurolicus australis*), which are the major prey of hoki (*Macruronus novaezelandiae*) and other valuable commercial species. Mesopelagic schools and layers typically occur at 100–500 m depth during the day, and migrate into the surface 200 m at night. Acoustic indices of the vertically migrating component were based on the total backscatter observed during the day multiplied by the proportion observed in the upper 200 m at night. Indices on the Chatham Rise were corrected for an estimated 20% of mesopelagic fish migrating into the acoustic deadzone (within 14 m of the sea surface), but this deadzone correction was not necessary in the Sub-Antarctic.

There was no clear trend in mesopelagic fish biomass on the Chatham Rise over the last 9 years – the estimate from 2009 was similar to estimates from 2001 and 2003, and higher than estimates in the other years. The time series of mesopelagic backscatter for the Sub-Antarctic area declined from 2001 to 2007, but has increased in the two most recent years. There were clear and consistent spatial patterns in mesopelagic fish distribution over all years. Abundance of mesopelagic fish was much higher on the Chatham Rise than in the Sub-Antarctic, with highest densities observed on the western Chatham Rise and lowest densities on the eastern Campbell Plateau. Abundance in areas of high mesopelagic fish density tended to be more variable between years.

Spatial patterns in mesopelagic fish abundance closely matched the distribution of hoki, but temporal changes in mesopelagic fish abundance were not strongly correlated with hoki biomass. We hypothesise that prey availability influences hoki distribution, but that hoki abundance is being driven by other factors such as recruitment variability and fishing. Surprisingly, there was no evidence for a link between hoki condition and mesopelagic prey abundance. There was a strong correlation between liver condition of similar size hoki on the Chatham Rise and Sub-Antarctic, which may be related to timing of spawning.

Key environmental variables were also extracted and updated from those presented in project ENV2007/04 (Hurst et al. in press). Updates include the Southern Oscillation Index, Kidson weather regimes and Trenberth pressure patterns. These are summarised monthly and with 3-monthly averages, from 1980. New extracts include sea surface temperature, sea surface height, and chlorophyll for subareas of the Chatham Rise and Southland/Sub-Antarctic regions. These are available from 1981, 1993 and 1997, respectively. Sea surface temperatures (SST) derived from satellite data have been compared to empirical CTD measurements made from relevant sub-areas of the Chatham Rise and Sub-Antarctic during trawl surveys. This showed good correlations, reassuring us that satellite-derived SST provided a realistic measure of sea surface temperature for these regions in years before CTD data were available.

There were no obvious correlations between mesopelagic fish abundance and environmental indices. Generalized additive models (GAM) suggested that mesopelagic abundance was influenced by the same key environmental factors of location, depth, temperature and prevailing weather conditions on both the Chatham Rise and Sub-Antarctic.

1. INTRODUCTION

Understanding change in the marine ecosystem is becoming increasingly important to provide context for fisheries management and decision making about sustainable fishing. Indicators are important for monitoring different types of change, and more than one type of indicator is required, particularly within the context of climate change. This work seeks to further our understanding of natural variability in productivity in relation to climate and how this translates through food webs to mesopelagic fish and, ultimately to the fish that feed on them. Section 13 (2) of the Fisheries Act requires the Minister to “set a total allowable catch that maintains the stock at or above a level that can produce the maximum sustainable yield, having regard to the interdependence of stocks”. In this context, mesopelagic fishes and the commercial species that forage on them can be considered interdependent stocks.

Mesopelagic fish form a major component of the diet of important fishstocks such as hoki (Dunn et al. 2009a, Horn & Dunn 2010, Connell et al. 2010), yet little is understood about how the distribution and abundance of mesopelagic fish influences the spatial distribution, abundance and growth of their predators. Estimates of abundance of mesopelagic fish will provide an indicator of food availability to piscivorous fishstocks. Trends and changes in mesopelagic biomass may be linked to climate cycles and influence fish condition. The distribution of mesopelagic fish may also influence the distribution of predator species in the water column, in turn affecting both vulnerability and catchability of trawl survey fish species that are assumed to be constant from year to year. The links between mesopelagic biomass and predator-prey consumption estimates are important for input to trophic models, and provide background information with which to make assessments about the status of fishstocks and changes in ecosystem indicators.

The overall objective of Ministry of Fisheries Research Project ENV2009/04 was to determine variability in the relative biomass and species composition of the mesopelagic fish community in relation to commercial fishstock abundance and distribution, and to climatic and oceanographic variables. Specific objectives were:

1. To evaluate relative changes in abundance of mesopelagic fish and other biological components from acoustic records collected during Chatham Rise and Sub-Antarctic trawl surveys.
2. To explore links between trends in mesopelagic biomass and climate variables and variations, and condition indices of commercial species in the Chatham Rise and Sub-Antarctic areas.

The report covers the analysis of existing acoustic data that has been collected and stored routinely during annual trawl surveys for hoki and middle depth species on the Chatham Rise and in the Sub-Antarctic since December 2000. Acoustic data collected from the water column during trawl surveys have the potential to determine both the relative abundance of mesopelagic fish from year to year and the distribution throughout the water column and survey areas (McClatchie & Dunford 2003, McClatchie et al. 2005, O’Driscoll et al. 2009). By exploring these data in conjunction with hydrographic data collected during the surveys (e.g. temperature, salinity) and remotely sensed data available from the survey time periods (e.g. SST, chlorophyll a), links to climate and hydrographic conditions may also be discernible.

McClatchie & Dunford (2003) estimated a biomass of 665 000 t of mesopelagic fish on the Chatham Rise and 438 000 t on the Campbell Plateau/Snares Shelf based on acoustic data collected during the 2000–01 trawl surveys (but see caveats in their discussion section). McClatchie et al. (2005) then examined the spatial distribution of mesopelagic backscatter from Chatham Rise surveys in 2001–03, and inferred that hoki abundance and condition was correlated with the abundance of their mesopelagic prey. More recent studies have also focused on the Chatham Rise. Work conducted in 2006/07 under NIWA’s Coasts and Oceans OBI successfully developed relative indices of mesopelagic biomass for Chatham Rise trawl surveys from 2001 to 2007 (excluding 2004 when no data were collected) (O’Driscoll et al. 2009). These results suggested that there was variability, but no statistically significant

trend, in abundance of mesopelagic fish over this period. Similar acoustic data exist for the Sub-Antarctic trawl series but have not been analysed in any detail since the work of McClatchie & Dunford (2003) and are not covered by the Coasts and Oceans OBI. Analyses of all Sub-Antarctic data from December 2000 to December 2008, and extension of the Chatham Rise time-series to include the surveys in January 2008 and 2009 were covered by this project.

This project has links to the Ministry of Fisheries Chatham Rise trophic study (ZBD2004/02, ENV2007/06), FRST projects on links between primary and secondary productivity (Coasts and Oceans OBI), and previous projects summarising climate and oceanographic trends and relating fisheries indices to them (SAM2005/02, ENV2007/04).

2. METHODS

2.1 Acoustic indices

Acoustic data have been collected during annual stratified random bottom trawl surveys for hoki and other species on both the Chatham Rise and Sub-Antarctic during the summer months of December and January since 2000–01 (Table 1). All surveys were carried out from the 70 m research stern trawler *Tangaroa*. Data were collected during daytime bottom trawls (with a constant tow speed of 3.5 knots) and while steaming (typically at 8–10 knots) between trawl stations both day and night. Surveys prior to May 2008 used the same custom-built CREST acoustic system (Coombs et al. 2003) with hull-mounted Simrad single-beam 12 kHz and 38 kHz transducers. In May 2008, the CREST system on *Tangaroa* was replaced by a new suite of Simrad EK60 echosounders with 18, 38, 70, 120, and 200 kHz transducers. The new multifrequency system provides more power for discriminating between acoustic mark types, but the 38 kHz data from the EK60 and CREST systems are comparable, allowing continuation of a consistent time-series. All 38 kHz data were collected with a transducer power output of 2 kW rms. Transmitted pulse length was 1 ms with 3 s between transmits. The 38 kHz transducer was calibrated regularly (usually once a year) with a 38.1 mm tungsten carbide sphere following standard procedures (Foote et al. 1987). Calibration coefficients for the CREST system were relatively stable and all CREST data were analysed using the calibration coefficients provided by Coombs et al. (2003). Data from the EK60 were analysed using calibration coefficients from a calibration on 30 May 2008 (calibration parameters given in Table 2 of O’Driscoll & Bagley (2009)). A constant sound absorption of 8.0 dB km⁻¹ and sound speed of 1500 m s⁻¹ was assumed for all surveys.

Analyses followed the methods of O’Driscoll et al. (2009). Acoustic data were analysed using standard echo integration methods (Simmonds & MacLennan 2005), as implemented in NIWA’s Echo Sounder Package (ESP2) software (McNeill, 2001). All echograms were visually scrutinised, and the bottom determined by a combination of an in-built bottom tracking algorithm and manual editing. Bad or missing pings (usually due to aeration in bad weather) were edited out. Only files with more than 90% good pings were considered of sufficient quality for echo integration.

Most mesopelagic fish undergo strong diurnal vertical migration, being concentrated at 100–500 m depth during the day, and migrating into the surface 200 m at night (McClatchie & Dunford 2003, McClatchie et al. 2005, O’Driscoll et al. 2009). We can use this behaviour to discriminate mesopelagic species from demersal fish and provide estimates of abundance. The rationale is that the mesopelagic fish of interest are mixed with demersal fish during the day, but migrate away and are separated from demersal fish at night (McClatchie & Dunford 2003). Based on a subset of their data, McClatchie & Dunford (2003) concluded that night estimates of backscatter in the upper 200 m (the nyctoepipelagic zone) “adequately captured” the scattering from vertically migrating mesopelagic fishes, but acknowledged that the proportion of the total mesopelagic fish community biomass represented by the nyctoepipelagic component was unknown. Using data from the Chatham Rise in 2001–07, O’Driscoll et al. (2009) found that there was a negative bias at night because an estimated 20% of the total daytime

backscatter on the Chatham Rise migrates to the surface 0–14 m, where it is too shallow to be detected by hull-mounted acoustics. O’Driscoll et al. (2009) suggested that unbiased relative estimates of mesopelagic backscatter for the Chatham Rise could be obtained by subtracting night estimates of backscatter which remains deeper than 200 m (the demersal component) from daytime estimates of total backscatter.

Day estimates were based on data recorded while bottom trawling only. Acoustic recording was manually started when the trawl doors entered the water and stopped when the gear was hauled off the bottom. This resulted in short (6–8 km) recordings at each random trawl location. Mean area backscattering coefficients were estimated for each trawl recording and then treated as random point samples to estimate survey mean and variance.

Night estimates were based on data recorded while steaming between 2000 h and 0500 h NZST (after O’Driscoll et al. 2009). To estimate abundance, we treated each night as a single random transect. The assumption of randomness is at least partly valid because the vessel was steaming between random trawl stations. These night ‘transects’ typically ranged in length from 30 to 160 km and there were between 17 and 27 nights with suitable acoustic data in each survey. Mean area backscattering coefficients were calculated for each ‘transect’, and then an overall survey estimate and variance obtained using the formulae of Jolly & Hampton (1990), as described by Coombs & Cordue (1995).

Acoustic data from each region (Chatham Rise and Sub-Antarctic) were stratified into broad sub-areas. Strata were defined *a priori* based on environmental variables.

Chatham Rise subareas:

1. NW: 174° 30'E, - 42° 45'S; 177° 00'E, - 42° 45'S; 177° 00'E, - 43° 30'S; 174° 30'E, - 43° 30'S
2. NE: 177° 00'E, - 42° 45'S; 174° 30'W, - 42° 45'S; 174° 30'W, - 43° 30'S; 177° 00'E, - 43° 30'S
3. SE: 177° 00'E, - 43° 30'S; 174° 30'W, - 43° 30'S; 174° 30'W, - 44° 45'S; 177° 00'E, - 44° 45'S
4. SW: 174° 30'E, - 43° 30'S; 177° 00'E, - 43° 30'S; 177° 00'E, - 44° 45'S; 174° 30'E, - 44° 45'S

Sub-Antarctic subareas:

1. Puysegur: 165° 00'E, - 46° 00'S; 168° 00'E, - 46° 00'S; 168° 00'E, - 48° 00'S; 165° 00'E, - 46° 00'S
2. West: 165° 00'E, - 48° 00'S; 169° 00'E, - 48° 00'S; 169° 00'E, - 54° 00'S; 165° 00'E, - 54° 00'S
3. East: 169° 00'E, - 46° 00'S; 176° 00'E, - 46° 00'S; 176° 00'E, - 54° 00'S; 169° 00'E, - 54° 00'S

Previously, O’Driscoll et al. (2009) divided the Chatham Rise into two strata (east and west of 177 °E) based on consistent observations of higher acoustic backscatter in the west. McClatchie & Dunford (2003) also subdivided the Chatham Rise into two strata at 176 °E, which was based on only one year’s data.

As well as annual estimates of mesopelagic abundance by strata, acoustic data were integrated in small-scale depth (50 m) and time (25 minute) bins to provide information on the spatial and vertical distribution of mesopelagic species within a survey.

2.2 Hoki abundance

Biomass indices for hoki were available for both areas up to and including surveys in January 2010. Doorspread biomass was estimated by the swept area method of Francis (1981, 1989) using the analysis programme SurvCalc (Francis 2009). The catchability coefficient (an estimate of the proportion of fish in the path of the net which are caught) is the product of vulnerability, vertical availability, and areal availability. These factors were set at 1 for the analysis, the assumptions being that fish were randomly distributed over the bottom, that no fish were present above the height of the headline, and that all fish within the path of the trawl doors were caught. Estimates of hoki biomass were calculated for all hoki

and for three discrete size classes (< 60 cm, 60–80 cm, and > 80 cm). Hoki catch rates (kg/km²) were also estimated for each individual trawl station, which allowed us to test association between hoki and mesopelagic prey at small spatial scales (see below).

2.3 Fish condition indices

Of the 25 species examined in the Chatham Rise feeding study, only four (hoki, Ray's bream, arrow squid, and alfonsino) had mesopelagic fish as a significant component of their diet (> 25% frequency occurrence) (Dunn et al. 2009a). Trawl-based abundance estimates and data on individual fish length and weight are available from these four species in every survey, but sample sizes for alfonsino, arrow squid, and Ray's bream are sometimes small, and species like Ray's bream and arrow squid are probably not representatively sampled in a bottom trawl survey. For these reasons, our analyses of trends in condition and abundance of piscivorous fish in relation to mesopelagic prey abundance were focused on hoki.

Two alternative indices of hoki condition were used: somatic condition based on the relationship between individual fish weight and length estimated from each survey, and liver condition index (LCI) based on the ratio of measured liver weight to fish gutted weight. The liver is the major lipid storage organ in hoki (MacDonald et al. 2002) and LCI may provide the best index of recent feeding conditions. Liver and gutted weight data were only available from the Sub-Antarctic since 2002 and from the Chatham Rise since 2004.

Exploratory analyses suggested that patterns in hoki liver condition were confounded by fish size and maturity state (e.g., O'Driscoll & Bagley 2009). A standardised analysis of LCI was attempted to separate year effects from other variables. Liver condition data were modelled using a lognormal generalised linear model following Dunn (2002). The dependent variable was estimated LCI per fish. Explanatory variables offered to the model included *year*, *area* (Chatham Rise or Sub-Antarctic), *sex*, *gonad stage*, *stratum* as categorical variables; and start latitude, start longitude, and fish length as continuous variables. Continuous variables were fitted as third-order polynomials. A forward stepwise multiple-regression fitting algorithm (Chambers & Hastie 1991) implemented in the R statistical programming language (R Development Core Team 2003) was used to fit all models. A stopping rule of 1% change in residual deviance was used. Year indices were standardised to the mean and were presented in canonical form (after Francis 1999). There were no zero values.

2.4 Environmental indices

Four main types of environmental data were assembled (Table 2). The subset of environmental variables was restricted to a subset of appropriate indices from the 11 categories of climatic and oceanographic indices relevant to New Zealand fisheries included by Hurst et al (in press). Environmental indices vary in terms of their spatial and temporal scales: in some cases (e.g. SOI) the same index is relevant for both the Sub-Antarctic and Chatham Rise; in other cases (e.g., SST, ocean colour) it was more appropriate to have separate environmental indices for the two areas (and subsets of the two areas).

Climatic indices include the Interdecadal Pacific Oscillation (IPO), monthly estimates of the Southern Oscillation Index (SOI), Kidson weather regimes and Trenberth pressure. Indices were updated to September 2009 (instead of February 2009 as originally proposed).

Sea surface temperature (SST, from September 1981 to January 2010), sea surface height (SSH, from November 1992 to January 2009) and ocean colour (chlorophyll, from September 1997 to December 2009) were extracted specifically for this project for four biologically relevant sub-areas on the Chatham Rise and six sub-areas in Sub-Antarctic (Figure 1). Sub-areas on the Chatham Rise were the same as

those used for the acoustic indices. The boundaries of the six environmental sub-areas in the Sub-Antarctic were:

1. Snares: between 165° 00'E and 170° 00'E, - 46° 00'S and - 49° 00'S
2. Auckland Is: between 166° 00'E and 168° 00'E, - 49° 00'S and - 51° 00'S
3. Puysegur: between 165° 00'E and 167° 00'E, - 46° 00'S and - 47° 00'S
4. Bounty: between 176° 00'E and 179° 00'W, - 47° 00'S and - 50° 00'S
5. West Sub-Antarctic: between 166° 00'E and 169° 00'E, - 49° 00'S and - 54° 00'S
6. East Sub-Antarctic: between 169° 00'E and 176° 00'E, - 48° 00'S and - 54° 00'S

Three of these sub-areas (Puysegur, west and east Sub-Antarctic) were broadly similar to strata used for acoustic indices (see above).

Data sources were: SST, NOAA OI daily SST analysis version 2 (AVHRR-only) as described by Reynolds et al. (2007); SSH, AVISO delayed-time, reference, merged, Mapped Sea Level Anomalies data set, as described by Dibaboure et al. (2009) and Ducet et al. (2000); Chlorophyll, SeaWiFS, Level 3, mapped monthly composite chlorophyll dataset, Reprocessing 5.2 (July 2007) as described in Thomas & Franz (2005).

Temperature data were also derived from measurements made using a calibrated Seabird SM-37 Microcat CTD during trawl surveys from December 2002 to ground-truth patterns observed in remotely derived data. Temperature data from earlier surveys were collected from an uncalibrated net-monitor and were not considered reliable.

2.5 Links between variables

Because the number of potential explanatory factors is great and the time-series of mesopelagic fish abundance is short (maximum of 8 years), statistical analyses of correlations between mesopelagic fish abundance and environmental variables and between mesopelagic fish abundance and hoki condition and abundance were relatively simple. Data were initially explored using dot-plots to determine if any relationships were obvious between the multiple time series. Where relationships appeared visually, factors were included in further analyses.

The association of mesopelagic biomass with environmental predictors was estimated using simple statistical tests, including a 2-sided Spearman's rank correlation, and an association test. In all statistical tests, the data (e.g., predictor and predictand) were restricted to the years that they had in common, and the test was not performed if this overlap was less than 5 years. The association test was a test of whether the extremes of the predictor and predictand occurred together (Dunn et al. 2009b), and allows for the hypothesis that extreme events in mesopelagic biomass and environmental indices might have a correlated effect, but the smaller year-to-year smaller fluctuations might not. Unlike the rank correlation test, the association test used only the upper and lower quantiles of the data, thereby ignoring the fluctuations around the median. Both the Spearman's rank correlation and association tests were assumed to be significant at the 5% level. The potential association was considered to be of interest only if both tests were significant. Predictor screening was not completed because of the exploratory nature of the analyses. However, predictor screening would be an important first step when developing predictive models (Francis 2006).

Some data sets were available at multiple spatial scales. For example, indices of mesopelagic backscatter were available from point samples at the scale of individual trawls (6–8 km), and for sub-areas (strata) as well as for the Chatham Rise and Sub-Antarctic as entire areas. The statistical tests of correlation and association were performed at the level of the entire Chatham Rise or Sub-Antarctic, and strata within these areas.

The data collected at an individual trawl level were investigated separately for the Chatham Rise and Sub-Antarctic using generalised additive models (GAMs), as implemented in the `mgcv` library of the statistical package R (Wood & Augustin 2002). The log of the mesopelagic biomass estimate was modelled using an identity function and Gaussian error term. The GAM model-building procedure followed the guidelines of Wood (2001), using penalized regression splines with backward model selection via generalised cross validation scores (Wood 2001, Wood & Augustin 2002). The potential predictors were either continuous variables smoothed using cubic splines, including longitude (tow mid-point), latitude (tow mid-point), depth (mean of start and end depth), surface temperature, and bottom temperature, continuous variables smoothed using linear models (Trenberth, Kidson regime, SOI, SST, SSH and IPO), or a categorical variable, year. Time lags in the predictors were not investigated using the GAMs.

For the simple statistical tests and GAMs, the Trenberth, Kidson regime, SOI, SST, SSH and IPO annual environmental indices were derived from monthly averages. The Chatham Rise trawl surveys took place predominantly during January, so the annual environmental indices were a mean of the monthly values for the January of the survey and the previous quarter (October to December). The Sub-Antarctic trawl surveys took place in December, so the annual environmental indices were a mean of the monthly values for the last quarter of the year (October to December).

Potential contact statistics (O’Driscoll et al. 2000) were used to assess the scale dependence of the spatial correlation between hoki (predators) and mesopelagic fish (prey). Potential contact is a distance-based method to describe spatial structure and association in sampled data from continuous two-dimensional distribution surface patterns. The advantages of this method are that, unlike covariance based methods such as geostatistics, it is robust to the presence of zeros, and can be used in an area with irregular boundaries and sampling (O’Driscoll et al. 2000). The test statistic is a measure of the potential contact between the predator (in the case hoki) and neighbouring prey (mesopelagic fish), and is defined as the expected density of prey (b) within a distance, t , of an average predator (a):

$$E[b(t)] = \frac{\sum_{i=1}^n a_i \overline{(b_{ij})}}{\sum_{i=1}^n a_i}$$

a_i and b_j are the measured densities of predators and prey at sample point i and j respectively. Hoki densities were based on (wingspread swept area) catch rates from the trawl survey and mesopelagic densities were based on acoustic estimates (see results).

To test whether an observed spatial association was significantly different from a random arrangement, we randomised the hoki density pattern by randomly reallocating hoki catch rates between sampling points (stations). The randomisation process was repeated 99 times and $E[b(t)]$ was calculated for each realisation. From these realisations we calculated the average potential contact for a random arrangement, $E[b(t)]_{ran}$, and the values of equivalent to the 5th percentile $E[b(t)]_5$, and the 95th percentile $E[b(t)]_{95}$.

We express our results as the ‘extra contact’ at distance t , $XC(t)$ where

$$XC(t) = E[b(t)] - E[b(t)]_{ran}$$

$XC(t)$ is the ‘extra’ density of prey within distance t . The ‘extra’ prey are those which are not expected if the predators were distributed randomly throughout the study area. $XC(t)$ has an expected value of 0 under a null hypothesis of complete spatial randomness. When individuals are aggregated $XC(t) > 0$. The upper and lower bounds for a random spatial distribution are given by:

$$XC(t)_5 = E[b(t)]_5 - E[b(t)]_{ran}$$

$$XC(t)_{95} = E[b(t)]_{95} - E[b(t)]_{ran}$$

$XC(t)_{95}$ represents the significance level of $p = 0.05$ for a one-sided test. Because we were only considering the hypothesis of association (i.e., positive correlation), when $XC(t) > XC(t)_{95}$ the association between predator and prey was considered statistically significant. No correction for edge bias was necessary in our analysis because the randomisation scheme used to generate the null model and calculate $XC(t)$ used the same sampling points, and makes the same assumptions about the distribution of organisms outside the study area as the data.

We used a Matlab routine to calculate $XC(t)$, $XC(t)_5$ and $XC(t)_{95}$ at distances $t = 10, 20, 30, \dots, 1000$ km. Results are presented as plots of $XC(t)$ as a function of t . Such plots allow comparison of association over a range of scales (Haase 1995). $XC(t)$ drops back to zero as t approaches the maximum separation of sampling points because all data become encompassed by the calculation.

To avoid spurious correlations, more emphasis was placed on environmental indices exhibiting more than one cycle during the analysis period (since 2001). For example, IPO will be of very limited value given the decadal time scales over which it changes and the recent shift to the negative phase in 2000. Time lags were considered where appropriate. For example, mesopelagic fish abundance might be related to favourable oceanographic conditions during early life history stages, so might be offset by several years (or a time period equivalent to the average age of the key species).

As with all correlation-based studies, it is important to note that significant correlations are not necessarily indicative of causation.

3. RESULTS

3.1 Acoustic indices

3.1.1 Chatham Rise

Survey dates were between 27 December and 25 January (e.g., ‘2001 survey’ was 28 December 2000 to 25 January 2001). Between 86 and 117 day acoustic point estimates were available from each survey from 2001 to 2009 (Table 1). Data in 2004 were collected using an uncalibrated ship’s echosounder only and are not suitable for quantitative analysis. Night ‘transects’ typically ranged in length from 30 to 160 km and there were between 17 and 27 nights with suitable acoustic data in each survey year (Table 1).

Expanding symbol plots of the distribution of total acoustic backscatter observed during daytime trawls and night transects are shown in Figures 2 and 3. The vertical distribution of backscatter is shown in Figure 4. Similar patterns of diurnal vertical migration were observed in all years. Most acoustic backscatter was concentrated at 200–500 m depth during the day, and migrated into the surface 200 m at night (Figure 4). This vertically migrating component was assumed to be dominated by mesopelagic fish (see McClatchie & Dunford, 2003 for rationale and caveats).

Day estimates of total acoustic backscatter over the Chatham Rise were consistently higher than night estimates (Figure 5). In the 8 survey years, night estimates of total backscatter (expressed as mean sa , averaged over the entire survey area) were 54–85% (mean 72%) of day estimates. In some years (e.g., 2003), the difference between day and night estimates was partly explained by sampling error, as day and night estimates were based on very different survey ‘designs’ (see Figures 2 and 3). For example, in

2003, there was one very high point estimate of total backscatter from a day trawl. This led to an increased difference between day and night estimates in 2003 and is reflected in the increased uncertainty associated with the day estimate from this year (Figure 5). However the consistent trend of lower observed backscatter at night could not be explained by survey design alone and was related to bias in night estimates (O’Driscoll et al. 2009).

The bias in night-time estimates occurs because some of the backscatter migrates very close to the surface at night (e.g., Figure 6), and may move into the surface ‘deadzone’ where it is not detectable by the vessel’s downward looking hull-mounted transducer. The approximate depth of the surface deadzone for *Tangaroa’s* 38 kHz transducer mounted at 6 m depth is 14 m. Based on comparison of paired day-night data, O’Driscoll et al. (2009) found that an estimated 20% of the total daytime backscatter migrates to the surface 0–14 m at night.

O’Driscoll et al (2009) recommended that the best estimate of mesopelagic fish abundance on the Chatham Rise was calculated by subtracting night estimates of the backscatter which remains deeper than 200 m from day estimates of total backscatter. Acoustic indices calculated using this equation are summarised in Table 3 and plotted in Figure 7 for the entire Chatham Rise and for the four sub-areas. The mesopelagic indices for the Chatham Rise are similar to estimates of total backscatter (see Figure 5). There has been no clear trend in mesopelagic fish abundance over the last 9 years. The estimate from 2009 was the second highest in the time series, but similar to estimates from 2001 and 2003 (Figure 7). Stratification into the four sub-areas did not have a strong influence on the overall acoustic index (Figure 7), probably because the distribution of stations has been relatively consistent between surveys (see Figure 2). However, the relative estimates of mesopelagic fish abundance varied between strata, with highest average abundance in the southwest and lowest abundance in the northeast (Table 3). Annual indices from the southwest Chatham Rise were also more variable than the other indices, with high values in 2001 and 2009 (Figure 7).

The mesopelagic indices based on the work of O’Driscoll et al (2009) can only be calculated for areas where sufficient data are available to estimate both the day estimate of total backscatter and the night estimate of backscatter deeper than 200 m. It also loses valuable information on spatial distribution that is obtained from point sample estimates of total backscatter (e.g., Figure 2). We derived an alternative method of estimating the amount of mesopelagic backscatter at each day trawl station by multiplying the total backscatter observed at the station by the estimated proportion of night-time backscatter in the same sub-area that was observed in the upper 200 m corrected for the estimated proportion in the surface deadzone:

$$sa(meso)_i = p(meso)_{y,s} * sa(all)_i$$

Where $sa(meso)_i$ is the estimated mesopelagic backscatter at station i , $sa(all)_i$ is the observed total backscatter at station i , and $p(meso)_{y,s}$ is the estimated proportion of mesopelagic backscatter in the same year y and stratum s as station i . $p(meso)_{y,s}$ was calculated from the observed proportion of night-time backscatter observed in the upper 200 m in year y and stratum s ($p(200)_{y,s}$) and the estimated proportion of the total backscatter in the surface deadzone, p_{sz} . p_{sz} was estimated as 0.2 by O’Driscoll et al (2009) and was assumed to be the same for all years and strata:

$$p(meso)_{y,s} = p_{sz} + p(200)_{y,s} * (1 - p_{sz})$$

Estimates of $p(meso)$ for each year and stratum are given in Table 4. Values ranged from 0.58 to 0.88 (mean 0.75) which indicates that an average of 75% of the total daytime backscatter at each station migrates into the upper 200 m at night and was therefore estimated to be from mesopelagic fish.

The overall acoustic abundance indices for the Chatham Rise calculated from estimates of $sa(meso)$ from daytime trawl samples was very similar to the indices calculated using the estimate of O’Driscoll

et al. (2009) (Figure 8), which reassured us that the corrections in Table 4 were appropriate. Distribution plots of mesopelagic backscatter estimated for each station are shown in Figure 9. These show similar patterns to total backscatter (see Figure 2). Simple regression analyses suggested that there was a trend of increasing mesopelagic backscatter towards the west, but no strong patterns associated with either depth or longitude (Figure 10). Although our east-west split at 177 °E was somewhat arbitrary, some longitudinal separation is clearly supported by the mesopelagic data. Although there was no trend apparent between the north and south Chatham Rise, these areas have different oceanographic regimes, and may have different assemblages of mesopelagic fish (Robertson et al. 1978), so we retained the north-south stratification. We chose not to stratify mesopelagic data further by depth.

3.1.2 Sub-Antarctic

Survey dates were between 11 November and 24 December (see Table 1), but surveys were labelled as the following year to facilitate comparison with the subsequent Chatham Rise survey (e.g., ‘2001 survey’ was 24 November to 23 December 2000). Between 56 and 102 day acoustic point estimates were available from each survey from 2001 to 2009 (see Table 1). There was a problem with synchronisation of scientific and ship’s echosounders in December 2004 (O’Driscoll & Bagley 2006), so data in 2005 (TAN0414) were not suitable for quantitative analysis due to the presence of acoustic interference. Night ‘transects’ typically ranged in length from 10 to 200 km and there were between 9 and 20 nights with suitable acoustic data in each survey year (see Table 1). The proportion of trawls and nights where acoustic data was considered suitable for quantitative analysis was lower than on the Chatham Rise because of poor weather conditions in some years. This is particularly apparent in 2003, where 38% of all acoustic recordings were considered too poor to be analysed quantitatively (i.e., had more than 10% incidence of noisy or missing transmits) (O’Driscoll & Bagley 2004).

Expanding symbol plots of the distribution of total acoustic backscatter observed during daytime trawls and night transects are shown in Figures 11 and 12. The vertical distribution of backscatter is shown in Figure 13. Vertical distribution of backscatter was more variable than on the Chatham Rise (see Figure 4), but diurnal vertical migration was still apparent (Figure 13). In some years marks were concentrated in a particular depth band during the day (e.g., around 350 m in 2002 and 2003), while in other years daytime marks occurred at all depths (e.g., 2006–09). We are not certain what is driving changes in vertical distribution patterns. However, CTD data show that there is considerable variability in the depth and strength of the thermocline between years (Figure 14), depending on the degree of solar heating and surface wind mixing. There was a particularly strong shallow thermocline in 2003, when daytime backscatter was concentrated at 350 m, with a weaker, deeper thermocline in subsequent years when daytime backscatter was more evenly distributed (Figures 13 and 14). There may also be different mesopelagic species composition between years, which we have no trawl data to test.

Vertical distribution of backscatter at night was more consistent, with much of the backscatter concentrated in the upper 200 m (see Figure 13). Unlike the Chatham Rise, there did not appear to be a bias in night acoustic estimates associated with a surface deadzone in the Sub-Antarctic. In fact, night estimates of total backscatter were always higher than day estimates (Figure 15). Close examination of echograms (e.g., Figure 16) suggested that fish were not ‘disappearing’ into the surface deadzone, but tended to remain at depths greater than 20 m at night. Because there was no apparent bias due to a surface deadzone, it would be possible to use night estimates of backscatter in the upper 200 m as an index of mesopelagic fish abundance in the Sub-Antarctic, as was done by McClatchie & Dunford (2003). This index is plotted in Figure 15 and shows a similar pattern to estimates of total day and night backscatter. However we were concerned that the quantity and quality of night data in the Sub-Antarctic was lower than the quality and quantity of day data. Key advantages of daytime data are:

- a) Day data were collected at stratified random trawl locations so there was good spatial coverage which followed a statistical survey design (see Figure 11). Night data were more patchy (see Figure 12).

- b) Fewer day data were rejected due to high incidence of missing pings (see Table 1). There were large gaps in the coverage of night transects in some years due to weather-related data quality (see Figure 12).
- c) Day data were collected at a constant speed of 3.5 knots and often running ‘with the weather’. This meant that there was less noise due to the vessel and the environment. Many night echograms exhibited vessel noise (see Figure 16). Because ambient and vessel noise is amplified by the time-varied gain (TVG) of the echosounder, noise from these sources is more apparent at greater range (depths). We were particularly concerned that there appeared to be a depth-related trend in total backscatter at night, but not during the day (Figure 17). This suggested the presence of noise in the night data, which may account for the positive bias in night estimates (see Figure 15).

We developed a day-based estimate of mesopelagic fish abundance in the Sub-Antarctic by multiplying the total backscatter observed at each station by the estimated proportion of night-time backscatter in the same sub-area and year that was observed in the upper 200 m:

$$sa(meso)_i = p(200)_{y,s} * sa(all)_i$$

This is analogous to the alternative method used for the Chatham Rise, except that no correction is applied for backscatter in the surface deadzone. Values of $p(200)_{y,s}$ are given in Table 5. The estimated acoustic indices calculated using this method are summarised in Table 6 and plotted in Figure 18 for the entire sub-Antarctic and for the three sub-areas. The mesopelagic indices for the Sub-Antarctic are similar to estimates of total backscatter (see Figure 15) and show a decreasing trend from 2001 to 2007, with an increase in the last two years. Indices from Puysegur showed a more extreme pattern (Figure 18). Because the station density at Puysegur was disproportionate to its small area (only 1.5% of total Sub-Antarctic area), stratification reduced the influence of Puysegur and flattened the decline observed in unstratified indices (Figure 18). Average mesopelagic abundance was highest and most variable at Puysegur, with lowest abundance in the east Sub-Antarctic (Table 6). Abundance in all three Sub-Antarctic strata was lower than observed on the Chatham Rise (see Table 3).

Distribution plots of mesopelagic backscatter estimated for each station are shown in Figure 19. These show similar patterns to total backscatter (see Figure 11). Simple regression analyses provided support for the three strata, showing higher values at Puysegur and a trend of increasing mesopelagic backscatter towards the west on the main Campbell Plateau (Figure 20). There were no strong patterns associated with depth (Figure 20).

3.2 Hoki abundance

Biomass indices for hoki on the Chatham Rise and Sub-Antarctic are summarised in Tables 7 and 8 and distribution of hoki catch rates are plotted in Figures 21 and 22. Hoki catch rates were also summarised by sub-area in Tables 7 and 8 to allow comparison with acoustic strata.

Hoki catch rates were higher on the Chatham Rise than in the Sub-Antarctic (Tables 7 and 8). On the Chatham Rise, hoki catch rates were highest in the southwest and lowest in the northeast (Table 7, Figure 21). In the Sub-Antarctic catch rates were highest at Puysegur (Table 8, Figure 22). Trends in hoki biomass indices over time have been well-documented for both series (e.g., O’Driscoll & Bagley 2009, Stevens et al. 2009). Hoki abundance on the Chatham Rise is driven by the recruitment of the three most recent year classes (roughly indexed by <60 cm fish in Table 7) and has fluctuated with variability in year-class strength. Hoki abundance in the Sub-Antarctic was at very low levels from 2004 to 2007 but has since increased.

3.3 Hoki condition

3.3.1 Somatic condition

Length-weight parameters estimated from hoki which are individually weighed and measured in each survey are derived annually and published in annual survey reports (e.g., O’Driscoll & Bagley 2009, Stevens et al. 2009). These are summarised in Table 9. To compare somatic condition between years we estimated the weight of a 75 cm hoki estimated from the survey length-weight parameters (Table 9). On average, 75 cm hoki were 40 g heavier on the Chatham Rise than in the Sub-Antarctic. Somatic condition was more variable on the Chatham Rise (range 1205–1295 g), peaking in 2002. In the Sub-Antarctic the observed range of fish weight was smaller (1195–1233 g), with a peak in 2006 (Table 9). This somatic condition index was not derived for sub-areas of the Chatham Rise and Sub-Antarctic, because we considered that liver condition would provide a better indicator of recent feeding.

3.3.2 Liver condition

Liver and gutted weight data were available from 11 051 individual hoki on the Sub-Antarctic since 2002 and 10 328 hoki from the Chatham Rise since 2004. Liver condition indices are summarised for each area and its strata in Tables 10 and 11.

As noted by O’Driscoll & Bagley (2009), there were consistent patterns in LCI between the Chatham Rise and Sub-Antarctic (Figure 23). Liver condition of hoki on the Chatham Rise was consistently higher than that for similar size fish from the Sub-Antarctic, as would be expected based on seasonal accumulation of lipid (MacDonald et al. 2002) – the Chatham Rise survey is a month later than the Sub-Antarctic survey and so fish on the Chatham Rise had an additional month to put on condition. The consistent pattern in liver condition of hoki from the Chatham Rise and Sub-Antarctic suggests that similar processes are affecting the two areas.

The standardised analyses of LCI revealed similar patterns to unstandardised indices (Figures 24 and 25). The explanatory power of the GLM models (R^2 values) were very low (Table 12), but predictive variables made sense. On the Chatham Rise, there was a decreasing trend in LCI with increasing fish length (i.e., smaller fish were in better condition). LCI on the Chatham Rise was also related to latitude, with lower condition along the central axis of the Rise (Figure 24). Latitude may be acting as a proxy for depth, which was not offered to the model. There was no evidence for a longitudinal gradient in condition on the Chatham Rise. In the Sub-Antarctic, there was a clear spatial pattern in LCI, with very low LCI at Puysegur (see Table 11), and increasing LCI with increasing longitude (i.e., better condition hoki in the east) (Figure 25). LCI was also related to macroscopic gonad stage, with fish that were macroscopically staged as partially spent or spent (stages 6 and 7) having lower LCI than immature or resting fish (stages 1 and 2). This pattern has been noted previously (O’Driscoll & Bagley 2009). Both the spatial pattern in LCI and the relationship with macroscopic gonad stage are consistent with our hypotheses about the spawning migration pattern of hoki in the Sub-Antarctic. We believe that there is a southeastward movement of fish from spawning areas on the WCSI and at Puysegur back to the Campbell Plateau. It therefore seems likely that fish which are at Puysegur or to the west are fish which are likely to have spawned more recently and therefore have lower LCI. Likewise, fish that can still be macroscopically staged as partially spent (mainly males with residual milt) or spent (mainly females) are likely to have spawned more recently than fish that are classified as resting. Indeed, the motivation for collecting liver weight data initially was to investigate whether this could be used as an index of proportion spawning in the Sub-Antarctic.

3.4 Environmental indices

Climatic indices include the Interdecadal Pacific Oscillation (IPO) (Figure 26), monthly estimates of the Southern Oscillation Index (SOI) (Figure 27), Kidson weather regimes (Figure 28) and Trenberth pressure (Figure 29). Indices were updated to September 2009 (instead of February 2009 originally proposed). Data from 1980 are presented here and update the longer time series presented by Hurst et al. (in press). Since 1999, the general trend in the IPO has been a move into the negative phase (Figure 26), and the SOI has moved to more years of La Niña events (positive SOI) and less El Niño events (negative SOI) than in the previous decade (Figure 27).

SST, SSH and chlorophyll monthly data are presented for the Chatham Rise (Figure 30) and Sub-Antarctic (Figure 31), monthly for the entire period, and by the individual months of the trawl surveys (January for the Chatham Rise and December for Sub-Antarctic). Note that chlorophyll data is missing for some months (particularly in 2008 and 2009 on the Chatham Rise and winter months in Sub-Antarctic) due to cloud, low sun angle or instrument outages. A mean value for the month was only calculated for each rectangle, for each month, if at least half of the grid points within the rectangle had valid data.

Trends in Chatham Rise SST are similar between subareas, although minor differences are apparent for the southeast Chatham Rise from 1982–2010 (Figure 30). SSH also shows considerable similarity between sub areas. Chlorophyll indices show more variability by area; most show higher values in 1998 and 2007, and two peaks in 2004, but other peak years vary (note there are no data for 2008). Trends in Sub-Antarctic SST and SSH are also similar between subareas, except for that SSH at the Bounties shows some different peaks and troughs (Figure 31). Chlorophyll indices show considerable variability by area, with Puysegur having the highest indices and peaking in 2003 and 2007; Auckland and west Sub-Antarctic peak in 2004.

Temperature data from CTD measurements are summarised in Tables 13 and 14. Surface estimates (approximately 5 m depth) were compared to satellite-derived SST by sub-area (Figures 32 and 33). This showed good correlations, reassuring us that satellite-derived SST provided a realistic measure of sea surface temperature for these regions in years before CTD data were available. Bottom temperatures (Tables 13 and 14) were confounded by tow depth. It would be possible to extract temperature data from any depth from CTD vertical profiles and also to calculate indices such as mixed layer depth. There was insufficient time available to do this as part of this project, but we recommend that it would be worth carrying out a more detailed analysis of CTD data collected on trawl surveys in the future.

3.5 Links between variables

Two alternative and simple presentations were used to compare time-series of indices within areas. Plots were created showing annual patterns for each of the selected indices in each area (Figures 34–35). Dot-plots were then used to carry out visual comparison between paired variables (Figures 36–37). Figures 34–37 show plots for the entire Chatham Rise and Sub-Antarctic but similar plots were also produced for subareas. There were strong correlations between some environmental variables (e.g., SST and surface CTD temperature shown in Figures 32 and 33), but this report focuses on factors associated with the mesopelagic acoustic index. The remainder of this section deals with the more detailed analyses carried out on:

1. Association between mesopelagic fish and hoki abundance;
2. Association between mesopelagic fish and hoki liver condition;
3. Association between mesopelagic fish and the environment.

3.5.1 Association between mesopelagic fish and hoki abundance

Visual inspection of time-series and dot-plots showed little correlation between annual indices of mesopelagic prey from acoustics and hoki abundance from trawl surveys. A comparison of scaled indices (relative to the mean) for the entire Chatham Rise and Sub-Antarctic is shown in Figure 38. Correlation between hoki and mesopelagic abundance was stronger in the Sub-Antarctic (Spearman rank correlation, $\rho = 0.43$), than on the Chatham Rise ($\rho = -0.20$), but was not significant in either area. Hoki abundance is driven by many factors, including recruitment and fishing, so the lack of a strong correlation with food availability (indexed as mesopelagic prey) was not surprising.

Comparison of hoki distribution (see Figures 21 and 22) and the distribution of mesopelagic backscatter (see Figures 9 and 19) were broadly similar and suggested spatial association between hoki and mesopelagic fish (Figure 39). As a crude representation, we noted that there was a very strong positive correlation ($\rho = 1.00$) between average mesopelagic backscatter and hoki catch rates in our seven strata when data from all years were combined (Figure 40). When data from individual years were compared the strength of the correlation decreased to 0.73 (Figure 40), but was still statistically significant. At the smallest spatial scale available, that of the individual trawl stations, there was a weak positive correlation ($\rho = 0.45$) between hoki catch rate and the estimate of mesopelagic backscatter (Figure 41).

Potential contact statistics detected significant spatial association between hoki and mesopelagic prey on the Chatham Rise in 7 of 8 years (Figure 42), and in 4 of 8 years in the Sub-Antarctic (Figure 43). Positive association occurred over a broad range of scales, but was usually highest at the scale of tens of kilometres (Table 15).

We conclude that there is spatial association between hoki and mesopelagic prey. The strength of this association is scale-dependent and varies between years, but there are consistent general patterns. Our results confirm the earlier observations by McClatchie et al. (2005) that hoki abundance and mesopelagic prey are both higher on the western Chatham Rise, with highest values of both indices on the southwest Chatham Rise. Lowest densities of both mesopelagic prey and hoki were in the eastern Sub-Antarctic.

3.5.2 Association between mesopelagic fish and hoki condition

Time-series and dot-plots suggested that there was a negative correlation between annual indices of mesopelagic prey from acoustics and hoki liver condition for both the Sub-Antarctic and Chatham Rise (Figure 44). This was disappointing; as we had hypothesised that hoki liver condition would be positively correlated with prey abundance, as an indicator of recent feeding. The spatial pattern in hoki liver condition also did not match the spatial distribution of mesopelagic prey. Highest liver condition on the Chatham Rise was in the southeast (see Table 10), which had only moderate mesopelagic fish abundance. There was no evidence for a longitudinal gradient in condition to support the hypothesis of McClatchie et al. (2005) that hoki were 'fatter' (i.e., in better condition) on the western Chatham Rise, where mesopelagic prey is more abundant. Similarly, lowest liver condition in the Sub-Antarctic was at Puysegur (see Table 11), which had the highest mesopelagic fish densities (see Table 6).

3.5.3 Exploratory analyses of the association between mesopelagic fish and the environment

Rank correlation and association tests were completed with no annual time lag, or one or two year time lags, for the Chatham Rise (Tables 16–18) and Sub-Antarctic (Tables 19–21).

For the Chatham Rise, there were no significant rank correlation and association tests with time lags of one or two years. The factors significantly correlated and associated with mesopelagic biomass on the Chatham Rise with no annual time lag were:

- SW Chatham Rise and ZS (Figure 45). The Trenberth ZS is an index of the air pressure difference between Kelburn and Invercargill, and a measure of the strength of westerly winds over the South Island. The positive correlation indicates higher mesopelagic biomass on Chatham Rise in years with increased westerly winds.
- NE Chatham Rise and LCI (Figure 46). The hoki liver condition index (LCI) is an index of fish condition. Although significant, the correlation is not convincing visually (Figure 46). The positive correlation indicates higher hoki condition in years when mesopelagic biomass was higher.

For the Sub-Antarctic, there were significant rank correlation and association tests with no annual time lag, and time lags of one and two years. The factors significantly correlated and associated with mesopelagic biomass in the Sub-Antarctic with no annual time lag were:

- EAST and IPO (Figure 47). The Interdecadal Pacific Oscillation (IPO) exerts a long-term influence over the El Niño/La Niña-Southern Oscillation (ENSO), and changes from positive to negative polarity every 20 to 30 years. During the positive IPO (for example, late 1970s to late 1990s), frequent El Niño events are common. A shift to a more positive IPO therefore brings more frequent cooler, windier weather over New Zealand. The positive correlation with IPO indicates higher mesopelagic biomass on Chatham Rise in years with cooler and windier weather.
- WEST and SST (Figure 48). The positive indicates higher mesopelagic biomass in warmer water, particularly in temperatures greater than about 12°C (Figure 48).

The factors significantly correlated and associated with mesopelagic biomass in the Sub-Antarctic with a one year time lag were:

- PUYSEGUR and SOI (Figure 49). The Southern Oscillation Index (SOI) is a measure of the difference in mean sea-level pressure between Tahiti (east Pacific) and Darwin (west Pacific), and is used to describe the ENSO. When the SOI is strongly negative, an El Niño event is taking place. The negative correlation indicates higher mesopelagic biomass in the Sub-Antarctic in years with increased westerly winds and cooler, less settled weather.

The factors significantly correlated and associated with mesopelagic biomass in the Sub-Antarctic with a two year time lag were:

- PUYSEGUR and Z3, ZS, and MZ2 (Figure 50). The three Trenberth indices have a similar meaning, with higher values of Z3 indicating stronger westerlies across the whole of New Zealand, ZS indicating stronger westerlies across southern New Zealand, and MZ2 indicating stronger northwesterlies across the southern North Island and South Island. The negative correlation between mesopelagic biomass in the Sub-Antarctic and Z3, ZS and MZ2 indicates less mesopelagic biomass in years with increased westerly winds.
- WEST and SOI (Figure 51). The negative correlation indicates higher mesopelagic biomass in the Sub-Antarctic in years with increased westerly winds and cooler, less settled weather. Although significant, the correlation is not convincing visually (Figure 51).

For the Chatham Rise, the final GAM was $\log(\text{mesopelagic biomass}) \sim \text{longitude} + \text{latitude} + \text{surface temperature} + \text{depth} + \text{Trough}$ ($n = 572$). All model terms were significant at $p \leq 0.001$, and the total deviance explained was 33.5%. Mesopelagic biomass was predicted to be substantially higher on the

Chatham Rise west of about 178° E, peaked at a latitude of around 43°45' S, increased with depth having peaks at around 450 m and 700 m, was highest at a surface temperature of about 15.5°C, and increased with greater prevalence of the Trough weather regime (Figure 52).

For the Sub-Antarctic, the final GAM was $\log(\text{mesopelagic biomass}) \sim \text{longitude} + \text{latitude} + \text{surface temperature} + \text{depth} + \text{year}$ ($n = 474$). All model terms were significant at $p \leq 0.001$, and the total deviance explained was 42.1%. Mesopelagic biomass was predicted to be substantially higher on the Sub-Antarctic west of about 168°E and east of about 173°E, peaked at a latitude of around 48° S, increased steadily with depth, had a distinct peak at a surface temperature of about 13°C, and decreased between 2003 and 2006 before increasing in 2007 and 2008 (Figure 53).

4. DISCUSSION

In this study, acoustic backscatter was used as a proxy for mesopelagic biomass (after McClatchie et al. 2005). One relationship between backscatter and biomass for mesopelagic fish on the Chatham Rise is derived by McClatchie & Dunford (2003), but there is still considerable uncertainty associated with the species involved, their size distributions, and their acoustic target strengths. Limited targeted trawling on the Chatham Rise was carried out in 2005–07 using a midwater ‘myctophid’ trawl with 10 mm codend and results are described by O’Driscoll et al. (2009). A total of 65 species or species groups were caught in 41 night-time midwater trawls. Catches from 19 trawls in the upper 200 m (nyctoepipelagic zone) averaged 5.73 kg total weight and were dominated by myctophid fish (64.3% by weight, genera identified included *Lampanyctodes*, *Lampanyctus*, *Diaphus*, *Symbolophorus*, and *Electrona*), and gelatinous zooplankton (17.3% by weight, mainly salps). Catches were lower in the 21 trawls deeper than 200 m (nyctobathypelagic zone), averaging 3.39 kg, with fewer myctophids (44.3% by weight), and higher proportions of squid (19.1%) and decapods (8.9%, mainly prawns).

More extensive mark identification trawling was carried out during a FRST-funded voyage to the Chatham Rise in May–June 2008. This included 30 trawls with the standard configuration of the midwater ‘myctophid’ trawl and 8 further deployments, with a multiple opening and closing codend (MIDOC), which allowed up to 5 nets to be fished at discrete depths. Results are currently being analysed to improve our knowledge of species composition and distribution of mesopelagic species contributing to the acoustic backscatter on the Chatham Rise. This study may allow us to provide separate estimates for different groups of mesopelagic species on the Chatham Rise in the future. It is unlikely we will be able to similarly discriminate estimates from the Sub-Antarctic because there has been no targeted mark identification trawling on mesopelagic species in this region.

We initially hypothesized that high hoki liver condition index would be associated with high mesopelagic biomass, but whilst this was supported by the correlation and association tests for the NE Chatham Rise, it was not supported in more detailed analyses. An alternative hypothesis could be that hoki with poorer condition focus on areas where mesopelagic biomass is highest, in order to feed heavily and regain condition. Hoki in better condition may live elsewhere, for example in areas where there are more natural refuges and natural mortality rates are lower (e.g., perhaps in deeper water). There are also indications from the spatial pattern in LCI and the relationship with macroscopic gonad stage that liver condition is related to the timing of spawning. A second alternative hypothesis is that LCI is not correlated with prey density, but with the amount of time that the fish have been feeding post-spawning. Consistent patterns in liver condition between the Chatham Rise and Sub-Antarctic (see Figure 23) are intriguing and, if this second hypothesis is correct, suggest that timing of spawning in the two stocks may be correlated between years. One way of investigating this idea further would be to examine the timing of hoki spawning from gonad stage data collected by observers and from market samples on the west coast South Island and Cook Strait. Unfortunately, this analysis was beyond the scope of the current project.

There were no obvious correlations between mesopelagic fish abundance and environmental indices. However, generalized additive models suggested that mesopelagic abundance was influenced by the same key environmental factors of location, depth, temperature and prevailing weather conditions on both the Chatham Rise and Sub-Antarctic. Similarly, location and depth have been previously found to explain most of the variation in abundance and composition of demersal fish on the Chatham Rise (Bull et al. 2001).

The GAM of mesopelagic biomass on the Chatham Rise did not have a year effect, but this was not surprising given that there was little variation over the time series. The main predictors of the variability of mesopelagic biomass chosen by the GAMs were location (latitude, longitude, depth), and could relate to the position of oceanographic features supporting enhanced primary productivity, specifically the location of the Sub Tropical Front. The Sub Tropical Front is also likely to be associated with the temperature effect, which was selected by the GAMs for both the Chatham Rise and Sub-Antarctic, and also identified as a potentially important factor in the correlation and association tests for the western Sub-Antarctic.

In the GAM for the Sub-Antarctic, when the year predictor was removed, the next best predictor was Trough. The predictors used in the GAM for the Sub-Antarctic would then have been the same as the GAM for the Chatham Rise. This is perhaps unexpected, given the geographic separation and differences in overall environment, e.g., average temperatures and timing of productivity (Dunn et al., 2009b). A similarity between the regions would be, however, consistent with the association suggested by the strong similarity in hoki liver condition index (see Figure 23). This suggests that although the timing and magnitude of mesopelagic productivity in the two areas may be different, the variability in mesopelagic biomass and hoki condition may be influenced by the same key factors.

The Trough Kidson regime is characterised by pressure troughs over and east of the country, and is linked with high rainfall, and below-normal temperatures in the south. The Trough regime typically brings wet, cool, and cloudy conditions to most of the country. With no annual time lag, or a one year lag, higher mesopelagic biomass on both the Chatham Rise and Sub-Antarctic were correlated with increased westerly winds, and also cooler conditions in the Sub-Antarctic. The effect of Trough in the GAMs, and wind or ENSO related indices in the correlation and association tests, may therefore indicate some consistency: windier and cooler conditions favour increased mesopelagic biomass. However, with a two year time lag a contrasting pattern was found for the Sub-Antarctic, suggesting either that a more complex association may exist, or that the correlations may be misleading.

Correlations or associations, whether identified from models such as GAMs, or statistical tests, do not evaluate the mechanism behind the correlation, and correlation does not necessarily imply causation. As a result, there is always a risk that the correlation was incorrect, or aliasing for something else, and the correlation might be misleading (Francis 2006). In addition, the time series used in this study were short, and must therefore be interpreted with caution. Over a short time period, random variability might easily look like a trend (Francis 2006). It is therefore important to continue to collect acoustic and environmental data to grow the available time series.

5. CONCLUSIONS

- There was no clear trend in mesopelagic fish biomass on the Chatham Rise over the last 9 years – the estimate from 2009 was similar to estimates from 2001 and 2003, and higher than estimates in the other years.
- The time series of mesopelagic backscatter for the Sub-Antarctic area declined from 2001 to 2007, but has increased in the two most recent years.

- There were clear and consistent spatial patterns in mesopelagic fish distribution over all years. Abundance of mesopelagic fish was much higher on the Chatham Rise than in the Sub-Antarctic, with highest densities observed on the western Chatham Rise and lowest densities on the eastern Campbell Plateau. Abundance in areas with high densities of mesopelagic fish tended to be more variable between years.
- Spatial patterns in mesopelagic fish abundance closely matched the distribution of hoki, but temporal changes in mesopelagic fish abundance were not strongly correlated with hoki biomass. We hypothesise that prey availability influences hoki distribution, but that hoki abundance is being driven by other factors such as recruitment variability and fishing.
- There was no evidence for a link between hoki condition and mesopelagic prey abundance. There was a strong correlation between liver condition of similar size hoki on the Chatham Rise and Sub-Antarctic, which may be related to timing of spawning
- There were no obvious correlations between mesopelagic fish abundance and environmental indices. Generalized additive models (GAM) suggested that mesopelagic abundance was influenced by the same key environmental factors of location, depth, temperature and prevailing weather conditions on both the Chatham Rise and Sub-Antarctic.
- It is important to continue to collect acoustic data to grow the available time series. Companion work under the FRST Coasts and Oceans OBI will assist us to discriminate mesopelagic species and may allow us to provide biomass estimates for different groups on the Chatham Rise in the future.

6. ACKNOWLEDGMENTS

We thank Dr James Renwick (NIWA) for providing the climate indices and Dr Mark Hadfield (NIWA) for carrying out the SST, SSH and Chlorophyll data extracts. Funding was provided by Ministry of Fisheries Research Project ENV2009/04. We acknowledge Dr Mary Livingston for her comments on a draft of this report.

7. REFERENCES

- Bull, B.; Livingston, M.E.; Hurst, R.; Bagley, N. (2001). Upper-slope fish communities on the Chatham Rise, New Zealand, 1992–99. *New Zealand Journal of Marine and Freshwater Research* 35: 795–815.
- Chambers, J.M.; Hastie, T.J. (1991). Statistical models in S. Wadsworth & Brooks-Cole, Pacific Grove, CA. 608 p.
- Connell, A.M.; Dunn, M.R.; Forman, J. (2010). Diet and dietary variation of New Zealand hoki *Macruronus novaezelandiae*. *New Zealand Journal of Marine and Freshwater Research* 44: 289–308.
- Coombs, R.F.; Cordue, P.L. (1995). Evolution of a stock assessment tool: acoustic surveys of spawning hoki (*Macruronus novaezelandiae*) off the west coast of South Island, New Zealand, 1985–91. *New Zealand Journal of Marine and Freshwater Research* 29: 175–194.
- Coombs, R.F.; Macaulay, G.J.; Knol, W.; Porritt, G. (2003). Configurations and calibrations of 38 kHz fishery acoustic survey systems, 1991–2000. *New Zealand Fisheries Assessment Report 2003/49*. 24 p.

- Dibaboure, G.; Lauret, O.; Mertz, F.; Rosmorduc, V.; Maheu, C. (2009). SSALTO/DUACS User Handbook : (M)SLA and (M)ADT Near-Real Time and Delayed Time Products. CLS-DOS-NT-06.034, SALP-MU-P-EA-21065-CLS, Issue 1 rev 10. http://www.avis.oceanobs.com/fileadmin/documents/data/tools/hdbk_duacs.pdf
- Ducet, N.; Le Traon, P. Y.; Reverdin, G. (2000). Global high-resolution mapping of ocean circulation from TOPEX/Poseidon and ERS-1 and -2. *Journal of Geophysical Research* 105(C8): 19477-19498.
- Dunn, A. (2002). Updated catch-per-unit-effort indices for hoki (*Macruronus novaezelandiae*) on the west coast South Island, Cook Strait, Chatham Rise, and sub-Antarctic for the years 1990 to 2001. *New Zealand Fisheries Assessment Report 2002/47*. 51 p.
- Dunn, M.; Horn, P.; Connell, A.; Stevens, D.; Forman, J.; Pinkerton, M.; Griggs, L.; Notman, P.; Wood, B. (2009a). Ecosystem-scale trophic relationships: diet composition and guild structure of middle-depth fish on the Chatham Rise. Final Research Report for Ministry of Fisheries Research Project ZBD2004-02, Objectives 1–5. 351 p.
- Dunn, M.R.; Hurst, R.; Renwick, J.; Francis, C.; Devine, J.; Mckenzie, A. (2009b). Fish abundance and climate trends in New Zealand. *New Zealand Aquatic Environment and Biodiversity Report 31*: 73 p.
- Foote, K.G.; Knudsen, H.P.; Vestnes, G.; MacLennan, D.N.; Simmonds, E.J. (1987). Calibration of acoustic instruments for fish density estimation: a practical guide. *ICES Cooperative Research Report 144*. 68 p.
- Francis, R.I.C.C. (1981) Stratified random trawl surveys of deep-water demersal fish stocks around New Zealand. *Fisheries Research Division Occasional Publication 32*. 28 p.
- Francis, R.I.C.C. (1989). A standard approach to biomass estimation from bottom trawl surveys. New Zealand Fisheries Assessment Research Document 89/3. 4 p. (Unpublished report held in NIWA library, Wellington.)
- Francis, R.I.C.C. (1999). The impact of correlations in standardised CPUE indices. New Zealand Fisheries Assessment Research Document 99/42. 30 p. (Unpublished report held in NIWA library, Wellington.)
- Francis, R.I.C.C. (2006). Measuring the strength of environment-recruitment relationships: the importance of including predictor screening within cross-validations. *ICES Journal of Marine Science* 63: 594–599.
- Francis, R.I.C.C. (2009). SurvCalc User Manual. 39 p. (Unpublished report held at NIWA, Wellington.)
- Haase, P. (1995). Spatial pattern analysis in ecology based on Ripley's K-function: introduction and methods of edge correction. *Journal of Vegetation Science* 6: 575–582.
- Horn, P.L.; Dunn, M.R. (2010). Inter-annual variability in the diets of hoki, hake and ling on the Chatham Rise from 1990 to 2009. *New Zealand Aquatic Environment and Biodiversity Report 2010/54*. 56 p.
- Hurst, R.J.; Renwick, J.A.; Sutton, P.J.H.; Uddstrom, M.J.; Kennan, S.C.; Law, C.S.; Rickard, G.J.; Korpela, A.; Stewart, C.; Evans, J. (in press). Climate and Oceanographic trends relevant to New Zealand fisheries. *New Zealand Aquatic Environment and Biodiversity Report No. XX*. 204 p.
- Jolly, G.M.; Hampton, I. (1990). A stratified random transect design for acoustic surveys of fish stocks. *Canadian Journal of Fisheries and Aquatic Sciences* 47: 1282–1291.
- MacDonald, G.A.; Hall, B.I.; Vlieg, P. (2002). Seasonal changes in hoki (*Macruronus novaezelandiae*)-Implications for quality and yield. *Journal of Aquatic Food Product Technology* 11(2): 35-51.
- McClatchie, S.; Dunford, A. (2003). Estimated biomass of vertically migrating mesopelagic fish off New Zealand. *Deep Sea Research Part I* 50: 1263–1281.
- McClatchie, S.; Pinkerton, M.; Livingston, M.E. (2005). Relating the distribution of a semi-demersal fish, *Macruronus novaezelandiae*, to their pelagic food supply. *Deep-Sea Research Part I* 52: 1489–1501.
- McNeill, E. (2001). ESP2 phase 4 user documentation. NIWA Internal Report 105. 31 p. (Unpublished report held in NIWA library, Wellington.)

- O'Driscoll, R.L.; Bagley, N.W. (2004). Trawl survey of middle depth species in the Southland and Sub-Antarctic areas, November–December 2003 (TAN0317). *New Zealand Fisheries Assessment Report 2004/49*. 58 p.
- O'Driscoll, R.L.; Bagley, N.W. (2006). Trawl survey of middle depth species in the Southland and Sub-Antarctic areas, November–December 2004 (TAN0414). *New Zealand Fisheries Assessment Report 2006/2*. 60 p.
- O'Driscoll, R.L.; Bagley, N.W. (2009). Trawl survey of middle depth species in the Southland and Sub-Antarctic areas, November–December 2008 (TAN0813). *New Zealand Fisheries Assessment Report 2009/56*. 67 p.
- O'Driscoll, R. L.; Gauthier, S.; Devine, J. (2009). Acoustic surveys of mesopelagic fish: as clear as day and night? *ICES Journal of Marine Science* 66: 1310–1317.
- O'Driscoll, R.L.; Schneider, D.C.; Rose, G.A.; Lilly, G.R. (2000). Potential contact statistics for measuring scale-dependent spatial pattern and association: an example of northern cod (*Gadus morhua*) and capelin (*Mallotus villosus*). *Canadian Journal of Fisheries and Aquatic Sciences* 57: 1355–1368.
- R Development Core Team (2003). R: A language and environment for statistical computing. R Foundation for Statistical Computing, Vienna. <http://www.R-project.org>.
- Reynolds, R.W.; Smith, T.M.; Liu, C.; Chelton, D.B.; Casey, K.S.; Schlax, M.G. (2007). Daily high-resolution-blended analyses for sea surface temperature. *Journal of Climate* 20(22): 5473-5496.
- Robertson, D.A.; Roberts, P.E.; Wilson, J.B. (1978). Mesopelagic faunal transition across the subtropical convergence east of New Zealand. *New Zealand Journal of Marine and Freshwater Research* 12: 295–312.
- Simmonds, E.J.; MacLennan, D.N. (2005). *Fisheries acoustics theory and practice*. 2nd edition. Blackwell Science, Oxford. 437 p.
- Stevens, D.W.; O'Driscoll, R.L.; Horn, P.L. (2009). Trawl survey of hoki and middle depth species on the Chatham Rise, January 2009 (TAN0901). *New Zealand Fisheries Assessment Report 2009/55*. 91 p.
- Thomas, D., Franz, B. (2005). Overview of SeaWiFS Data Processing and Distribution, updated 21 July 2009. http://oceancolor.gsfc.nasa.gov/DOCS/SW_proc.html.
- Wood S.N. (2001). mgcv: GAMs and generalized ridge regression for R. *R News* 1: 20–25.
- Wood, S.N.; Augustin, N.H. (2002). GAMs with integrated model selection using penalized splines and applications to environmental modelling. *Ecological Modelling* 157: 157–177.

Table 1: Summary of acoustic data collection.

Area	Survey	Dates	“Year”	No. valid trawl stations	No. stations suitable acoustic data ^c	No. night-time acoustic recordings
Chatham Rise	TAN0101	28 Dec 2000 – 25 Jan 2001	2001	119	117	27
	TAN0201	5–25 Jan 2002	2002	107	102	26
	TAN0301	29 Dec 2002 – 21 Jan 2003	2003	115	117	22
	TAN0401 ^a	27 Dec 2003 – 23 Jan 2004	2004	110	0	0
	TAN0501	27 Dec 2004 – 23 Jan 2005	2005	106	86	24
	TAN0601	27 Dec 2005 – 23 Jan 2006	2006	96	88	17
	TAN0701	27 Dec 2006 – 23 Jan 2007	2007	101	100	22
	TAN0801	27 Dec 2007 – 23 Jan 2008	2008	101	103	23
	TAN0901	27 Dec 2008 – 23 Jan 2009	2009	108	105	23
	TAN0012	24 Nov – 24 Dec 2000	2001	103	97	20
Sub-Antarctic	TAN0118	19 Nov – 18 Dec 2001	2002	106	102	20
	TAN0219	23 Nov – 22 Dec 2002	2003	105	97	19
	TAN0317	11 Nov – 11 Dec 2003	2004	81	56	9
	TAN0414 ^b	24 Nov – 23 Dec 2004	2005	90	0	0
	TAN0515	24 Nov – 21 Dec 2005	2006	96	88	20
	TAN0617	24 Nov – 23 Dec 2006	2007	91	70	15
	TAN0714	24 Nov – 23 Dec 2007	2008	98	80	18
	TAN0813	24 Nov – 23 Dec 2008	2009	95	92	19

^a Acoustic data were not recorded on TAN0401 as this objective was not supported by MFish.

^b No suitable acoustic data were recorded on TAN0414 due to acoustic interference with another echosounder.

^c Number of stations with suitable acoustic data can exceed number of valid trawl stations as acoustic data was available from some tows where gear performance was unsuitable for estimation of trawl biomass

Table 2: Environmental variables available for this study.

Index no.	Category	Sub-category	Data or indices	Available from ENV2007-04 to:	Update or new development relevant to this study	Status
1	Climatic	Southern Oscillation Index (SOI)	Seasonal, annual	May 2008	September 2009	Updated
1	Climatic	Wind and pressure patterns (Kidson synoptic types, Trenberth indices)	Monthly	December 2007	September 2009	Updated
2	Oceanographic	Sea Surface Temperatures (SST)	i. Regional mean monthly anomalies	June 2008	January 2010	Updated
			ii. Monthly means and anomalies	June 2008	January 2010	
	Oceanographic	Sea Surface Temperatures (SST)	i. <i>Tangaroa</i> survey SST (from net-mounted CTD)	NA	Relevant surveys	Derived to January 2010
			ii. Comparable monthly SST indices for Chatham Rise and Sub-Antarctic, by up to 4 subareas	NA	New, proposed under this project	Derived to January 2010
3	Oceanographic	Sea surface height (SSH)	Comparable monthly SSH indices for Chatham Rise and Sub-Antarctic	NA	New, proposed under ENV2009-08	Derived to January 2009
4	Oceanographic	Ocean colour (Chl)	ii. Temporal and spatial Chl indices for Chatham Rise and Sub-Antarctic	NA	New, proposed under ENV2009-08	Derived to December 2009

Table 3: Mesopelagic indices for the Chatham Rise. Indices were derived by subtracting estimates of average backscatter that remains deeper than 200 m at night from estimates of average total daytime backscatter in each area (after O'Driscoll et al. 2009). Unstratified indices for the Chatham Rise were calculated as the unweighted average over all available acoustic data. Stratified indices were obtained as the weighted average of stratum estimates, where weighting was the proportional area of the stratum (northwest 11.3% of total area, southwest 18.7%, northeast 33.6%, southeast 36.4%).

Survey	Year	Unstratified				Northeast		Northwest		Southeast		Southwest		Stratified	
		Mean	c.v.	Mean	c.v.	Mean	c.v.	Mean	c.v.	Mean	c.v.	Mean	c.v.	Mean	c.v.
TAN0101	2001	46.3	11	21.5	22	60.6	17	37.2	16	94.1	18	45.2	9		
TAN0201	2002	36.8	9	25.6	20	39.6	17	35.3	20	55.2	15	36.2	10		
TAN0301	2003	43.7	12	34.3	31	30.9	17	58.2	22	58.6	14	47.1	13		
TAN0501	2005	29.5	11	28.1	19	44.6	25	25.7	14	24.6	44	28.4	12		
TAN0601	2006	37.7	10	30.7	17	47.6	19	41.1	17	35.5	26	37.3	10		
TAN0701	2007	32.1	10	25.1	16	42.1	15	28.3	19	36.3	26	30.3	10		
TAN0801	2008	28.4	9	17.2	14	27.8	43	39.8	12	33.1	17	29.6	9		
TAN0901	2009	46.9	13	24.9	37	56.2	18	40.6	19	89.4	20	46.2	12		
All		38.1	4	25.5	9.4	44.5	7	37.9	6	55.6	8	37.8	4		

Table 4: Estimates of the proportion of total day backscatter in each stratum and year on the Chatham Rise which is assumed to be mesopelagic fish ($p(meso)_{y,s}$). Estimates were derived from the observed proportion of night backscatter in the upper 200 m corrected for the proportion of backscatter estimated to be in the surface acoustic deadzone (see text for details).

Year	Stratum			
	Northeast	Northwest	Southeast	Southwest
2001	0.64	0.83	0.81	0.88
2002	0.58	0.78	0.66	0.86
2003	0.67	0.82	0.81	0.77
2005	0.72	0.83	0.73	0.69
2006	0.69	0.77	0.76	0.80
2007	0.67	0.85	0.73	0.80
2008	0.61	0.64	0.84	0.85
2009	0.58	0.75	0.83	0.86
All	0.64	0.80	0.77	0.84

Table 5: Estimates of the proportion of total day backscatter in each stratum and year in the Sub-Antarctic which is assumed to be mesopelagic fish ($p(200)_{y,s}$). Estimates were derived from the observed proportion of night backscatter in the upper 200 m with no correction for the surface acoustic deadzone (see text for details).

Year	Stratum		
	East	Puysegur	West
2001	0.64	0.66	0.58
2002	0.56	0.39	0.57
2003	0.54	0.77	0.60
2004	0.60	0.66	0.67
2006	0.59	0.38	0.54
2007	0.55	0.32	0.56
2008	0.56	0.46	0.51
2009	0.63	0.58	0.62
All	0.59	0.52	0.57

Table 6: Mesopelagic indices for the Sub-Antarctic. Indices were derived by multiplying daytime estimates of total backscatter by the estimated proportion of night backscatter in the upper 200 m (see Table 5) and calculating averages in each area (after O'Driscoll et al. 2009). Unstratified indices were calculated as the unweighted average over all available acoustic data. Stratified indices were obtained as the weighted average of stratum estimates, where weighting was the proportional area of the stratum (Puysegur 1.5% of total area, west 32.6%, east 65.9%).

Survey	Year	Unstratified			East		Puysegur		West		Stratified	
		Mean	c.v.		Mean	c.v.	Mean	c.v.	Mean	c.v.	Mean	c.v.
TAN0012	2001	14.1	9	10.8	12	28.8	10	12.6	17	11.6	10	
TAN0118	2002	13.3	17	9.2	16	29.9	45	13.1	11	10.8	10	
TAN0219	2003	10.4	12	6.8	13	31.2	28	9.0	7	7.9	8	
TAN0317	2004	9.8	10	8.1	23	18.9	15	9.2	8	8.6	14	
TAN0515	2006	8.0	7	7.8	10	6.0	7	8.7	12	8.0	8	
TAN0617	2007	4.5	6	4.8	10	3.4	13	4.7	9	4.7	7	
TAN0714	2008	6.4	8	5.7	15	7.3	12	6.2	12	5.9	11	
TAN0813	2009	9.9	11	7.0	12	13.3	12	12.3	23	8.9	12	
All		9.8	5	7.8	6	15.6	14	9.5	6	8.4	4	

Table 7: Hoki abundance indices for the Chatham Rise. Biomass indices were calculated based on trawl survey strata. Hoki catch rates are also summarised for each of the four acoustic strata.

Survey	Year	Biomass ('000 t)												Catch rate (kg/km ²)				
		< 60 cm			60–80 cm			>80 cm			Northeast		Northwest		Southeast		Southwest	
		Index	c.v.	All hoki	Index	c.v.	All hoki	Index	c.v.	All hoki	Mean	c.v.	Mean	c.v.	Mean	c.v.	Mean	c.v.
TAN0101	2001	60.3	10	26.6	17	27.1	11	6.6	8	367	21	523	25	547	20	467	22	
TAN0201	2002	74.4	11	23.8	25	43.2	14	7.3	10	723	25	588	27	538	20	643	43	
TAN0301	2003	52.6	9	30.8	18	16.2	10	5.5	10	315	15	783	47	289	15	790	22	
TAN0401	2004	52.7	13	18.7	26	28.5	15	5.5	8	305	24	199	44	398	24	366	25	
TAN0501	2005	84.6	12	50.9	14	26.1	13	7.5	13	495	20	1 311	35	846	19	809	31	
TAN0601	2006	99.2	11	53.0	17	39.4	11	6.8	13	599	30	860	36	660	17	988	20	
TAN0701	2007	70.5	8	38.0	13	26.2	10	6.5	7	307	13	863	27	555	18	878	26	
TAN0801	2008	76.9	11	39.6	20	30.0	9	7.3	6	397	20	967	35	580	17	2 021	71	
TAN0901	2009	144.1	11	84.4	16	46.7	9	12.4	11	693	23	1 693	24	884	15	2 239	22	
TAN1001	2010	97.5	15	44.8	21	40.5	16	12.2	15	490	22	888	34	604	21	1 163	32	
All										459	8	893	11	596	6	1 019	18	

Table 8: Hoki abundance indices for the Sub-Antarctic. Biomass indices were calculated based on trawl survey strata. Hoki catch rates are also summarised for each of the three acoustic strata.

Survey	Year	Biomass ('000 t)												Catch rate (kg/km ²)			
		< 60 cm			60–80 cm			> 80 cm			East		Puysegur		West		
		Index	c.v.	All hoki	Index	c.v.	All hoki	Index	c.v.	All hoki	Mean	c.v.	Mean	c.v.	Mean	c.v.	
TAN0012	2001	56.4	12	0.2	62	14.6	17	41.6	12	175	13	146	28	256	22		
TAN0118	2002	39.4	15	0.6	39	7.4	27	31.4	15	131	19	222	25	224	26		
TAN0219	2003	40.5	14	2.5	51	3.0	23	34.9	15	121	16	238	32	186	28		
TAN0317	2004	14.7	13	1.9	26	1.5	27	11.3	14	52	21	346	41	55	17		
TAN0414	2005	18.1	12	4.4	34	1.8	22	11.9	9	51	19	911	44	108	39		
TAN0515	2006	20.7	13	1.9	25	2.6	23	16.1	14	62	15	272	25	132	22		
TAN0617	2007	14.8	11	1.2	25	5.6	17	8.0	11	57	43	162	21	116	20		
TAN0714	2008	46.0	16	3.0	37	13.7	19	29.3	18	395	58	219	57	239	14		
TAN0813	2009	48.3	14	2.7	39	8.6	13	37.1	16	207	18	391	30	202	25		
TAN0911	2010	66.1	16	12.5	60	18.6	17	35.1	13	208	20	1 080	36	525	53		
All										149	16	395	17	205	14		

Table 9: Estimated length-weight parameters for hoki from Chatham Rise and Sub-Antarctic trawl surveys, and derived weight of a 75 cm fish (W(75 cm)), which was used as an index of somatic condition. $W = aL^b$ where W is weight (g) and L is length (cm).

Area	Survey	Year	LW parameters		W(75 cm) (g)
			a	b	
Chatham Rise	TAN0101	2001	0.004088	2.926636	1256
	TAN0201	2002	0.003959	2.941069	1295
	TAN0301	2003	0.003463	2.967778	1271
	TAN0401	2004	0.002895	3.003977	1242
	TAN0501	2005	0.003572	2.948285	1205
	TAN0601	2006	0.004478	2.904336	1250
	TAN0701	2007	0.003930	2.933382	1244
	TAN0801	2008	0.003118	2.988453	1251
	TAN0901	2009	0.004304	2.914802	1257
	TAN1001	2010	0.004210	2.916284	1237
		ALL			1251
Sub-Antarctic	TAN0012	2001	0.005603	2.844446	1208
	TAN0118	2002	0.005681	2.842391	1214
	TAN0219	2003	0.004172	2.914928	1219
	TAN0317	2004	0.003975	2.922135	1198
	TAN0414	2005	0.003785	2.933285	1197
	TAN0515	2006	0.005824	2.840234	1233
	TAN0617	2007	0.004363	2.903530	1214
	TAN0714	2008	0.004172	2.914241	1215
	TAN0813	2009	0.005024	2.871200	1215
	TAN0911	2010	0.004245	2.906240	1195
		ALL			1211

Table 10: Hoki liver condition indices for the Chatham Rise and each of the four acoustic strata.

Survey	Year	Chatham Rise		Northeast		Northwest		Southeast		Liver condition index	
		Mean	c.v.	Mean	c.v.	Mean	c.v.	Mean	c.v.	Mean	c.v.
TAN0401	2004	2.89	1.6	2.88	2.4	2.73	5.0	3.04	3.1	2.79	3.5
TAN0501	2005	3.78	1.3	3.62	1.8	3.66	9.8	3.81	2.3	4.20	3.0
TAN0601	2006	3.69	1.2	3.71	1.8	3.67	5.0	3.90	2.0	3.32	2.5
TAN0701	2007	3.50	1.2	3.36	1.8	3.59	2.6	3.60	2.3	3.65	3.1
TAN0801	2008	3.57	1.0	3.28	1.6	3.39	2.8	4.03	2.1	3.67	2.1
TAN0901	2009	3.33	1.1	3.03	1.6	3.55	2.4	3.50	2.2	3.54	2.6
TAN1001	2010	3.10	1.0	3.09	1.7	3.13	2.1	3.06	2.1	3.13	2.8
All		3.41	0.4	3.27	0.7	3.34	1.2	3.59	0.9	3.49	1.1

Table 11: Hoki liver condition indices for the Sub-Antarctic and each of the three acoustic strata.

Survey	Year	Sub-Antarctic		East		Puysegur		West		Liver condition index	
		Mean	c.v.	Mean	c.v.	Mean	c.v.	Mean	c.v.	Mean	c.v.
TAN0118	2002	2.94	1.7	3.45	2.3	2.48	3.8	2.49	2.8	2.49	2.8
TAN0219	2003	2.73	1.8	3.11	2.9	1.99	3.5	2.68	2.6	2.68	2.6
TAN0317	2004	2.76	2.2	3.17	3.4	2.24	5.6	2.55	3.0	2.55	3.0
TAN0414	2005	3.07	2.0	3.45	3.3	2.28	5.9	2.99	2.8	2.99	2.8
TAN0515	2006	3.10	1.6	3.20	2.6	2.27	3.9	3.36	2.4	3.36	2.4
TAN0617	2007	2.88	1.7	3.01	3.4	2.27	4.3	3.02	2.2	3.02	2.2
TAN0714	2008	3.15	1.6	3.42	2.5	2.07	4.5	3.34	2.1	3.34	2.1
TAN0813	2009	2.63	1.6	2.96	2.2	1.87	4.7	2.58	2.6	2.58	2.6
TAN0911	2010	2.49	1.7	2.74	2.5	1.96	5.5	2.34	2.5	2.34	2.5
All		2.85	0.6	3.16	0.9	2.16	1.5	2.82	0.9	2.82	0.9

Table 12: Variables retained in GLM analysis of LCI for each model and corresponding total R² values.

Model	Variable	R ²
Chatham Rise	<i>year</i>	3.57
	<i>fish length</i>	4.86
	<i>start latitude</i>	5.87
Sub-Antarctic	<i>year</i>	1.43
	<i>start longitude</i>	5.56
	<i>gonad stage</i>	7.10
	<i>start latitude</i>	8.10

Table 13: Temperature data from CTD measurements for the Chatham Rise and each of the four acoustic strata.

Survey	Year	Chatham Rise		Northeast		Northwest		Southeast		Mean temperature (°C)	
		Surface	Bottom	Surface	Bottom	Surface	Bottom	Surface	Bottom	Surface	Bottom
TAN0301	2003	15.4	8.2	15.4	8.4	15.5	8.6	15.5	8.1	15.2	7.7
TAN0401	2004	15.7	8.1	15.8	8.5	16.4	8.1	15.7	8.0	15.3	7.7
TAN0501	2005	13.7	8.2	13.7	8.3	14.8	8.8	13.0	8.0	13.9	7.6
TAN0601	2006	15.5	8.0	16.1	8.3	15.6	8.3	15.4	8.0	14.6	7.5
TAN0701	2007	14.3	8.2	14.7	8.9	14.5	7.9	13.6	7.8	13.7	7.8
TAN0801	2008	15.9	8.1	16.4	8.1	16.8	8.5	15.5	8.4	15.0	7.6
TAN0901	2009	16.4	8.2	16.9	8.5	16.6	8.6	16.0	7.9	15.7	7.5
TAN1001	2010	14.1	8.1	14.0	8.2	15.4	8.4	13.6	8.1	13.1	7.7
All		15.1	8.2	15.4	8.4	15.5	8.4	14.7	8.1	14.6	7.6

Table 14: Temperature data from CTD measurements for the Sub-Antarctic and each of the three acoustic strata.

Survey	Year	Sub-Antarctic		East		Puysegur		West		Mean temperature (°C)	
		Surface	Bottom	Surface	Bottom	Surface	Bottom	Surface	Bottom	Surface	Bottom
TAN0219	2003	10.3	6.7	9.4	6.0	12.8	6.9	10.4	7.1	10.4	7.1
TAN0317	2004	8.8	6.9	8.3	6.4	11.6	8.1	8.6	7.2	8.6	7.2
TAN0414	2005	9.3	7.0	8.7	6.5	11.3	7.3	9.0	7.4	9.0	7.4
TAN0515	2006	10.5	6.8	9.3	6.4	14.3	7.4	10.3	7.1	10.3	7.1
TAN0617	2007	9.2	6.9	8.4	6.4	11.6	7.4	8.8	7.2	8.8	7.2
TAN0714	2008	9.5	6.7	8.6	6.1	12.3	7.1	9.4	7.2	9.4	7.2
TAN0813	2009	9.4	6.9	8.7	6.5	12.4	7.4	9.4	7.3	9.4	7.3
TAN0911	2010	9.0	7.0	8.1	6.5	11.6	7.1	9.2	7.4	9.2	7.4
All		9.5	6.9	8.6	6.4	12.3	7.3	8.9	7.2	8.9	7.2

Table 15: Estimated spatial scales at which we detected significant positive associations between hoki and mesopelagic fish (see Figures 42 and 43). NS indicates no significant positive association was observed.

Area	Survey	Year	Scale, t (km)		
			Minimum	Maximum	Peak
Chatham Rise	TAN0101	2001	10	30	10
	TAN0201	2002		NS	
	TAN0301	2003	30	510	30
	TAN0501	2005	10	50	20
	TAN0601	2006	10	250	10
	TAN0701	2007	10	480	10
	TAN0801	2008	180	320	200
	TAN0901	2009	10	720	10
	Sub-Antarctic	TAN0012	2001		NS
TAN0118		2002		NS	
TAN0219		2003	180	560	200
TAN0317		2004	100	270	100
TAN0515		2006		NS	
TAN0617		2007		NS	
TAN0714		2008	10	30	10
TAN0813		2009	10	350	10

Table 16: Probability of no significant relationship between Chatham Rise total mesopelagic biomass and environmental or biotic estimates with no annual time lag using S, Spearman’s rank correlation, and A, association test, for the entire Chatham Rise (ALL), and subsets of the Chatham Rise as defined in the text (NE, NW, SE, SW). The probabilities are reported to two significant figures. The shading indicates significant relationships, at the 5% (0.05) level.

	ALL		NE		NW		SE		SW	
	S	A	S	A	S	A	S	A	S	A
Hoki	0.57	0.25	0.96	1	0.96	0.25	0.74	1	0.42	0.25
LCI	0.19	0.05	0.037	0.05	0.82	0.05	0.87	0.05	0.19	0.2
CTD.Surf	0.4	0.033	0.33	0.033	0.96	0.033	0.27	0.033	0.21	0.033
CTD.Bot	0.54	0.17	0.79	0.033	0.96	0.033	0.7	0.033	0.79	0.033
SST	0.96	0.25	0.78	1	0.57	0.25	0.1	1	0.42	0.25
SSH	0.071	0.071	0.002	1	0.65	0.25	0.61	1	0.35	0.25
CHL	0.71	0.071	0.4	0.071	0.43	0.071	0.4	0.25	0.73	0.25
Z1	0.78	0.071	0.82	0.25	0.49	0.25	0.74	0.071	0.69	0.071
Z2	0.82	0.071	0.023	1	0.76	0.036	0.84	0.25	0.45	0.012
Z3	0.39	0.071	0.49	0.25	0.29	0.25	1	0.071	0.21	0.071
Z4	0.78	0.012	0.23	0.071	0.78	0.071	0.32	0.071	0.82	0.071
M1	0.39	0.012	0.65	0.071	0.65	0.071	0.29	0.25	0.46	0.071
M2	0.87	0.071	0.29	0.012	0.82	0.071	1	0.036	0.87	0.071
M3	0.18	0.012	0.87	0.071	0.96	0.071	0.015	0.071	0.57	0.012
ZN	0.73	0.012	0.96	0.25	0.73	0.25	0.32	0.071	0.96	0.071
ZS	0.047	0.071	0.29	1	0.49	0.036	0.16	1	0.028	0.036
MZ1	0.82	0.012	0.26	1	0.32	0.012	0.35	1	0.49	0.036
MZ2	0.18	0.071	0.23	1	0.57	0.036	0.53	0.25	0.071	0.012
MZ3	0.87	0.071	0.35	0.036	0.82	0.25	0.78	0.012	1	0.25
MZ4	0.69	0.012	0.73	0.25	0.91	0.25	0.2	0.012	0.93	0.071
Trough	0.96	0.25	0.32	1	0.46	0.25	0.46	0.25	0.87	0.25
Zonal	0.82	0.25	0.74	0.071	0.61	0.25	0.78	0.25	0.61	0.25
Blocking	0.65	0.25	0.23	1	0.35	0.25	0.46	1	0.46	0.25
IPO	0.69	0.071	0.49	0.25	0.78	0.012	0.74	0.25	0.46	0.012
SOI	0.53	0.25	0.12	1	0.21	0.012	0.49	1	0.35	0.036

Table 17: Probability of no significant relationship between Chatham Rise total mesopelagic biomass and environmental or biotic estimates with a one year annual time lag using S, Spearman's rank correlation, and A, association test, for the entire Chatham Rise (ALL), and subsets of the Chatham Rise as defined in the text (NE, NW, SE, SW). The probabilities are reported to two significant figures. The shading indicates significant relationships, at the 5% (0.05) level.

	ALL		NE		NW		SE		SW	
	S	A	S	A	S	A	S	A	S	A
Hoki	0.16	0.012	0.01	0.071	0.69	0.071	0.57	0.036	0.18	0.071
LCI	0.042	0.17	0.87	0.17	0.79	0.033	0.072	0.17	0.47	0.033
CTD.Surf	0.29	0.14	0.53	0.14	0.094	0.14	1	0.14	0.7	0.024
CTD.Bot	0.43	1	0.48	0.024	0.34	0.14	0.25	1	0.25	0.14
SST	0.036	1	0.53	0.071	0.028	0.071	1	0.071	0.14	0.012
SSH	0.32	0.071	0.64	0.14	0.014	0.14	0.53	1	0.43	1
CHL	0.43	1	0.23	0.14	0.43	0.14	0.43	1	0.85	1
Z1	0.82	1	1	0.14	0.15	0.14	0.25	1	0.43	1
Z2	0.78	1	0.88	0.14	0.12	0.14	0.64	1	0.64	1
Z3	1	1	0.82	0.14	0.12	0.14	0.12	1	0.48	1
Z4	0.38	0.14	0.071	0.14	0.7	0.14	0.38	0.14	0.88	0.14
M1	0.38	0.024	0.052	0.14	0.76	0.14	0.59	1	0.76	1
M2	0.64	1	0.25	0.14	0.94	0.024	0.59	1	0.48	0.14
M3	0.071	0.024	0.43	0.14	0.12	0.14	0.43	1	0.18	1
ZN	0.88	0.14	0.53	0.14	0.43	0.14	0.29	1	0.64	1
ZS	0.94	1	0.94	0.14	0.00045	0.14	0.34	1	0.82	1
MZ1	0.88	1	0.12	0.14	0.94	0.14	0.88	1	0.59	1
MZ2	0.78	1	0.76	0.14	0.0068	0.14	0.22	1	0.82	1
MZ3	0.38	0.14	0.53	0.14	1	0.14	0.82	1	0.15	1
MZ4	0.16	0.14	0.27	0.14	0.61	0.14	0.021	1	0.61	1
Trough	0.78	0.14	0.48	0.14	0.34	0.14	0.48	0.14	0.94	0.14
Zonal	0.88	1	0.38	0.14	0.43	0.14	0.18	1	0.22	1
Blocking	0.48	1	0.48	0.14	0.94	0.14	0.76	1	0.094	1
IPO	0.18	1	0.64	0.14	0.34	0.14	1	1	0.071	1
SOI	0.15	1	0.094	0.14	0.43	0.14	0.38	1	0.43	1

Table 18: Probability of no significant relationship between Chatham Rise total mesopelagic biomass and environmental or biotic estimates with a two year annual time lag using S, Spearman’s rank correlation, and A, association test, for the entire Chatham Rise (ALL), and subsets of the Chatham Rise as defined in the text (NE, NW, SE, SW). The probabilities are reported to two significant figures. The shading indicates significant relationships, at the 5% (0.05) level.

	ALL		NE		NW		SE		SW	
	S	A	S	A	S	A	S	A	S	A
Hoki	0.59	1	1	0.14	0.64	0.14	0.64	1	0.22	1
LCI	0.33	0.17	0.11	0.17	0.79	0.033	0.4	1	0.79	0.17
CTD.Surf	0.82	1	0.82	0.14	0.48	0.14	0.25	1	0.22	1
CTD.Bot	0.7	0.14	0.88	0.14	0.88	0.14	0.036	1	0.76	1
SST	0.62	0.033	0.38	0.14	0.53	0.14	0.34	1	0.22	0.14
SSH	1	1	0.87	0.033	0.87	1	0.4	0.17	0.27	0.17
CHL	0.68	0.17	0.5	0.17	0.91	1	0.46	0.17	0.42	0.17
Z1	0.4	0.033	0.7	1	0.61	0.17	0.27	0.17	0.79	0.17
Z2	0.33	0.17	0.87	0.033	0.62	1	0.62	0.033	0.21	0.17
Z3	0.072	0.033	0.27	1	0.79	0.17	0.019	0.17	0.62	0.17
Z4	0.96	0.17	0.79	1	0.7	0.17	0.7	0.17	0.87	0.17
M1	0.87	0.17	0.54	1	0.87	1	0.96	0.17	0.96	0.17
M2	0.54	0.17	0.96	1	0.33	1	0.79	0.17	0.62	0.17
M3	0.47	0.17	0.4	1	0.62	0.17	0.62	0.17	0.62	0.033
ZN	0.87	0.17	0.87	1	0.79	0.17	0.62	0.17	0.96	0.17
ZS	0.47	0.033	0.072	0.17	0.79	1	0.4	0.17	0.87	0.17
MZ1	0.96	0.033	0.47	1	0.21	1	0.7	0.17	0.79	0.17
MZ2	0.47	0.033	0.072	0.17	0.79	1	0.4	0.17	0.87	0.17
MZ3	0.87	0.17	0.87	1	0.54	1	0.62	0.17	0.96	0.17
MZ4	0.79	0.17	0.47	1	0.21	0.033	0.96	0.17	0.7	0.033
Trough	0.33	0.17	0.87	1	0.62	0.033	0.62	0.17	0.16	0.033
Zonal	0.072	0.17	0.79	1	0.47	0.17	0.042	0.17	0.4	0.17
Blocking	0.96	0.033	0.62	0.033	0.33	1	0.87	0.033	0.87	0.17
IPO	0.33	0.17	0.62	1	0.87	1	0.62	0.17	0.11	0.17
SOI	0.96	0.17	0.96	1	0.7	1	0.79	0.17	0.87	0.17

Table 19: Probability of no significant relationship between Sub-Antarctic total mesopelagic biomass and environmental or biotic estimates with no annual time lag using S, Spearman’s rank correlation, and A, association test, for the entire Sub-Antarctic (ALL), and subsets of the Sub-Antarctic as defined in the text (PUYSEGUR, EAST, WEST). The probabilities are reported to two significant figures. The shading indicates significant relationships, at the 5% (0.05) level.

	ALL		PUYSEGUR		EAST		WEST	
	S	A	S	A	S	A	S	A
Hoki	0.29	0.071	0.91	0.25	1	0.25	0.29	0.071
LCI	0.53	1	0.64	1	0.29	0.14	0.023	1
CTD.Surf	0.87	1	0.96	1	0.96	1	0.079	1
CTD.Bot	0.27	1	0.87	1	0.21	1	0.27	0.17
SST	0.12	0.012	0.42	0.25	0.14	0.012	0.028	0.0024
SSH	0.38	1	0.53	1	0.34	1	0.34	1
CHL	0.1	0.036	0.18	1	0.16	0.036	0.028	0.071
Z1	0.7	1	0.53	1	0.7	1	0.64	1
Z2	0.052	1	0.88	0.14	0.052	1	0.12	1
Z3	0.53	1	0.88	1	0.53	1	0.64	1
Z4	0.43	0.14	0.64	0.14	0.43	0.14	0.38	0.14
M1	0.88	1	0.88	1	0.88	1	0.82	1
M2	0.7	1	0.76	1	0.7	1	0.48	0.14
M3	0.38	1	0.59	1	0.38	1	0.38	1
ZN	0.82	1	1	1	0.82	1	0.76	1
ZS	0.34	1	0.64	1	0.34	1	0.59	1
MZ1	0.94	0.14	0.76	1	0.94	0.14	0.76	1
MZ2	0.34	1	0.64	1	0.34	1	0.59	1
MZ3	0.82	1	1	1	0.82	1	0.7	1
MZ4	0.76	1	0.88	1	0.76	1	0.64	1
Trough	0.052	0.14	0.25	0.14	0.052	0.14	0.052	0.14
Zonal	0.48	1	1	1	0.48	1	0.53	1
Blocking	0.48	1	0.88	1	0.48	1	0.48	1
IPO	0.16	0.012	0.058	0.25	0.047	0.012	0.14	0.012
SOI	0.052	1	0.43	1	0.052	1	0.036	1

Table 20: Probability of no significant relationship between Sub-Antarctic total mesopelagic biomass and environmental or biotic estimates with a one year annual time lag using S, Spearman’s rank correlation, and A, association test, for the entire Sub-Antarctic (ALL), and subsets of the Sub-Antarctic as defined in the text (PUYSEGUR, EAST, WEST). The probabilities are reported to two significant figures. The shading indicates significant relationships, at the 5% (0.05) level.

	ALL		PUYSEGUR		EAST		WEST	
	S	A	S	A	S	A	S	A
Hoki	0.96	0.25	0.46	0.25	0.26	0.25	1	0.25
LCI	0.65	0.036	0.61	0.25	0.42	0.012	0.16	0.25
CTD.Surf	1	0.14	0.53	0.024	0.34	0.14	0.82	0.14
CTD.Bot	0.76	0.14	0.7	0.14	0.64	0.14	0.88	0.14
SST	0.43	0.024	0.43	0.14	0.64	0.024	0.094	0.14
SSH	0.62	0.17	0.072	0.17	0.7	0.17	0.33	0.17
CHL	1	0.14	0.22	0.14	1	0.14	0.88	0.14
Z1	0.33	0.17	0.96	0.033	0.33	0.17	0.47	0.17
Z2	0.62	0.17	0.87	0.17	0.62	0.17	0.87	0.17
Z3	0.87	0.17	0.79	0.033	0.87	0.17	0.87	0.17
Z4	0.79	0.17	0.072	0.17	0.79	0.17	0.47	0.17
M1	0.7	0.17	0.072	0.17	0.7	0.17	0.54	0.17
M2	0.21	0.17	0.072	0.17	0.21	0.17	0.21	0.17
M3	0.79	0.17	0.042	0.17	0.79	0.17	0.47	0.17
ZN	0.87	0.17	0.11	0.17	0.87	0.17	0.62	0.17
ZS	0.87	0.17	0.54	0.033	0.87	0.17	0.87	0.17
MZ1	0.0048	0.17	0.62	0.033	0.0048	0.17	0.072	0.17
MZ2	0.87	0.17	0.54	0.033	0.87	0.17	0.87	0.17
MZ3	0.4	0.17	0.16	0.17	0.4	0.17	0.4	0.17
MZ4	0.87	0.17	0.11	0.17	0.87	0.17	0.62	0.17
Trough	0.96	0.17	0.27	0.17	0.96	0.17	0.79	0.17
Zonal	0.87	0.17	0.54	0.17	0.87	0.17	0.62	0.17
Blocking	0.87	0.17	0.27	0.17	0.87	0.17	0.87	0.033
IPO	0.014	0.14	0.052	0.14	0.014	0.14	0.0068	0.14
SOI	0.16	0.17	0.042	0.033	0.16	0.17	0.11	0.17

Table 21: Probability of no significant relationship between Sub-Antarctic total mesopelagic biomass and environmental or biotic estimates with a two year annual time lag using S, Spearman’s rank correlation, and A, association test, for the entire Sub-Antarctic (ALL), and subsets of the Sub-Antarctic as defined in the text (PUYSEGUR, EAST, WEST). The probabilities are reported to two significant figures. The shading indicates significant relationships, at the 5% (0.05) level.

	ALL		PUYSEGUR		EAST		WEST	
	S	A	S	A	S	A	S	A
Hoki	0.15	0.14	0.76	0.14	0.48	0.14	0.052	0.14
LCI	0.43	0.14	0.052	0.14	0.59	0.14	0.76	0.14
CTD.Surf	0.53	1	0.29	1	0.34	0.024	0.88	1
CTD.Bot	0.18	1	0.88	1	0.023	1	0.22	1
SST	0.47	0.17	0.79	0.033	0.21	0.17	0.87	0.17
SSH	0.75	0.05	1	0.05	1	0.05	0.19	0.05
CHL	0.87	0.17	0.79	0.033	0.54	0.17	0.87	0.17
Z1	0.87	0.2	0.1	0.05	0.87	0.2	0.87	0.05
Z2	0.28	0.2	0.19	0.05	0.28	0.2	1	0.05
Z3	0.87	0.05	0	0.05	0.87	0.05	0.5	0.05
Z4	0.19	0.2	0.87	0.05	0.19	0.2	0.1	0.05
M1	0.28	0.2	0.62	0.05	0.28	0.2	0.28	0.05
M2	0.39	0.2	0.87	0.05	0.39	0.2	0.19	0.05
M3	0.19	0.2	0.87	0.05	0.19	0.2	0.1	0.05
ZN	0.28	0.2	0.62	0.05	0.28	0.2	0.28	0.05
ZS	0.62	0.05	0.037	0.05	0.62	0.05	0.62	0.05
MZ1	0.62	0.05	0.28	0.05	0.62	0.05	1	0.05
MZ2	0.62	0.05	0.037	0.05	0.62	0.05	0.62	0.05
MZ3	0.28	0.2	0.62	0.05	0.28	0.2	0.28	0.05
MZ4	0.19	0.2	0.87	0.05	0.19	0.2	0.1	0.05
Trough	0.75	0.2	0.28	0.05	0.75	0.2	0.75	0.05
Zonal	0.39	0.2	0.19	0.05	0.39	0.2	0.87	0.05
Blocking	0.5	0.2	0.62	0.05	0.5	0.2	0.39	0.05
IPO	0.042	0.17	0.072	0.033	0.042	0.17	0.019	0.17
SOI	0.28	0.05	0.62	0.05	0.28	0.05	0.037	0.05

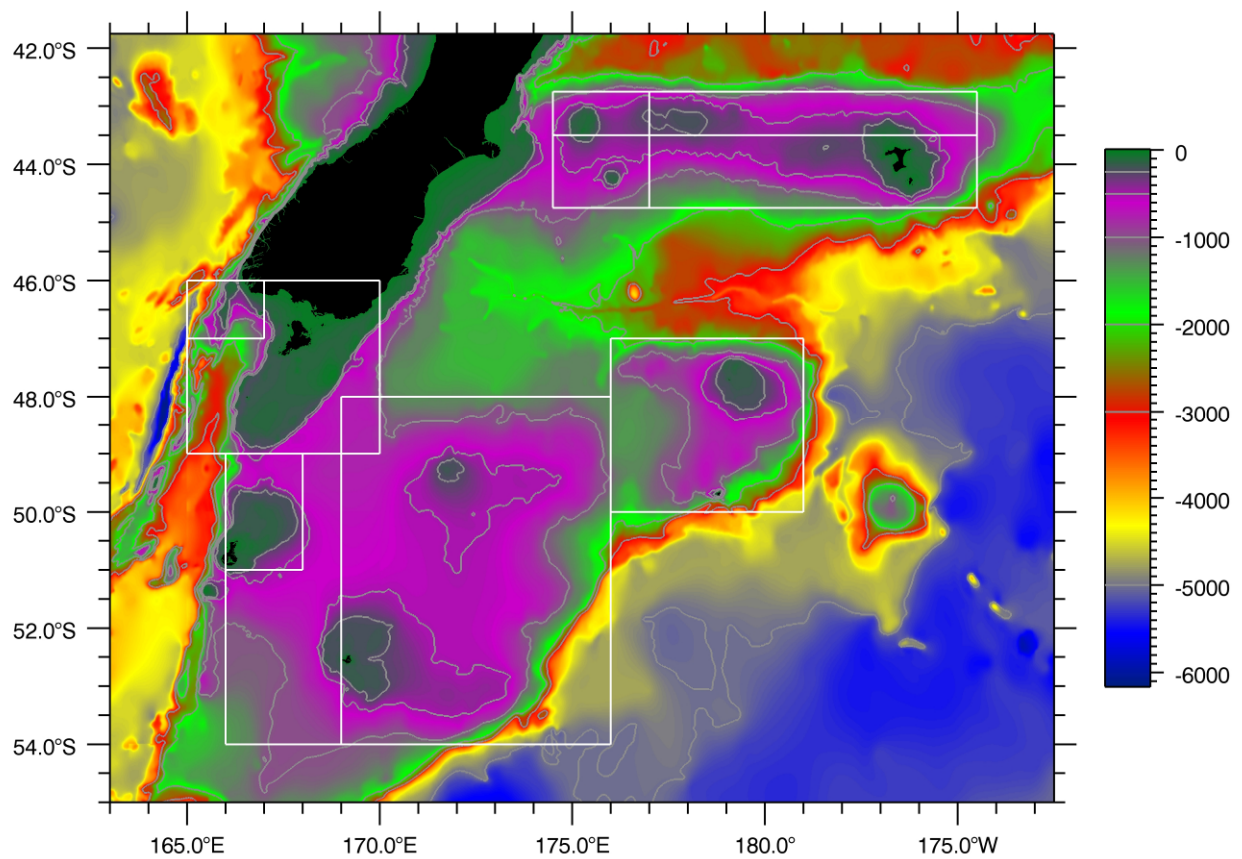


Figure 1: Areas for which SST, SSH and chlorophyll indices were derived: Anticlockwise from top left hand corner: Chatham Rise: northwest, southwest, southeast, northeast; Sub-Antarctic: Puysegur, Snares, Auckland, west Sub-Antarctic, east Sub-Antarctic, Bounty. Colours represent bathymetry (in metres). Acoustic indices were derived for the same four sub-areas on the Chatham Rise and three slightly broader areas on the Sub-Antarctic (see area definitions in text).

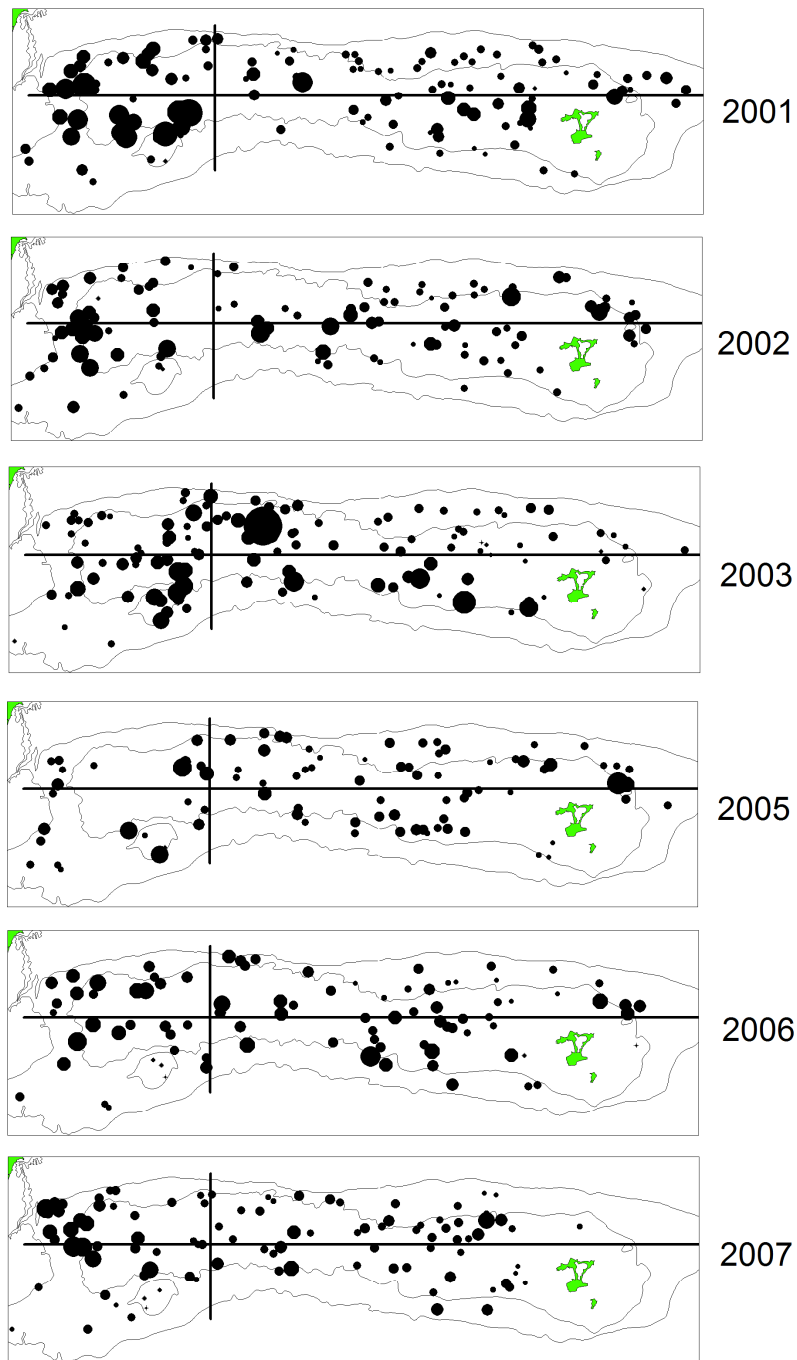


Figure 2: Spatial distribution of total acoustic backscatter on the Chatham Rise observed during day trawl stations. Circle area is proportional to the acoustic backscatter (maximum symbol size = $500 \text{ m}^2/\text{km}^2$). Lines separate the four acoustic strata.

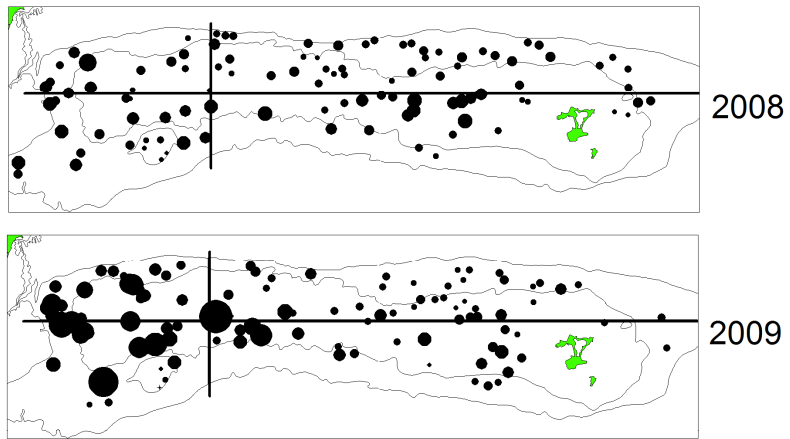


Figure 2 continued: Spatial distribution of total acoustic backscatter on the Chatham Rise observed during day trawl stations. Circle area is proportional to the acoustic backscatter (maximum symbol size = $500 \text{ m}^2/\text{km}^2$). Lines separate the four acoustic strata.

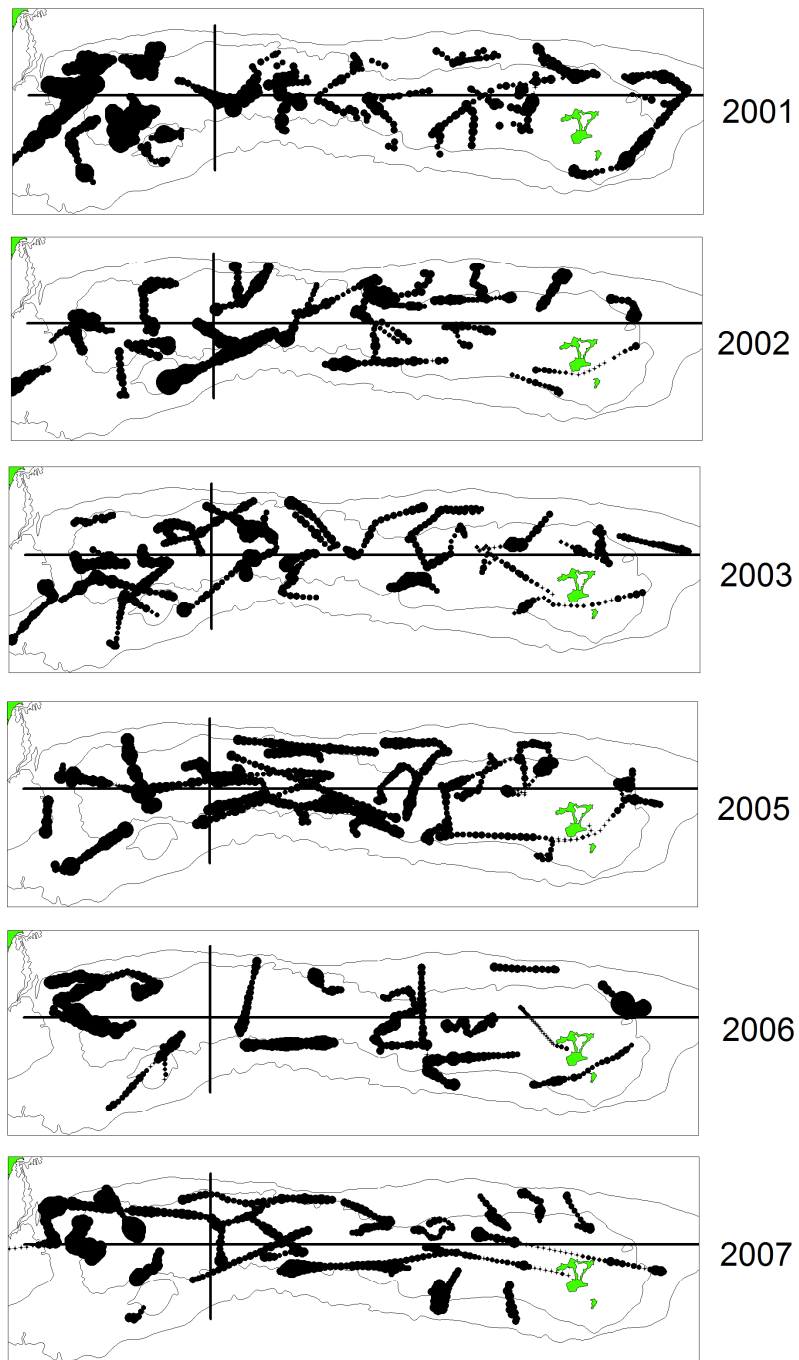


Figure 3: Spatial distribution of total acoustic backscatter on the Chatham Rise observed during night transects. Circle area is proportional to the acoustic backscatter (maximum symbol size = $500 \text{ m}^2/\text{km}^2$). Lines separate the four acoustic strata.

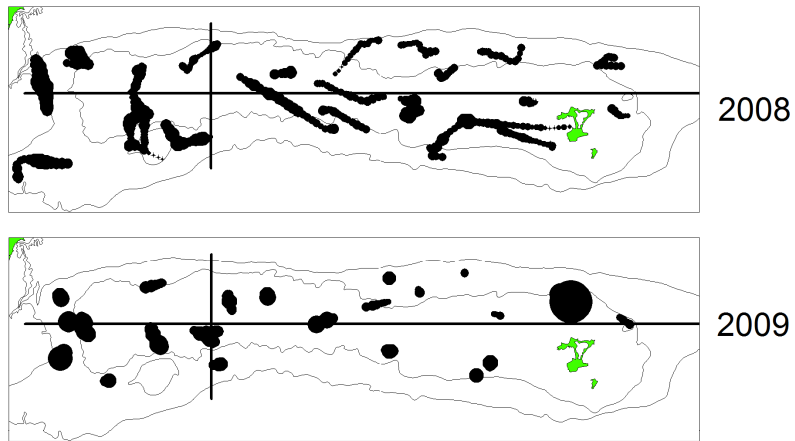


Figure 3 continued: Spatial distribution of total acoustic backscatter on the Chatham Rise observed during night transects. Circle area is proportional to the acoustic backscatter (maximum symbol size = $500 \text{ m}^2/\text{km}^2$). Lines separate the four acoustic strata.

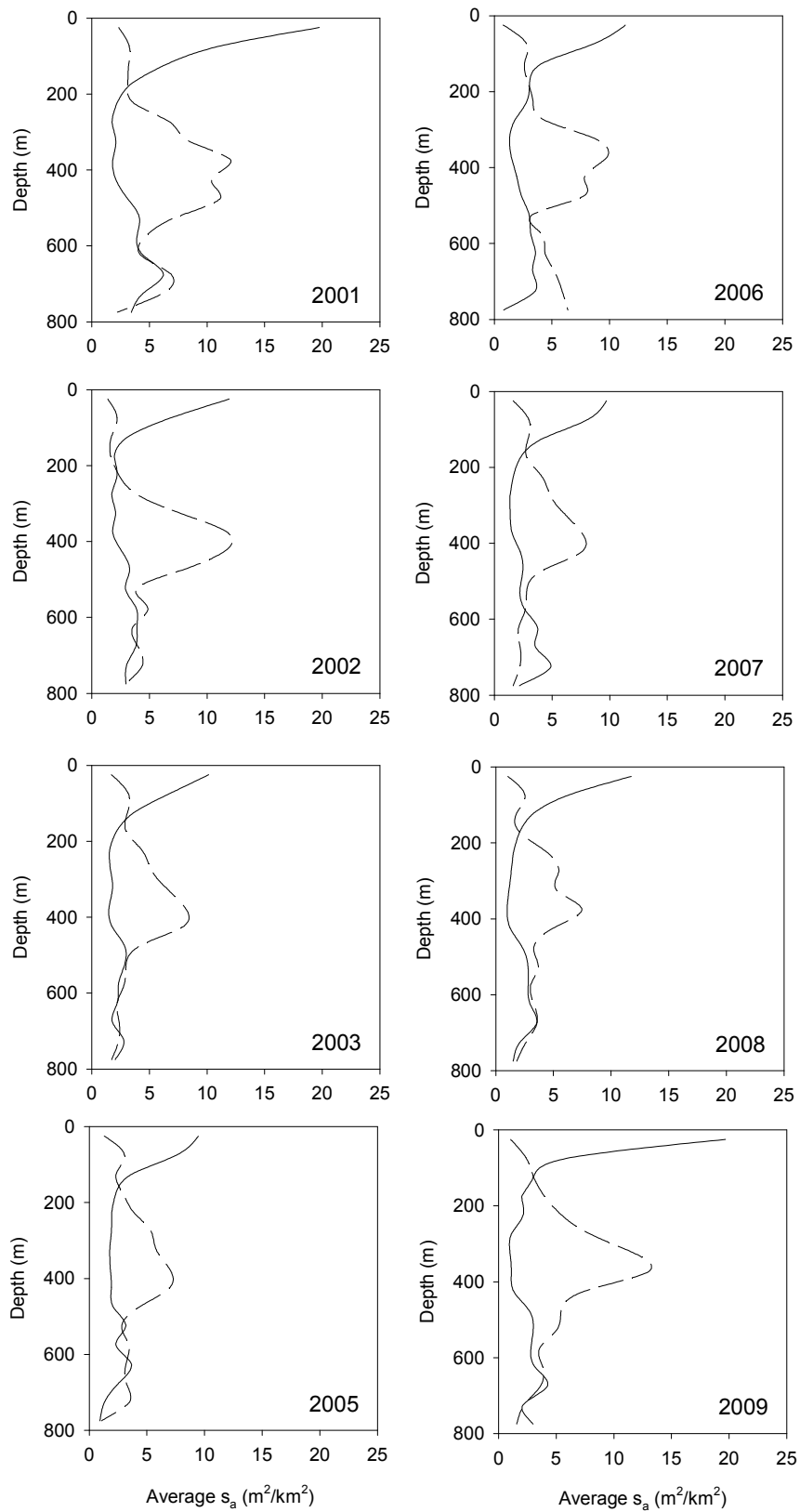


Figure 4: Vertical distribution of total acoustic backscatter integrated in 50 m depth bins on the Chatham Rise observed during the day (dashed lines) and at night (solid lines) in 2001–09.

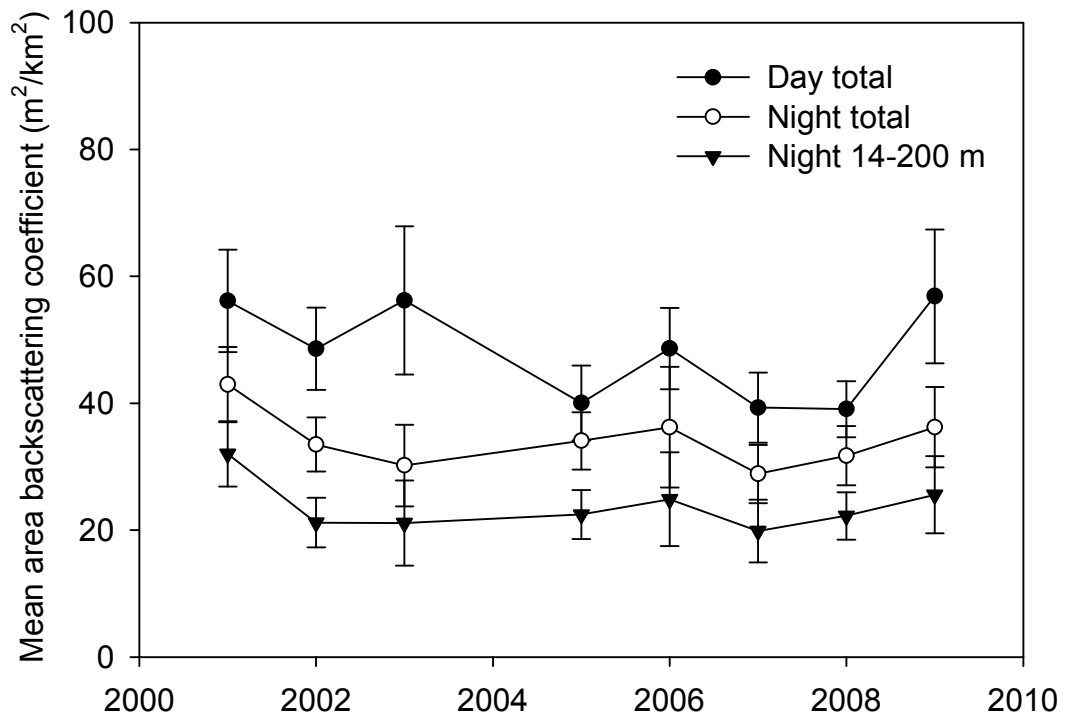


Figure 5: Total acoustic abundance indices for the Chatham Rise based on (strata-averaged) mean areal backscatter (sa). Error bars are ± 2 standard errors.

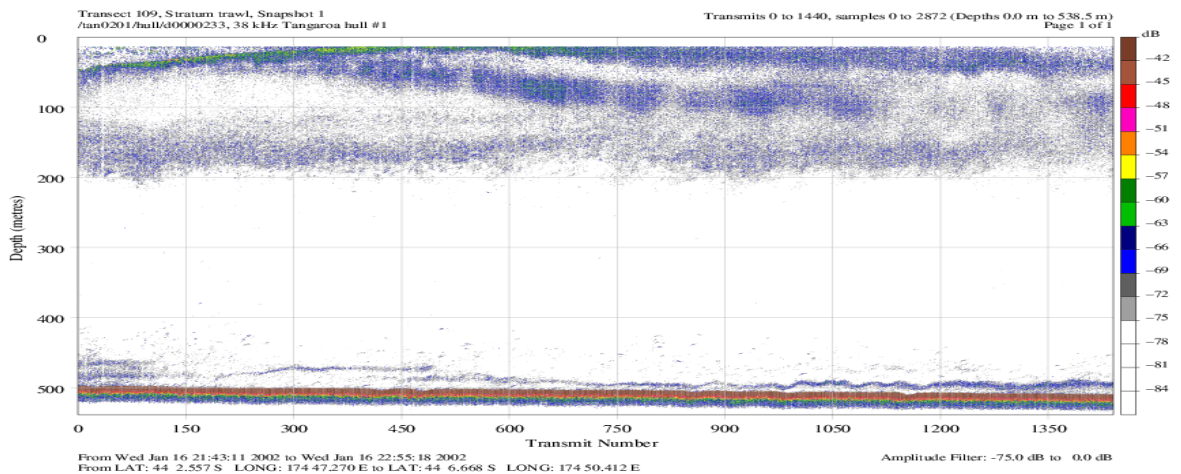
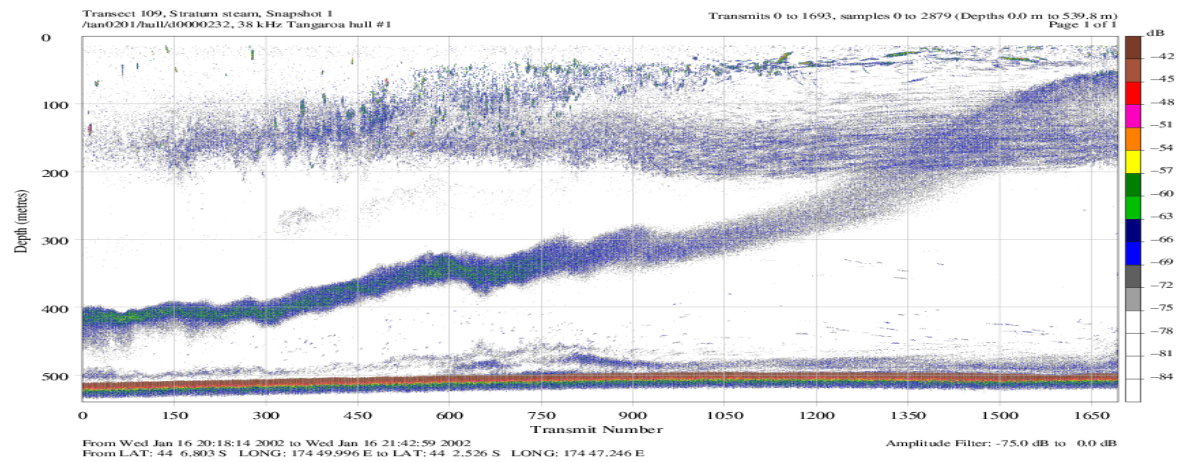
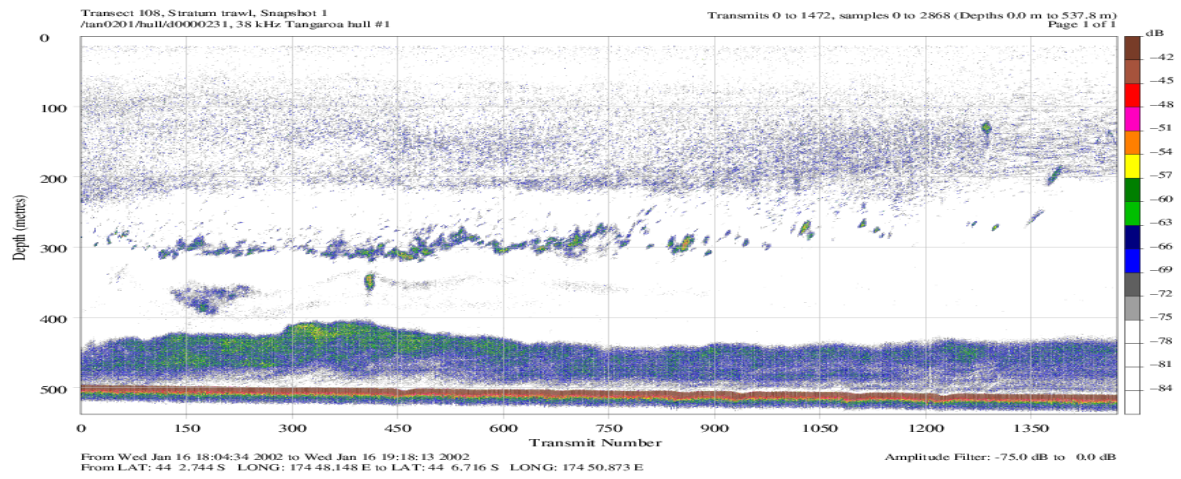


Figure 6: Series of repeated transects over the same area in daylight (17:04–18:18 NZST), at dusk (19:18–20:42) and at night (20:43–21:55) showing ascension of mesopelagic layers on the Chatham Rise (from O’Driscoll et al. 2009).

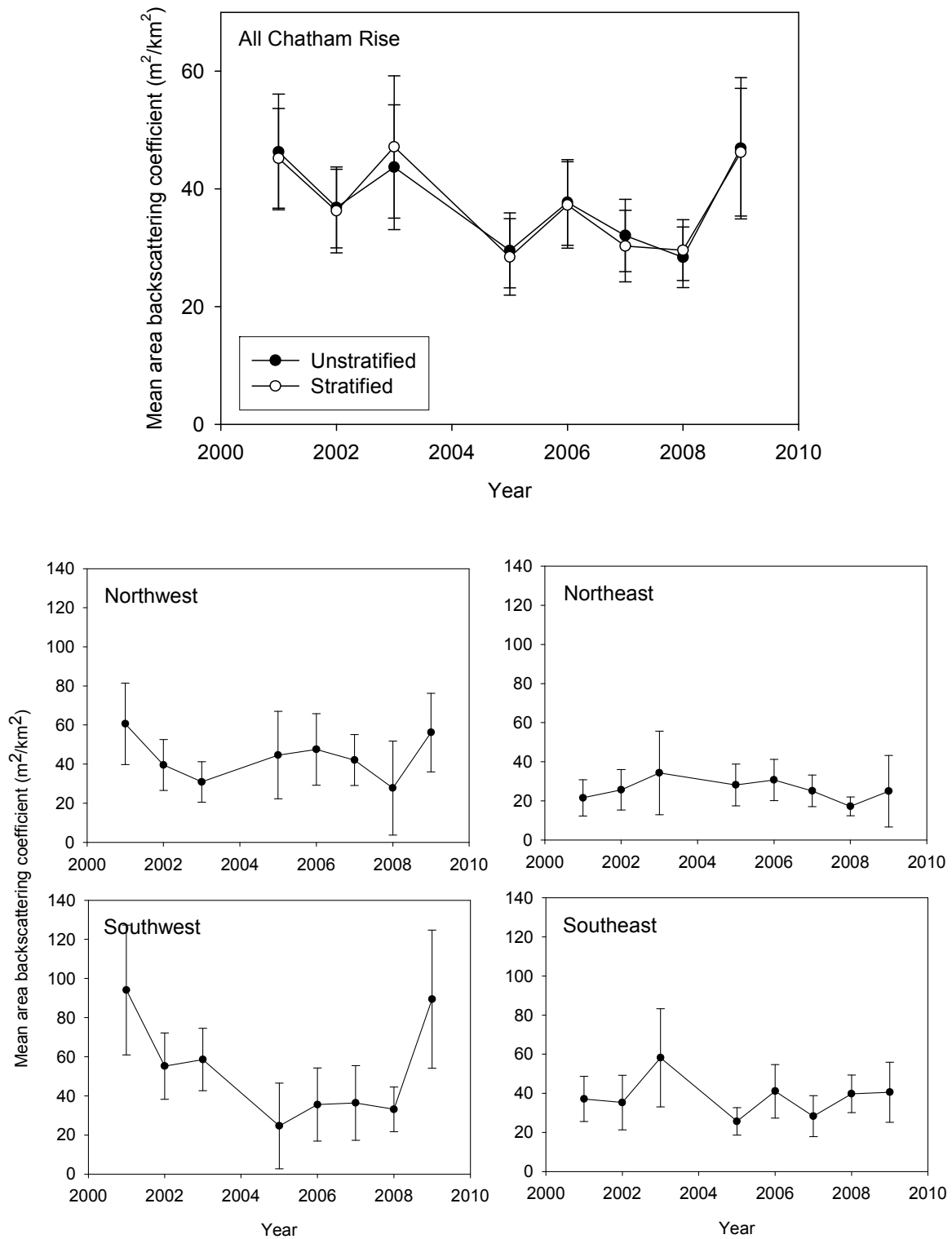


Figure 7: Time-series of mesopelagic indices on the Chatham Rise (values in Table 3). Upper plot shows index for entire Chatham Rise with and without stratification into four sub-areas. Lower panels show indices for the individual strata. Error bars are ± 2 standard errors.

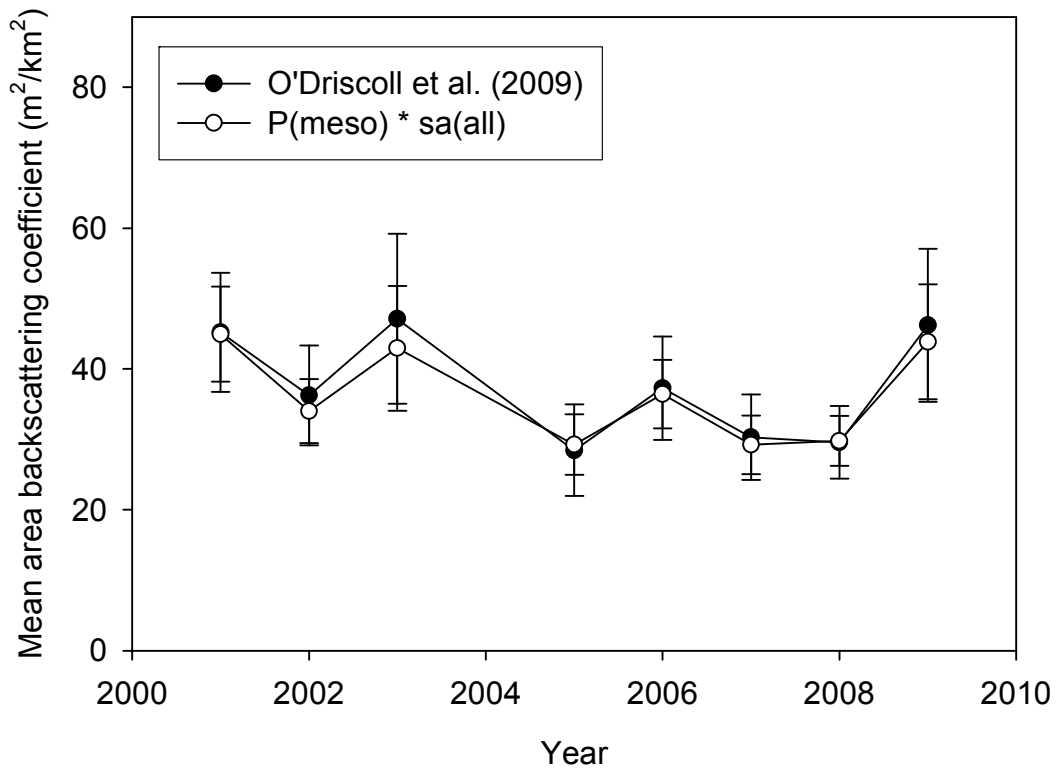


Figure 8: Comparison of stratified time-series of mesopelagic indices on the Chatham Rise calculated using the methods of O'Driscoll et al. (2009) (values in Table 3 and Figure 7) and based on multiplying the total backscatter observed at each station by the estimated proportion of night-time backscatter in the same sub-area observed in the upper 200 m corrected for the estimated proportion in the surface deadzone (see Table 4). Error bars are ± 2 standard errors.

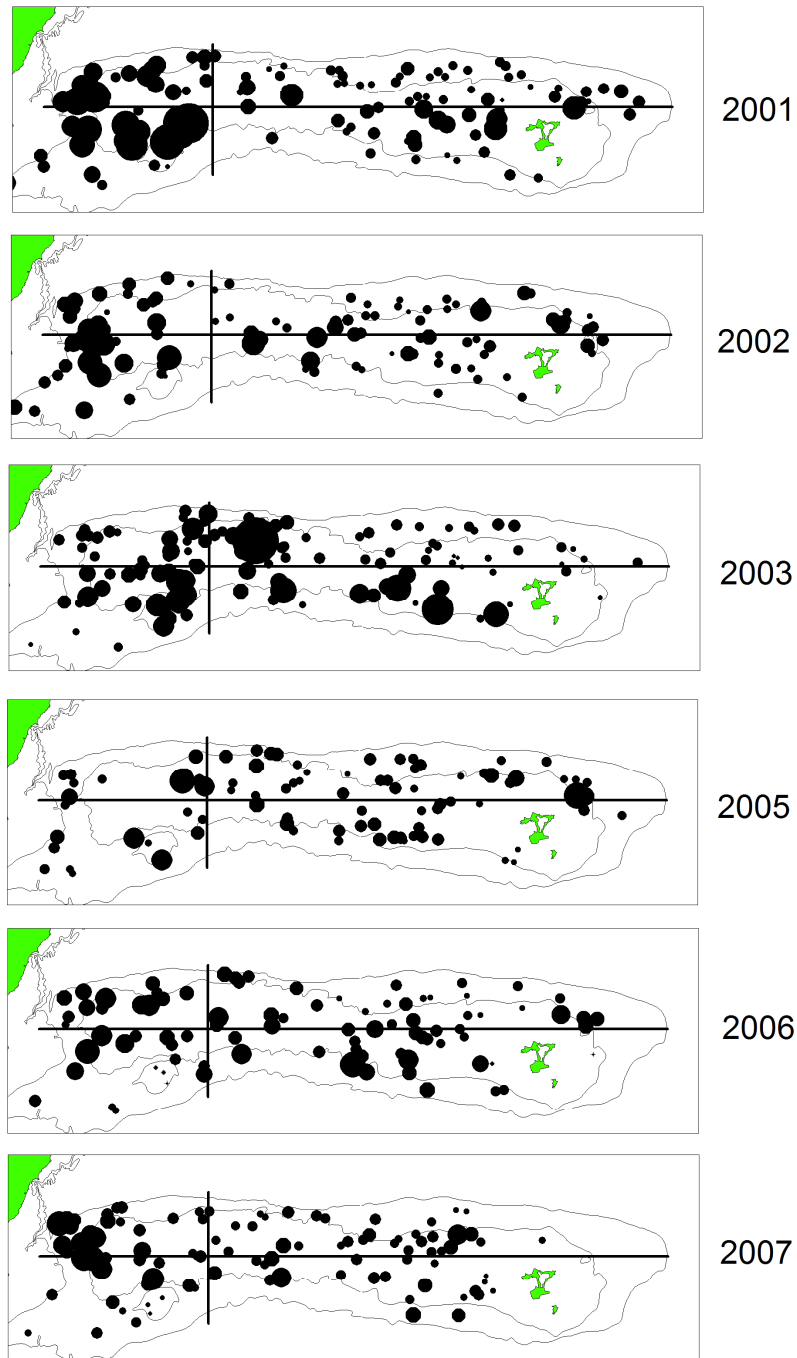


Figure 9: Spatial distribution of acoustic backscatter estimated to be from mesopelagic fish on the Chatham Rise. Circle area is proportional to the acoustic backscatter (maximum symbol size = $250 \text{ m}^2/\text{km}^2$). Lines separate the four acoustic strata.

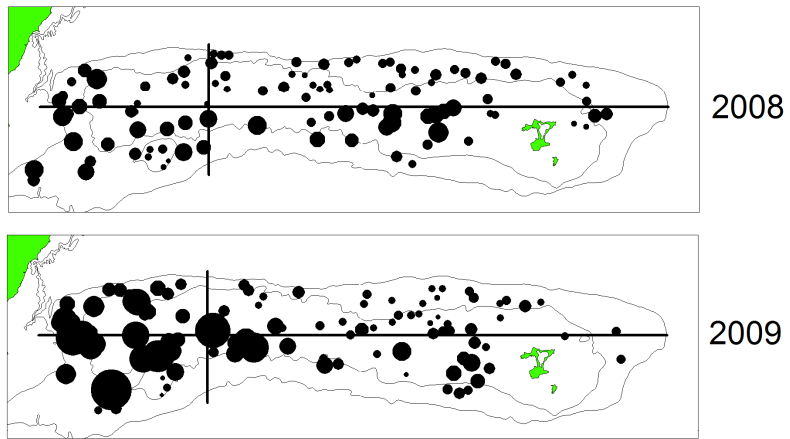


Figure 9 continued: Spatial distribution of acoustic backscatter estimated to be from mesopelagic fish on the Chatham Rise. Circle area is proportional to the acoustic backscatter (maximum symbol size = $250 \text{ m}^2/\text{km}^2$). Lines separate the four acoustic strata.

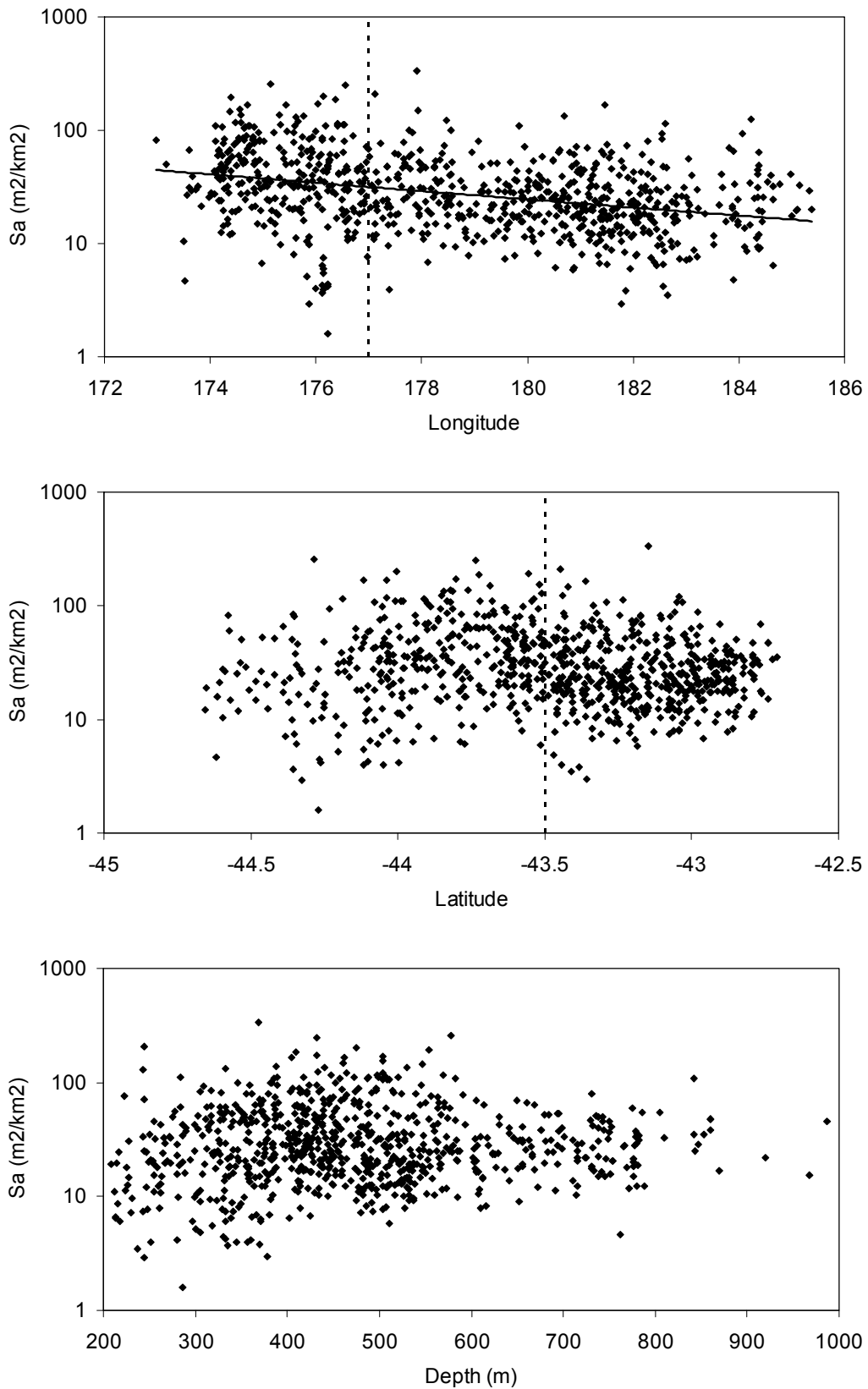


Figure 10: Relationships between point estimates of mesopelagic backscatter (see Figure 9) and longitude, latitude, and depth. Dotted lines show separation between strata used in this report.

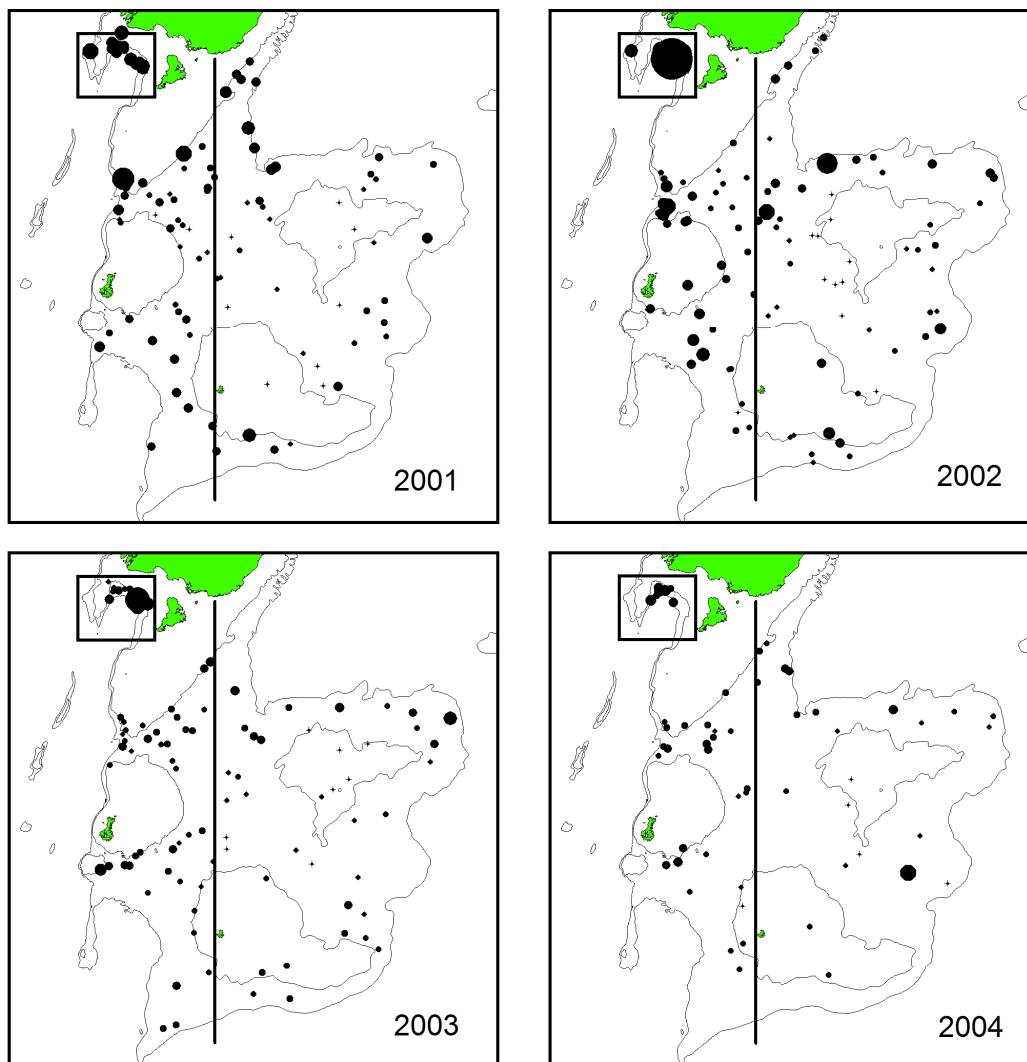


Figure 11: Spatial distribution of total acoustic backscatter in the Sub-Antarctic observed during day trawl stations. Circle area is proportional to the acoustic backscatter (maximum symbol size = 500 m²/km²). Lines separate the three acoustic strata.

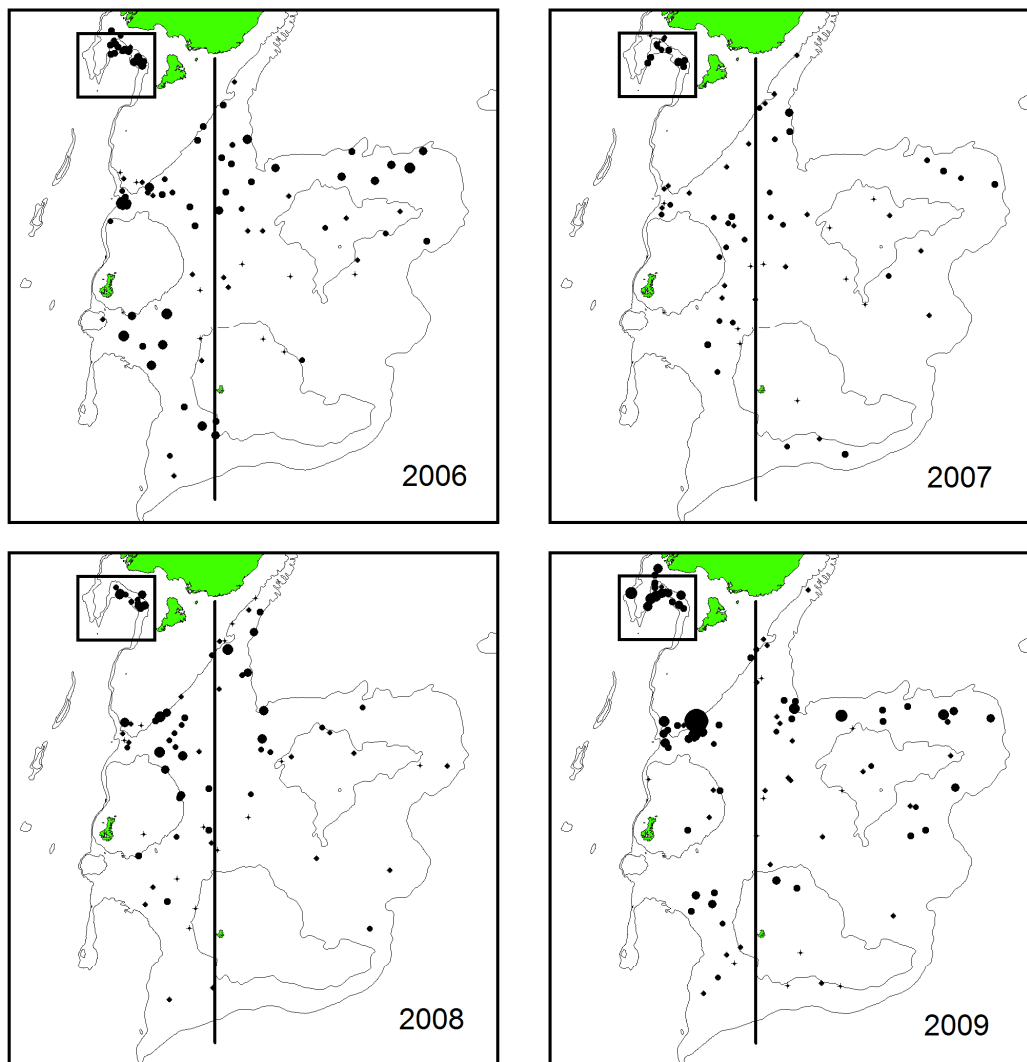


Figure 11 continued: Spatial distribution of total acoustic backscatter in the Sub-Antarctic observed during day trawl stations. Circle area is proportional to the acoustic backscatter (maximum symbol size = 500 m²/km²). Lines separate the three acoustic strata.



Figure 12: Spatial distribution of total acoustic backscatter in the Sub-Antarctic observed during night steams. Circle area is proportional to the acoustic backscatter (maximum symbol size = 500 m²/km²). Lines separate the three acoustic strata.

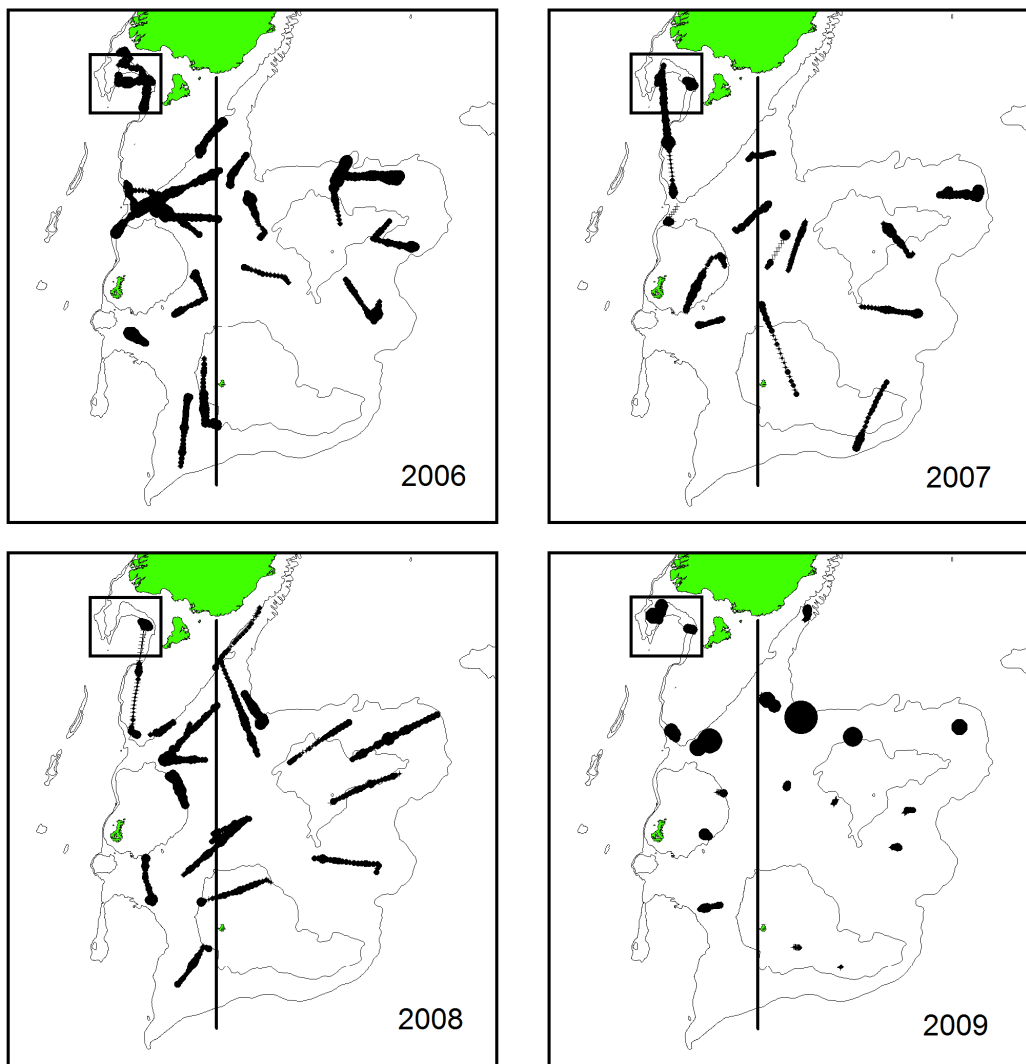


Figure 12 continued: Spatial distribution of total acoustic backscatter in the Sub-Antarctic observed during night steams. Circle area is proportional to the acoustic backscatter (maximum symbol size = 500 m²/km²). Lines separate the three acoustic strata.

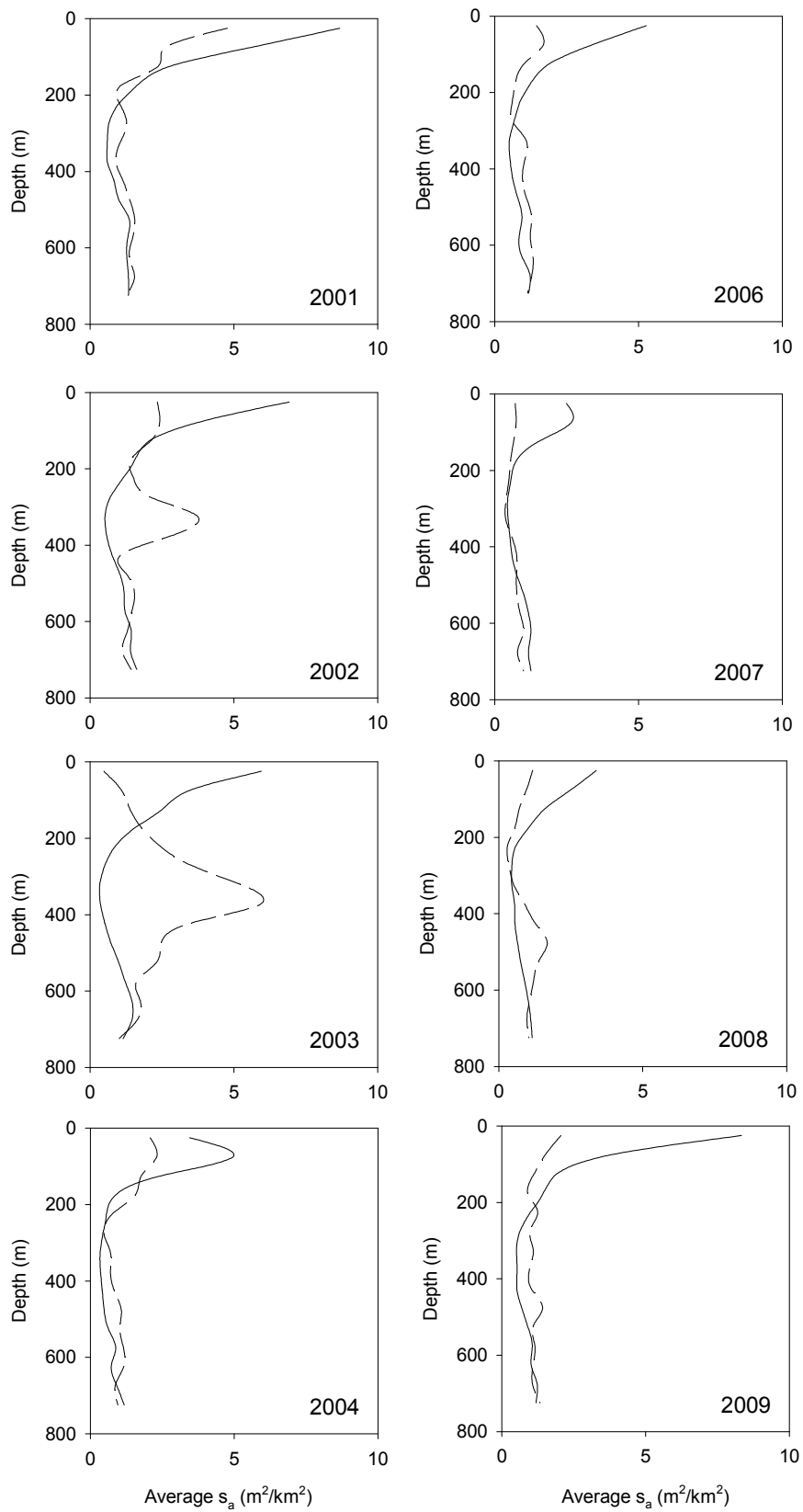


Figure 13: Vertical distribution of total acoustic backscatter integrated in 50 m depth bins on the Sub-Antarctic observed during the day (dashed lines) and at night (solid lines) in 2001–09.

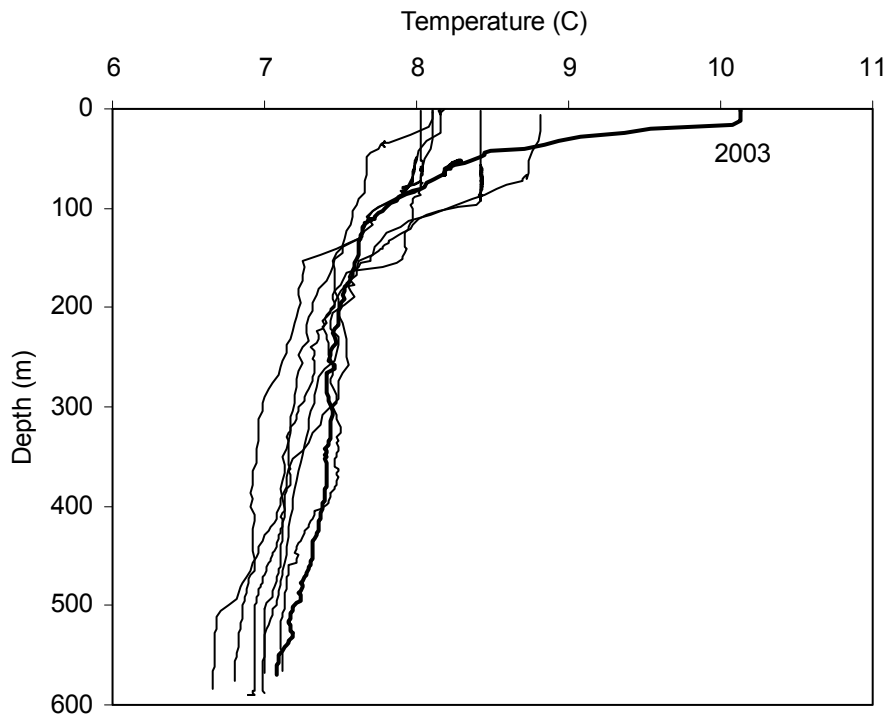


Figure 14: Comparison of vertical profiles of temperature from the net-mounted CTD on tows in stratum 9 at approximately 50 45' S and 169 00' E in 2003 (TAN0219 station 54, on 6 December), 2004 (TAN0317 station 45, on 29 November), 2005 (TAN0414 station 54, on 14 December), 2006 (TAN0515 station 42, on 6 December), 2007 (TAN0617 station 33, on 5 December), 2008 (TAN0714 station 40, on 7 December), and 2009 (TAN0813 station 17, on 30 November). The profile from 2003 is the bold line.

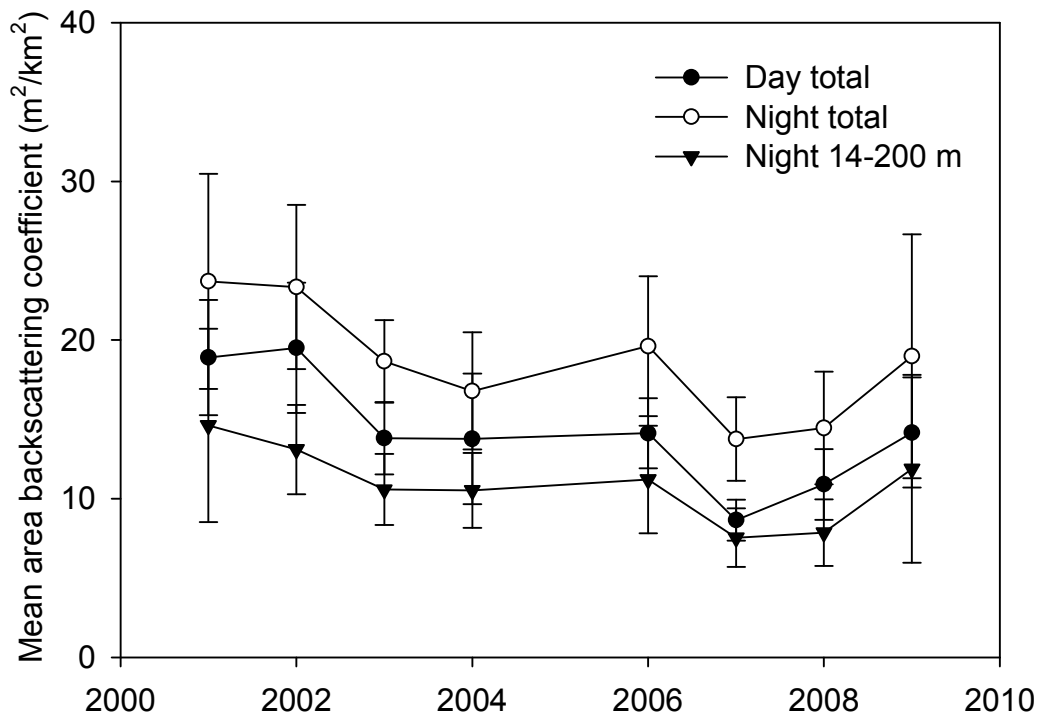


Figure 15: Total acoustic abundance indices for the Sub-Antarctic based on (strata-averaged) mean areal backscatter (sa). Error bars are ± 2 standard errors.

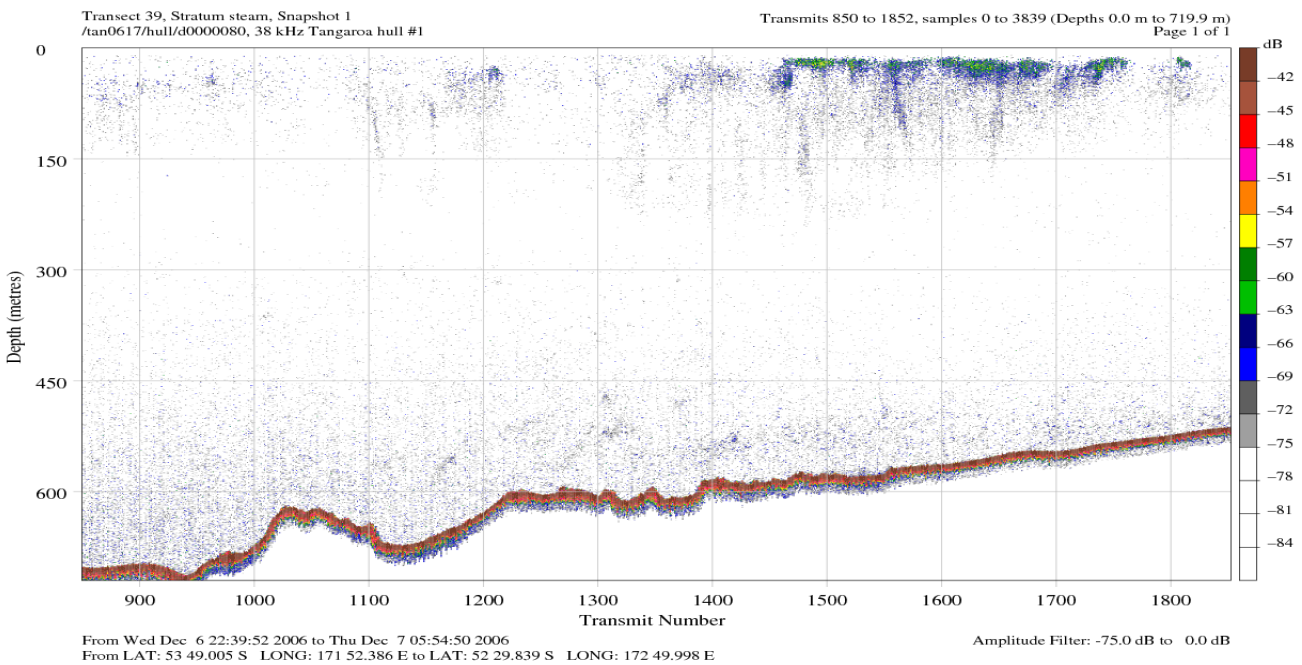
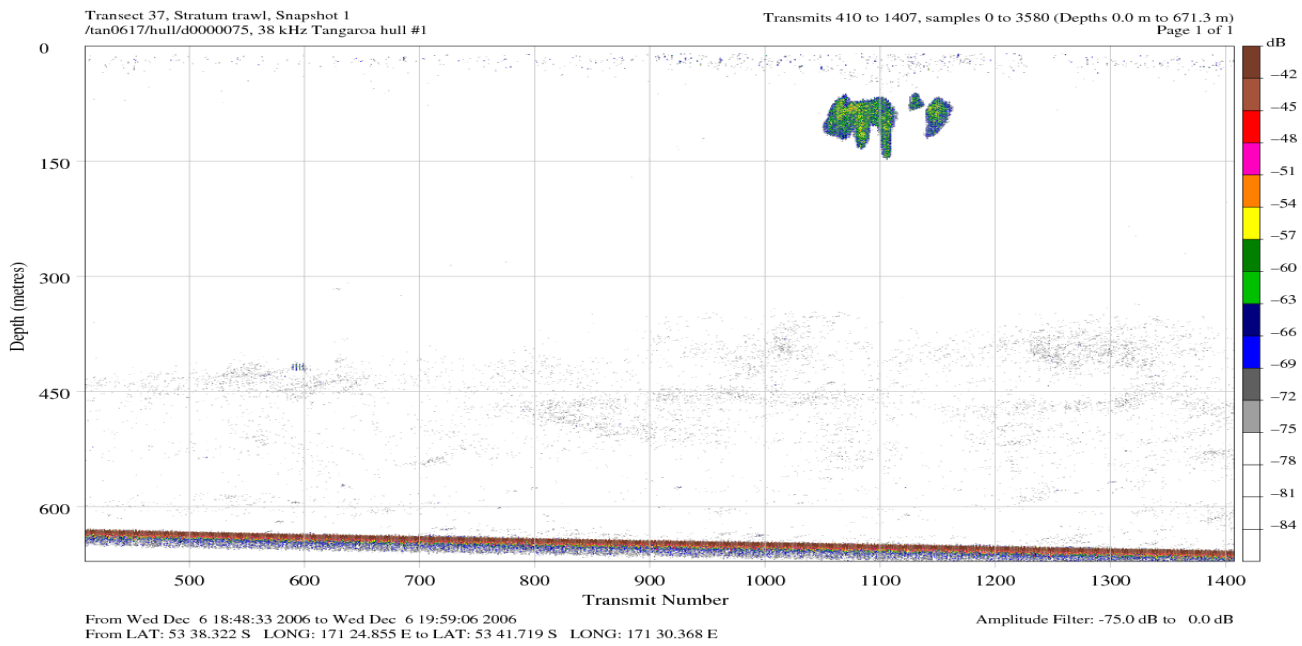


Figure 16: Consecutive acoustic recordings in a similar location in daylight (18:08–18:59 NZST) and at night (22:25–23:26) showing ascension of mesopelagic marks in the Sub-Antarctic. Note blue haze at depths greater than 450 m at night (lower panel) which is noise caused by the vessel.

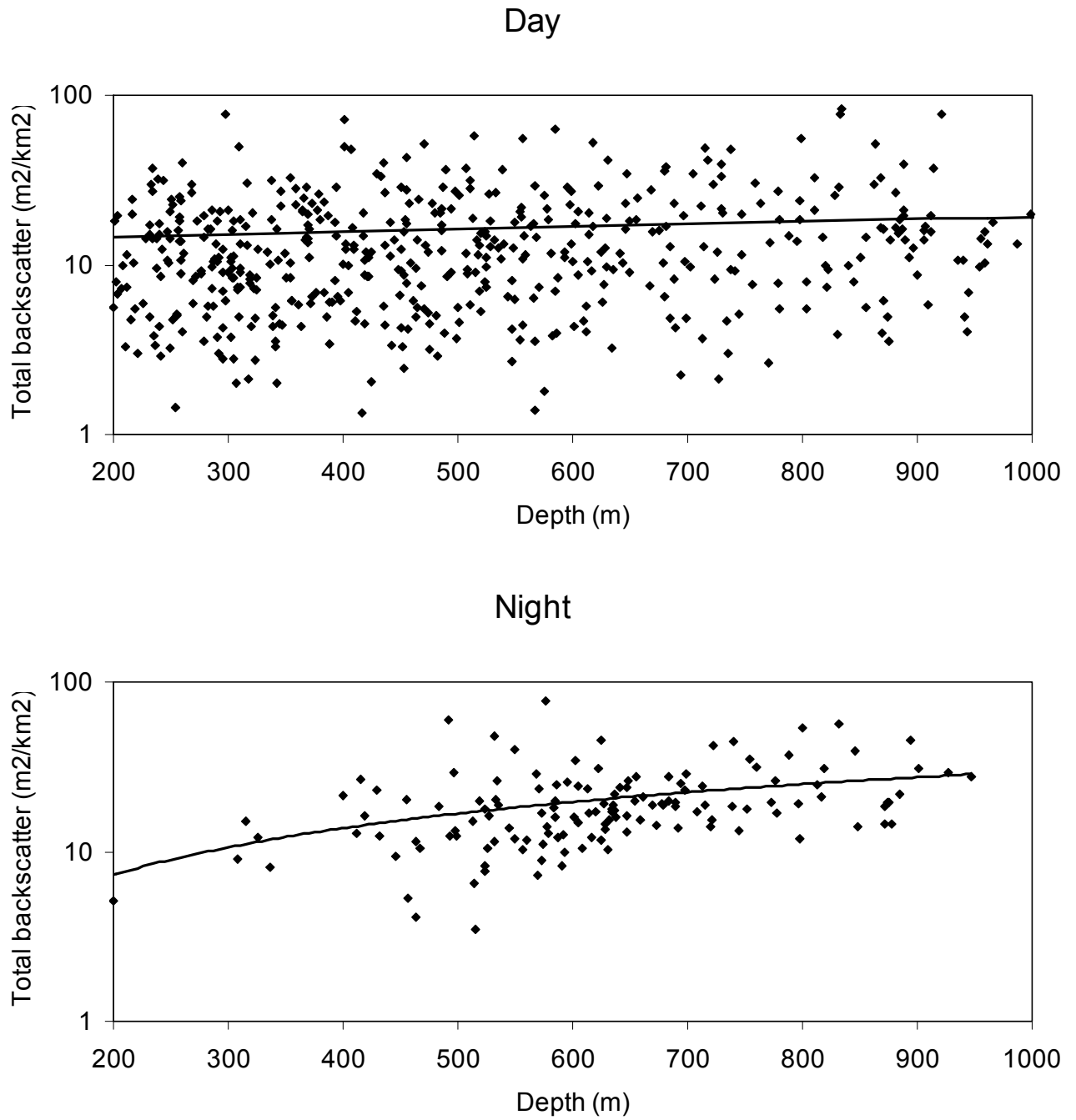


Figure 17: Depth-related patterns in total acoustic backscatter in recordings made during day trawls and night steams. Lines are fitted 2nd-order polynomials. We interpret the stronger increase in backscatter with increasing depth in night recordings as evidence that these data were affected by vessel noise (see text for details).

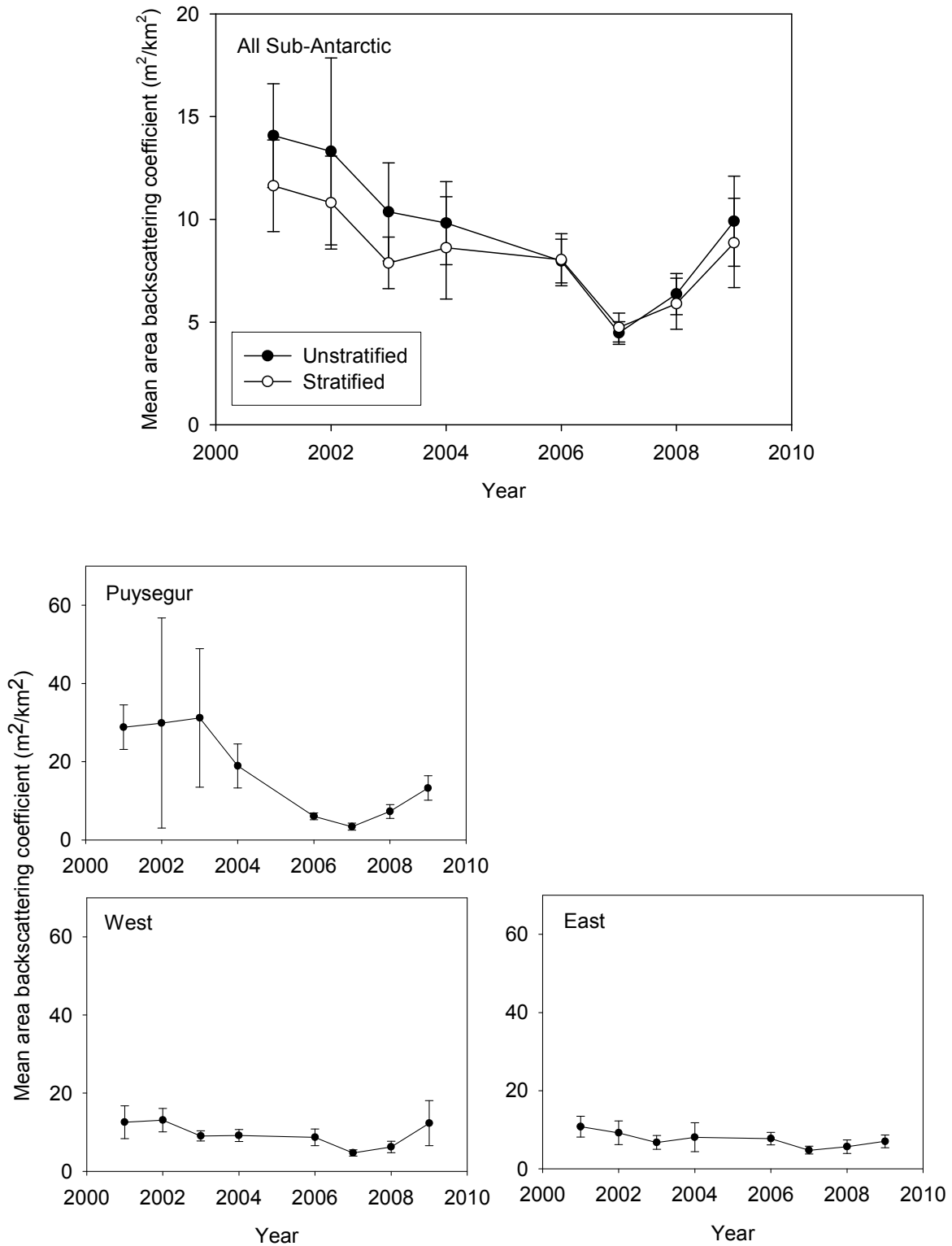


Figure 18: Time-series of mesopelagic indices on the Sub-Antarctic (values in Table 6). Upper plot shows index for entire Sub-Antarctic with and without stratification into three sub-areas. Lower panels show indices for the individual strata. Error bars are ± 2 standard errors.

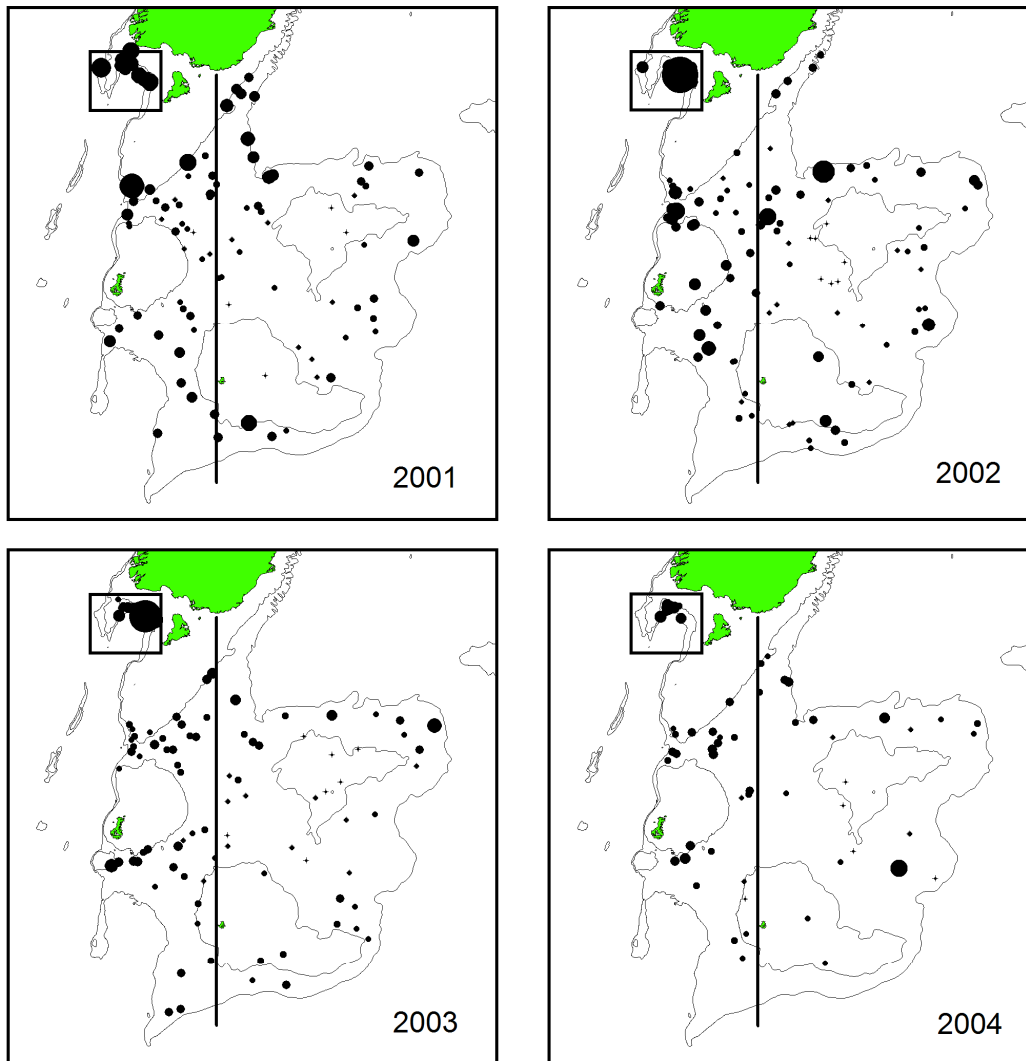


Figure 19: Spatial distribution of acoustic backscatter estimated to be from mesopelagic fish in the Sub-Antarctic. Circle area is proportional to the acoustic backscatter (maximum symbol size = 250 m²/km²). Lines separate the three acoustic strata.

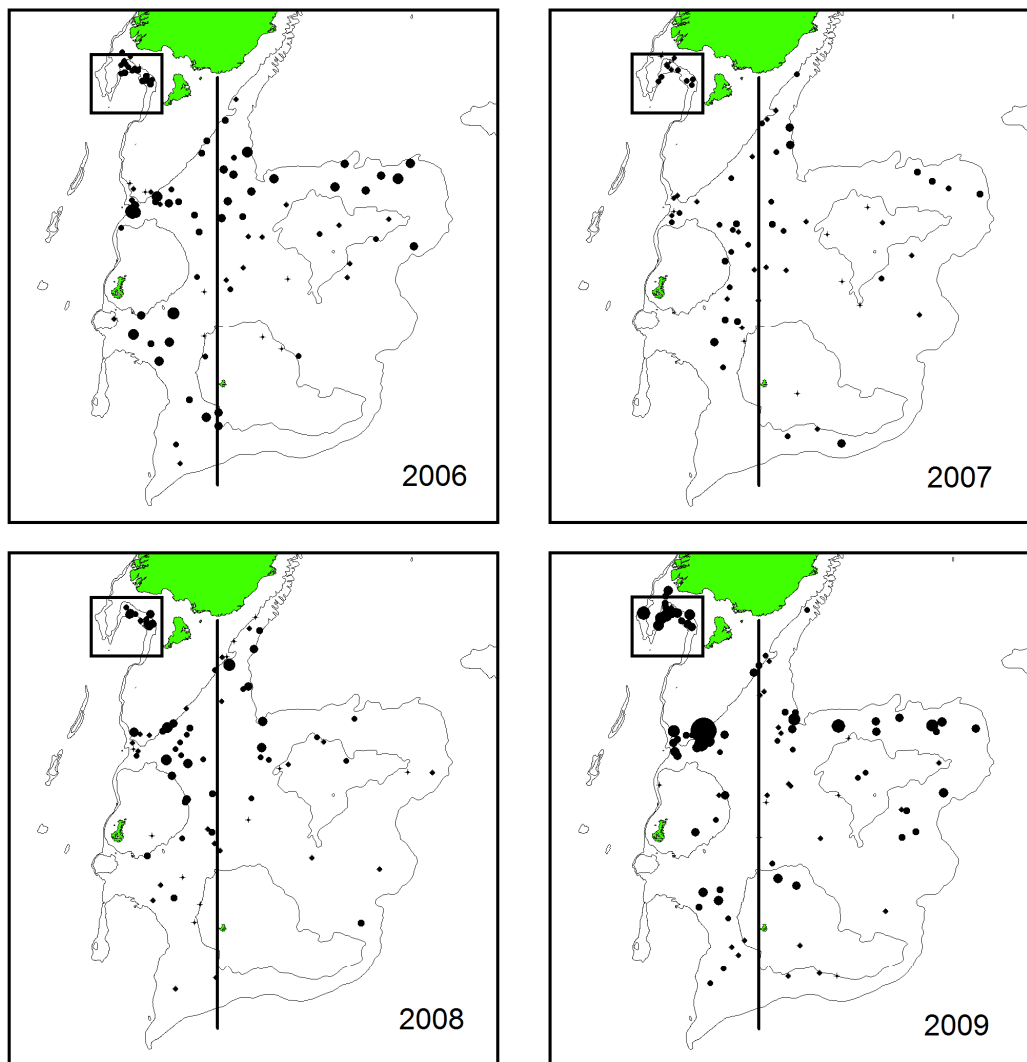


Figure 19 continued: Spatial distribution of acoustic backscatter estimated to be from mesopelagic fish in the Sub-Antarctic. Circle area is proportional to the acoustic backscatter (maximum symbol size = $250 \text{ m}^2/\text{km}^2$). Lines separate the three acoustic strata.

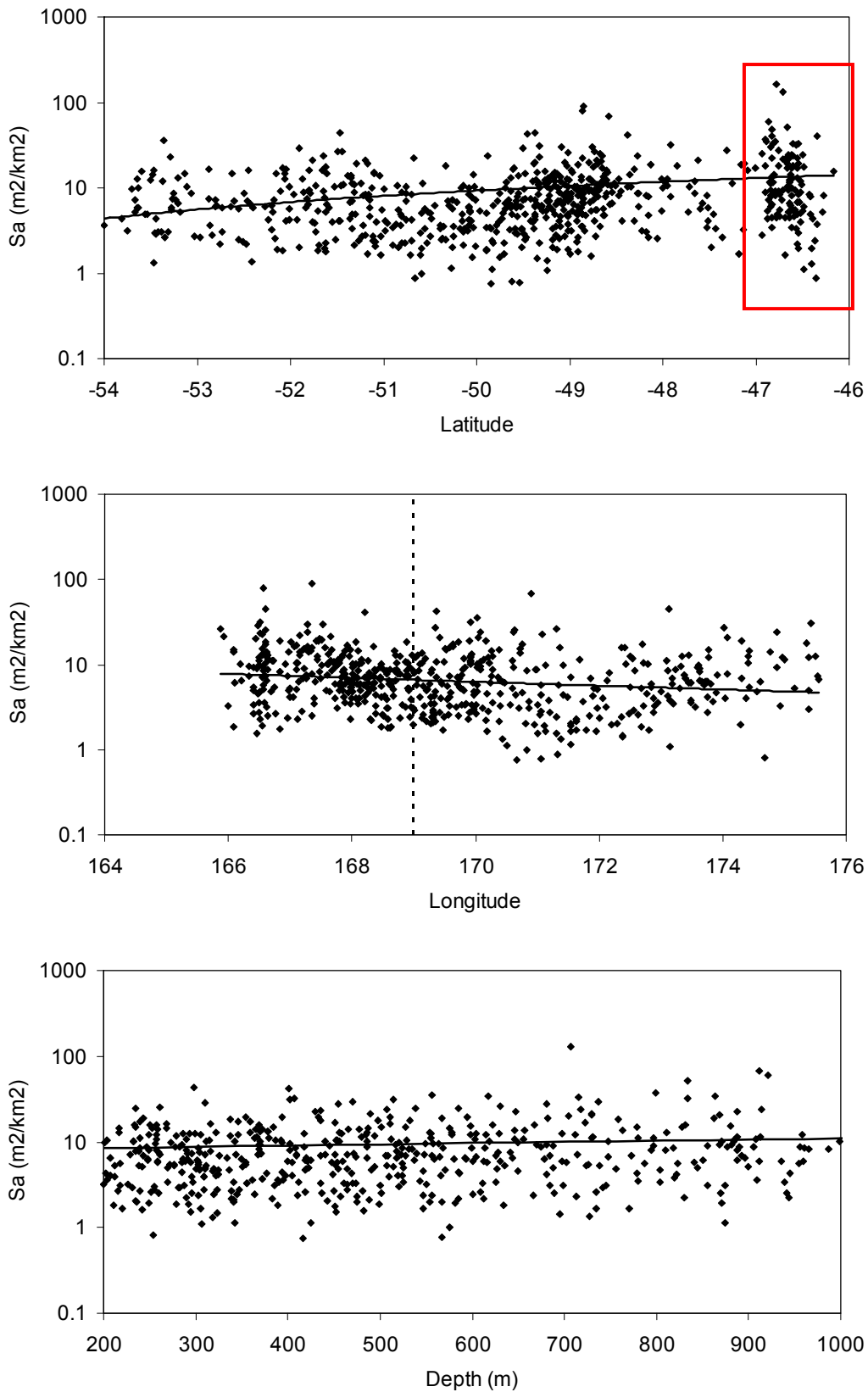


Figure 20: Relationships between point estimates of mesopelagic backscatter (see Figure 19) and latitude, longitude, and depth. Red box in upper panel shows Puysegur stratum. Dotted line in middle panel shows separation between east and west Sub-Antarctic (with Puysegur excluded).

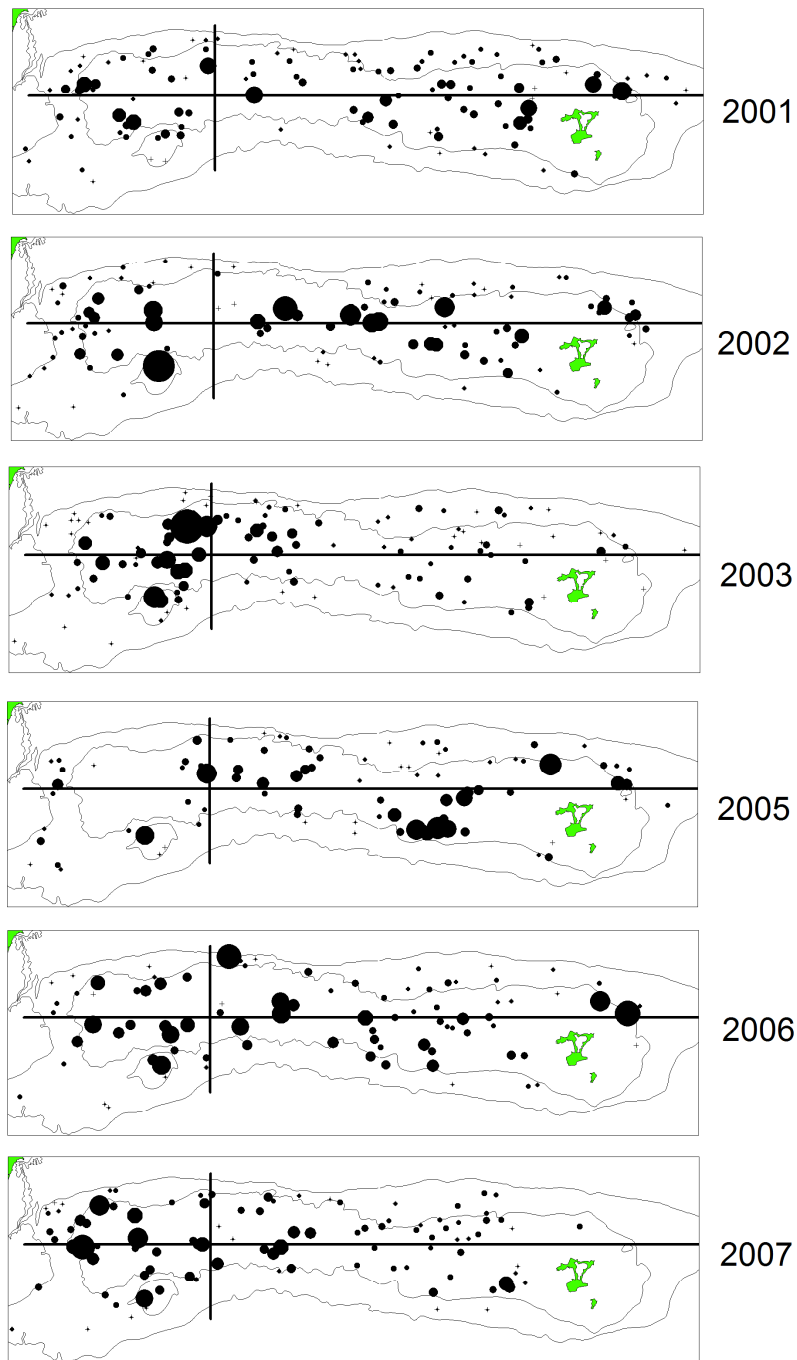


Figure 21: Spatial distribution of hoki catch rates on the Chatham Rise observed during trawl surveys where acoustic data were also available. Circle area is proportional to the catch rate (maximum symbol size = 10 000 kg/km²). Lines separate the four acoustic strata.

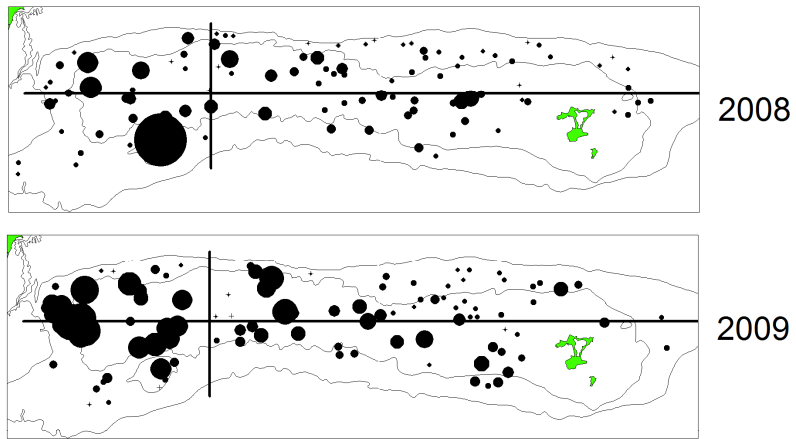


Figure 21 continued: Spatial distribution of hoki catch rates on the Chatham Rise observed during trawl surveys where acoustic data were also available. Circle area is proportional to the catch rate (maximum symbol size = 10 000 kg/km²). Lines separate the four acoustic strata.

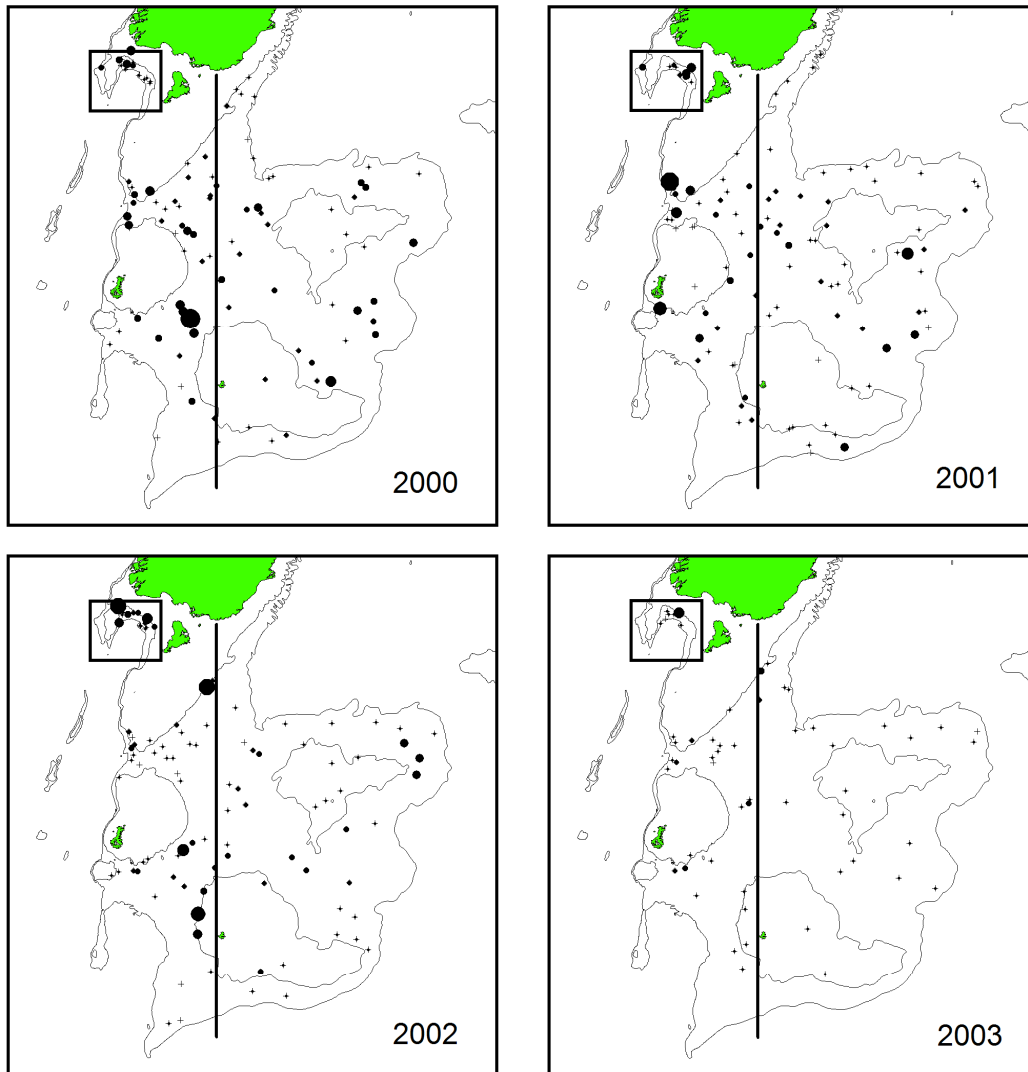


Figure 22: Spatial distribution of hoki catch rates in the Sub-Antarctic observed during trawl surveys where acoustic data were also available. Circle area is proportional to the catch rate (maximum symbol size = 10 000 kg/km²). Lines separate the three acoustic strata.

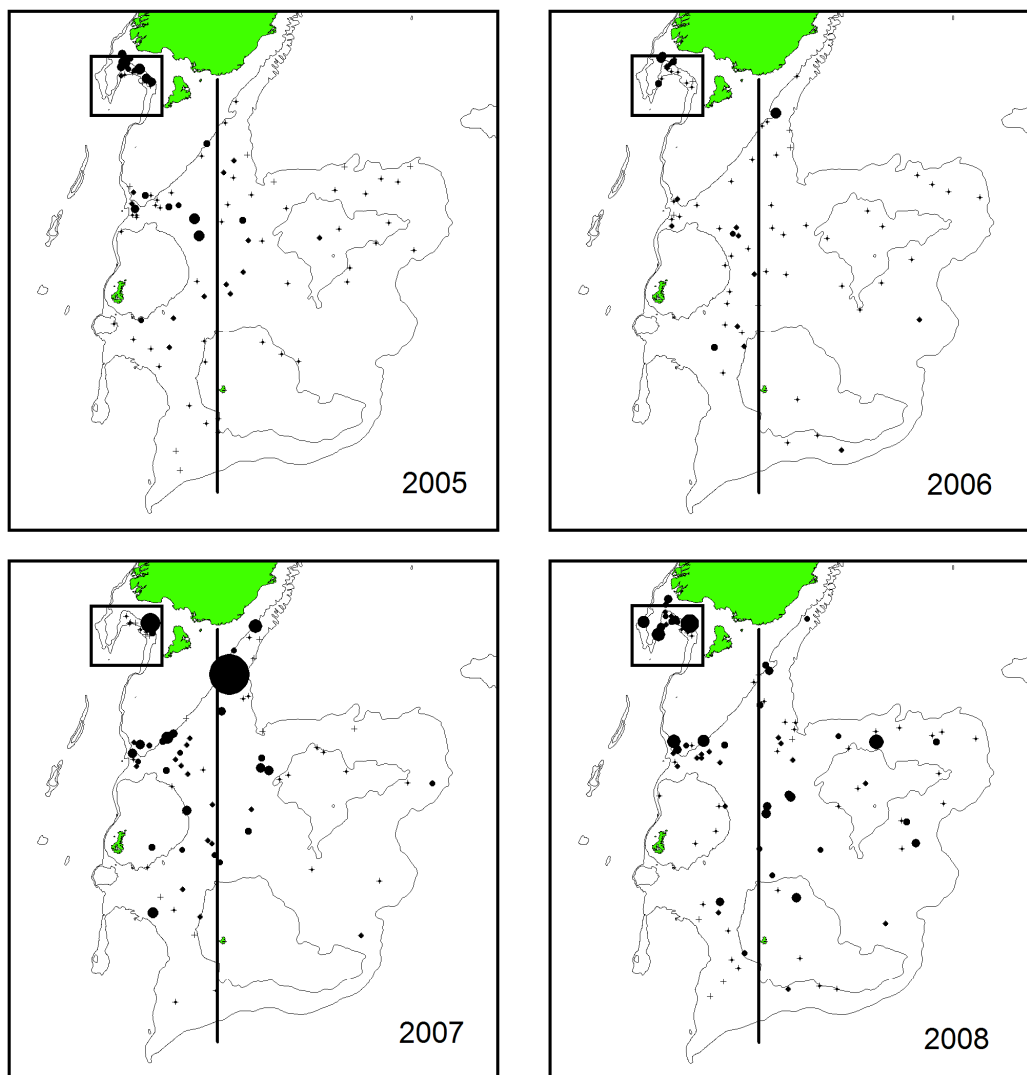


Figure 22 continued: Spatial distribution of hoki catch rates in the Sub-Antarctic observed during trawl surveys where acoustic data were also available. Circle area is proportional to the catch rate (maximum symbol size = 10 000 kg/km²). Lines separate the three acoustic strata.

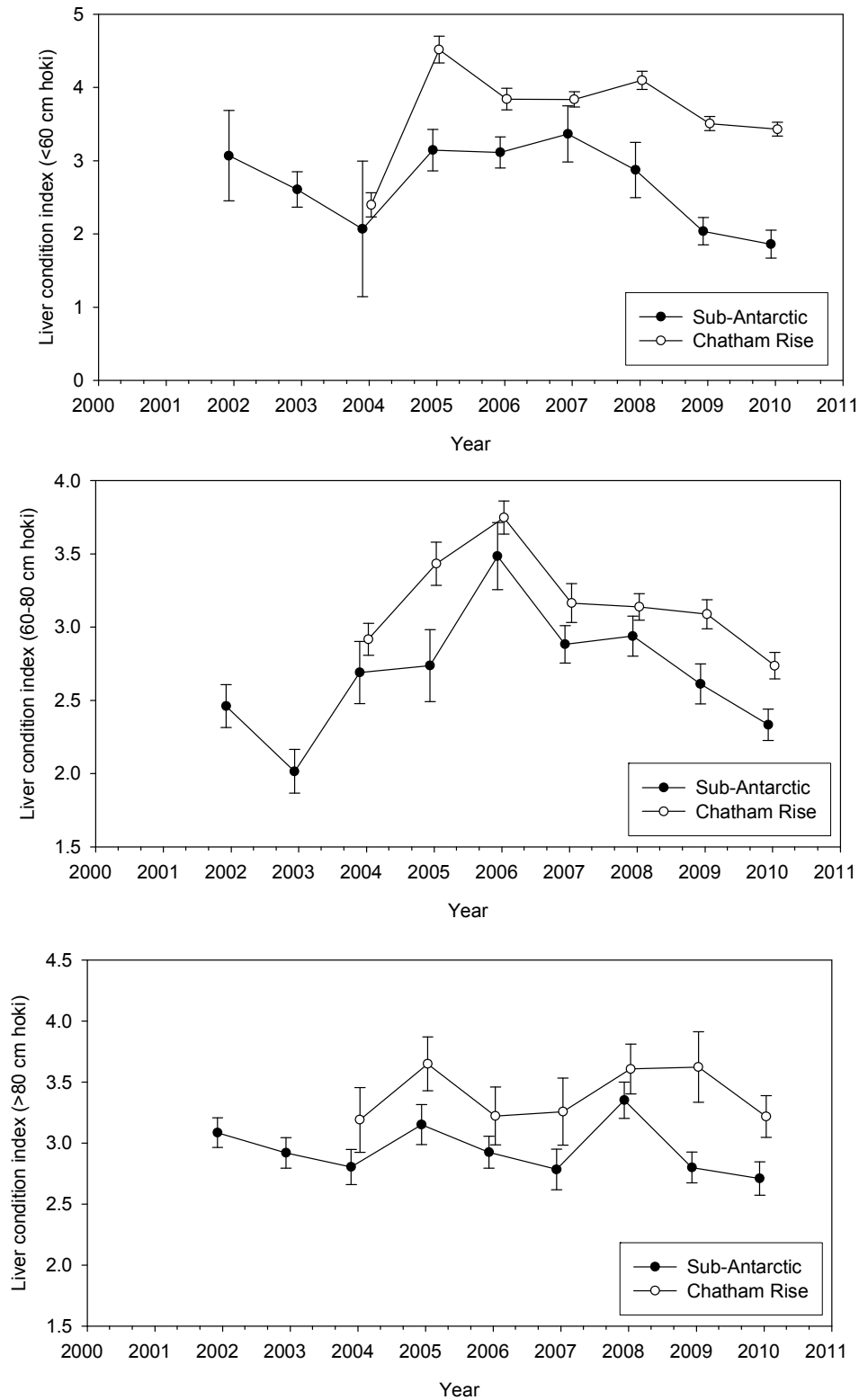
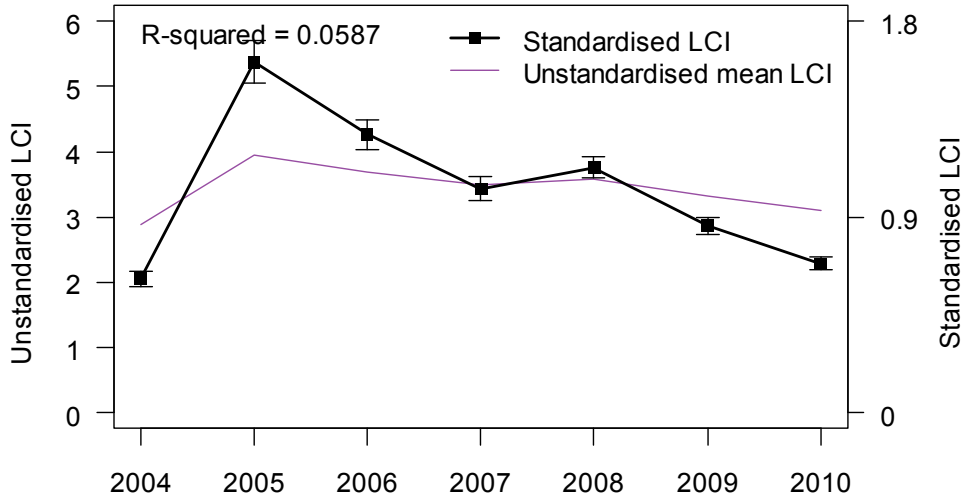


Figure 23: Comparison of liver condition indices of hoki on the Sub-Antarctic and Chatham Rise for three size-classes of hoki: <60 cm (upper panel); 60–80 cm (middle panel); and >80 cm (lower panel).

(a)



(b)

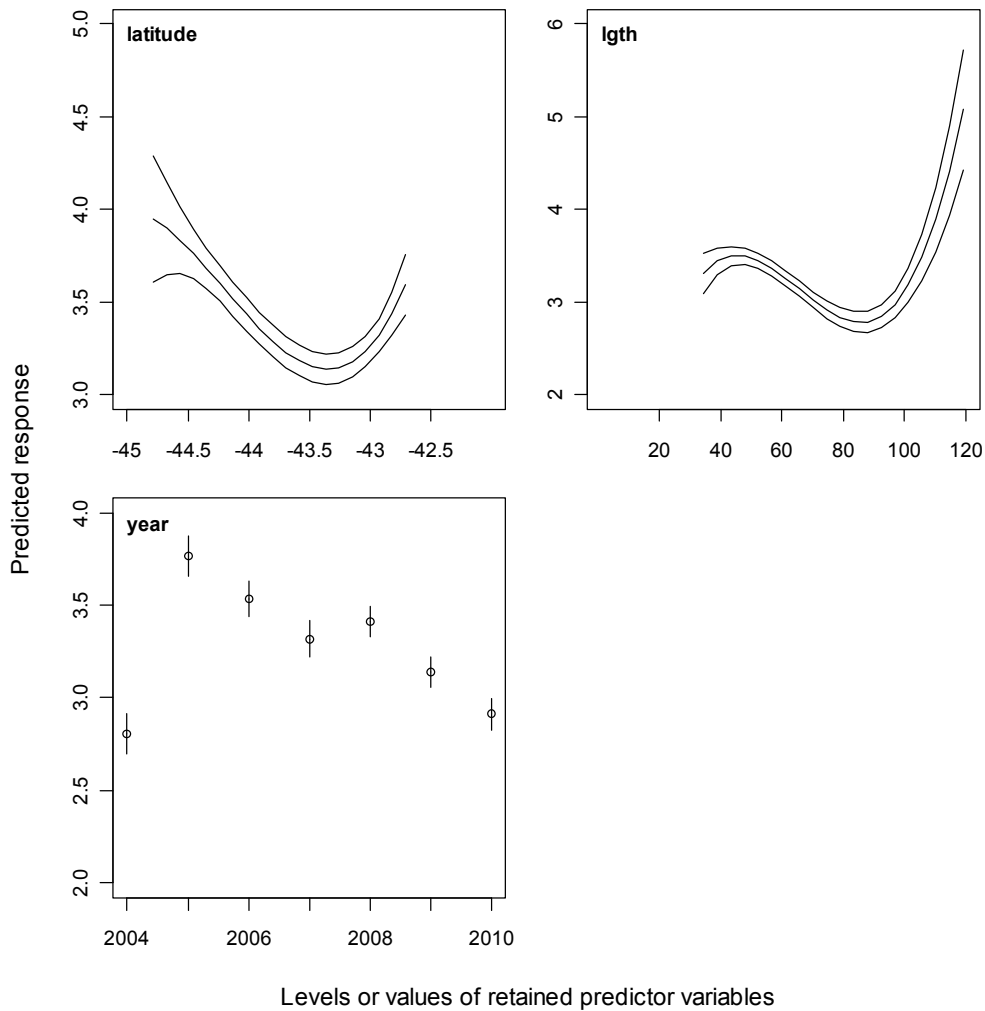
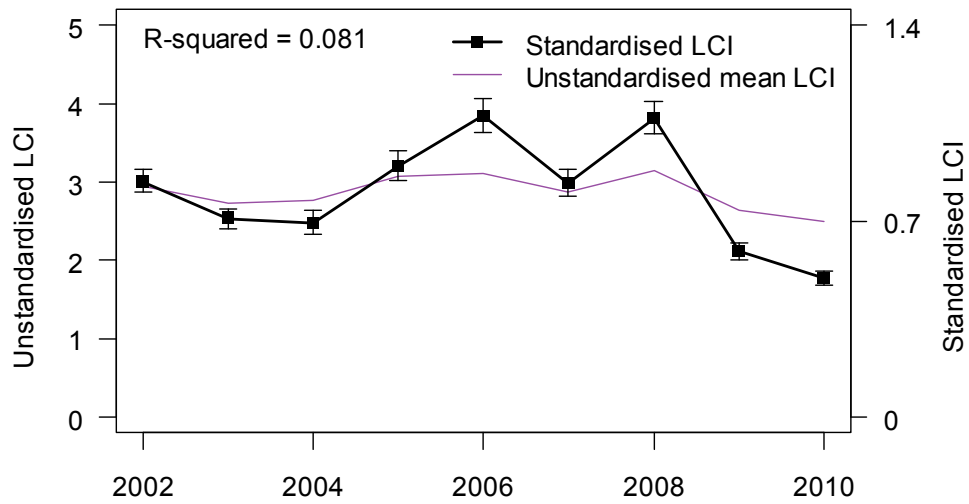


Figure 24: GLM model of LCI on the Chatham Rise: (a) Model arithmetic, geometric and standardised CPUE indices. (b) Predictor variables retained in the GLM analysis and their distributions by factor levels.

(a)



(b)

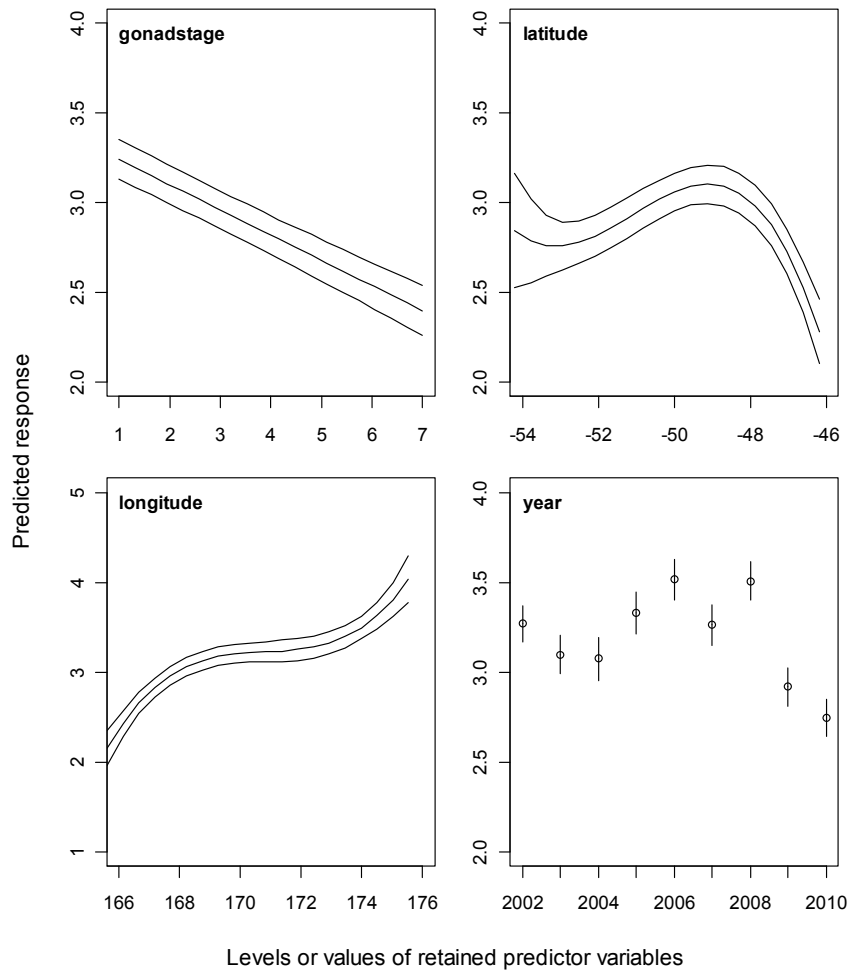


Figure 25: GLM model of LCI in the Sub-Antarctic: (a) Model arithmetic, geometric and standardised CPUE indices. (b) Predictor variables retained in the GLM analysis and their distributions by factor levels.

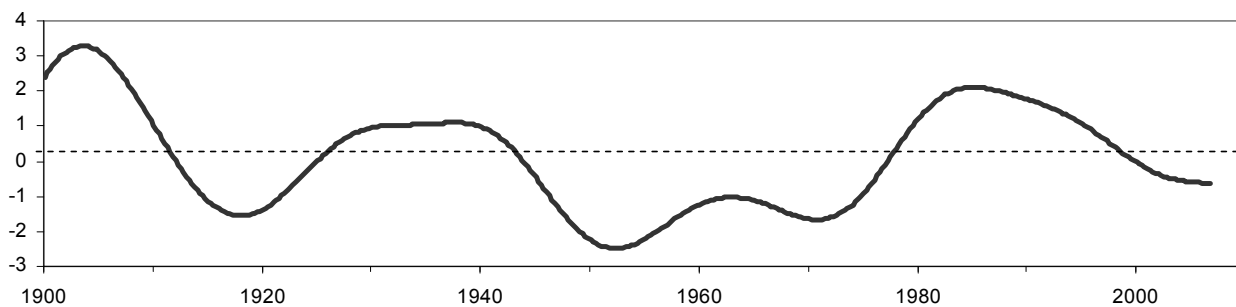


Figure 26: Interdecadal Pacific Oscillation index (13 year filter).

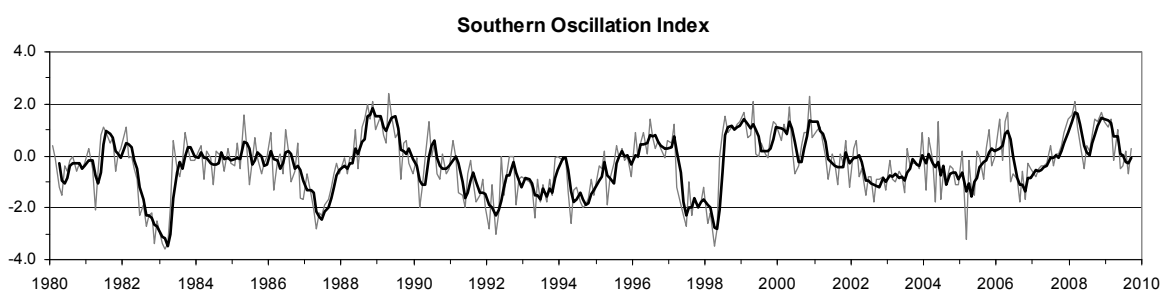


Figure 27: Southern Oscillation index wind anomalies over New Zealand, monthly with 3-monthly averages

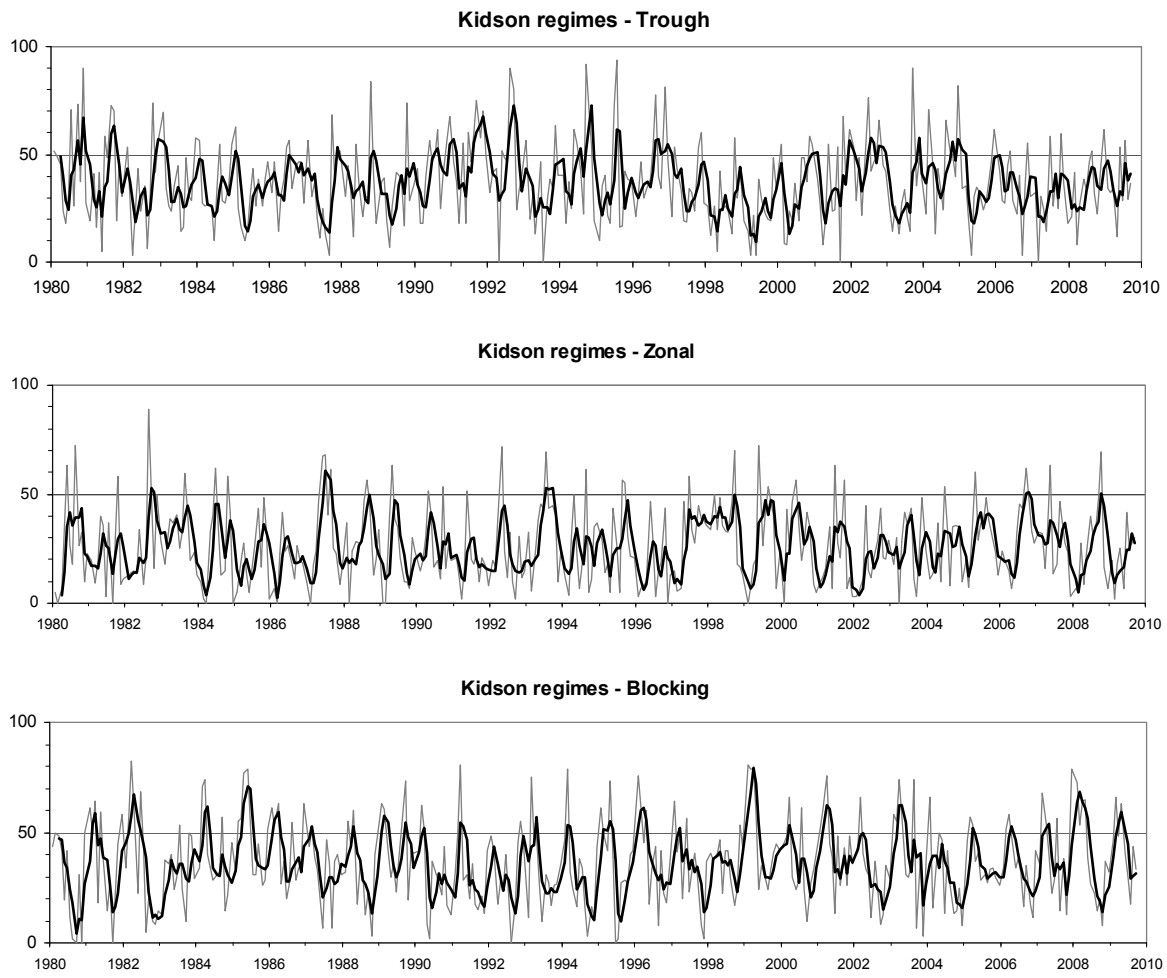


Figure 28: Kidson weather regimes, monthly with 3-monthly averages.

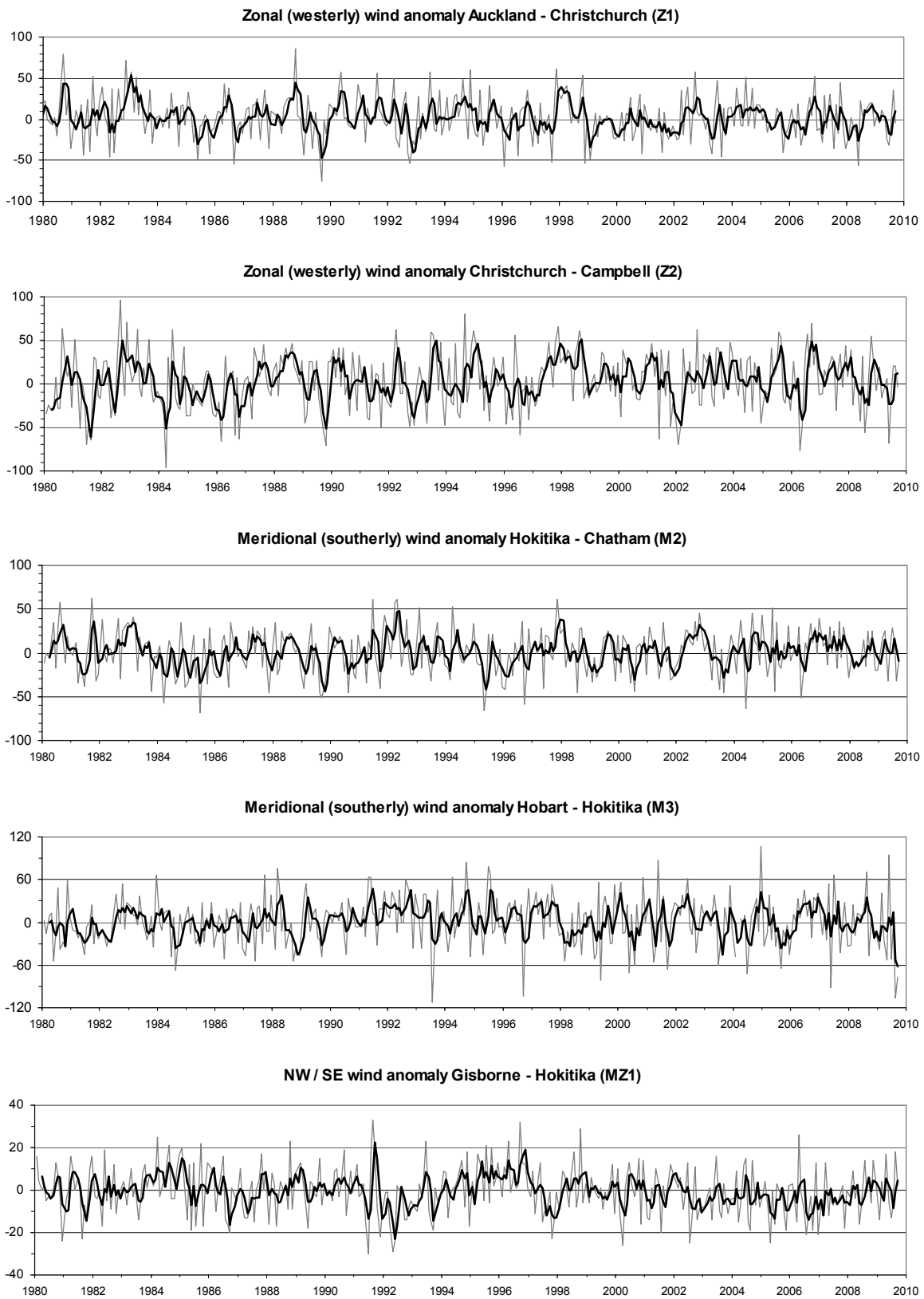


Figure 29: Trenberth wind anomalies over New Zealand, monthly with 13-month running averages

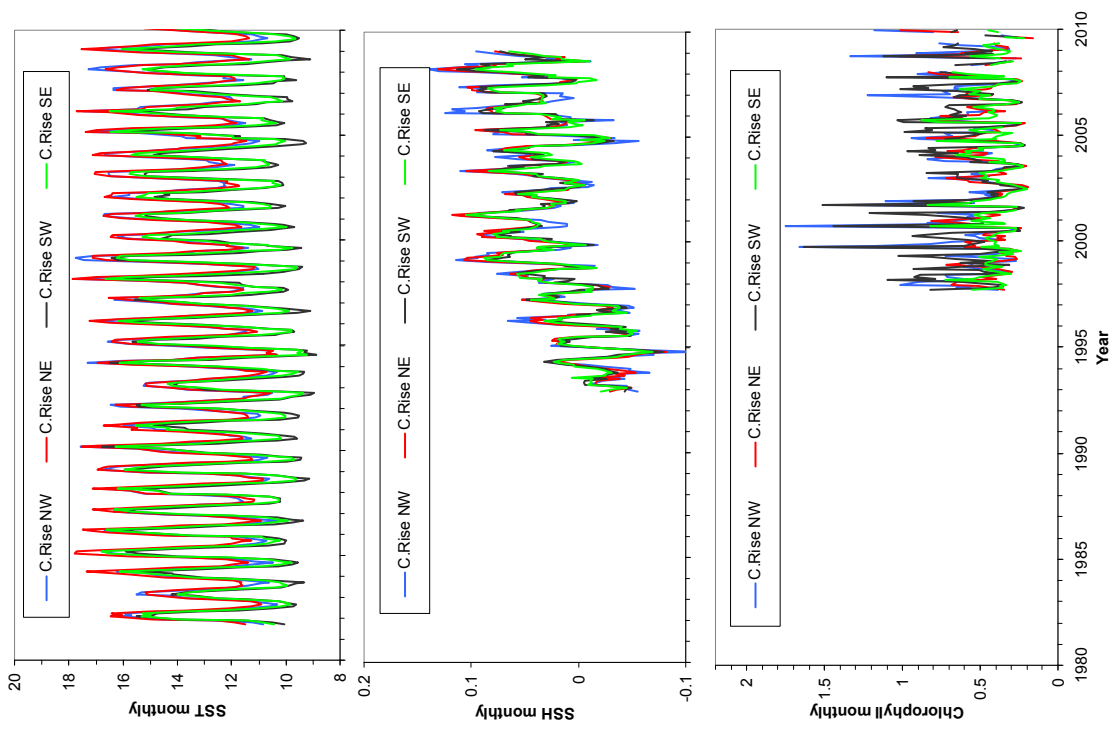
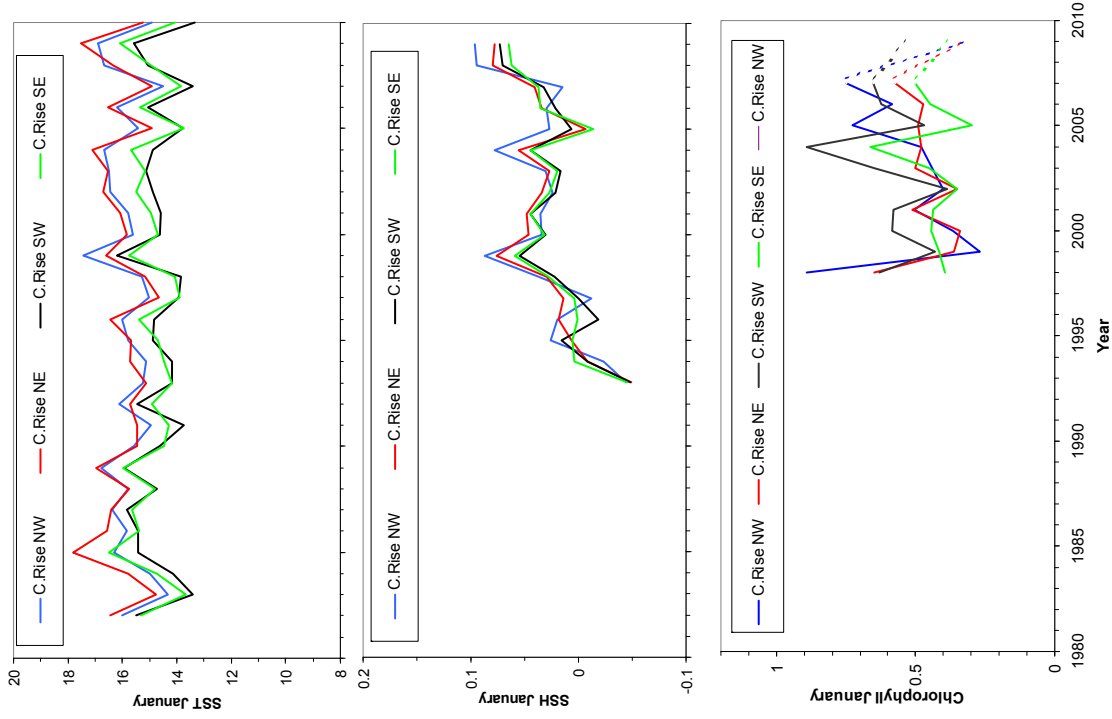


Figure 30: Chatham Rise SST, SSH and Chlorophyll indices, 1985–2010: left panel monthly; right panel January.

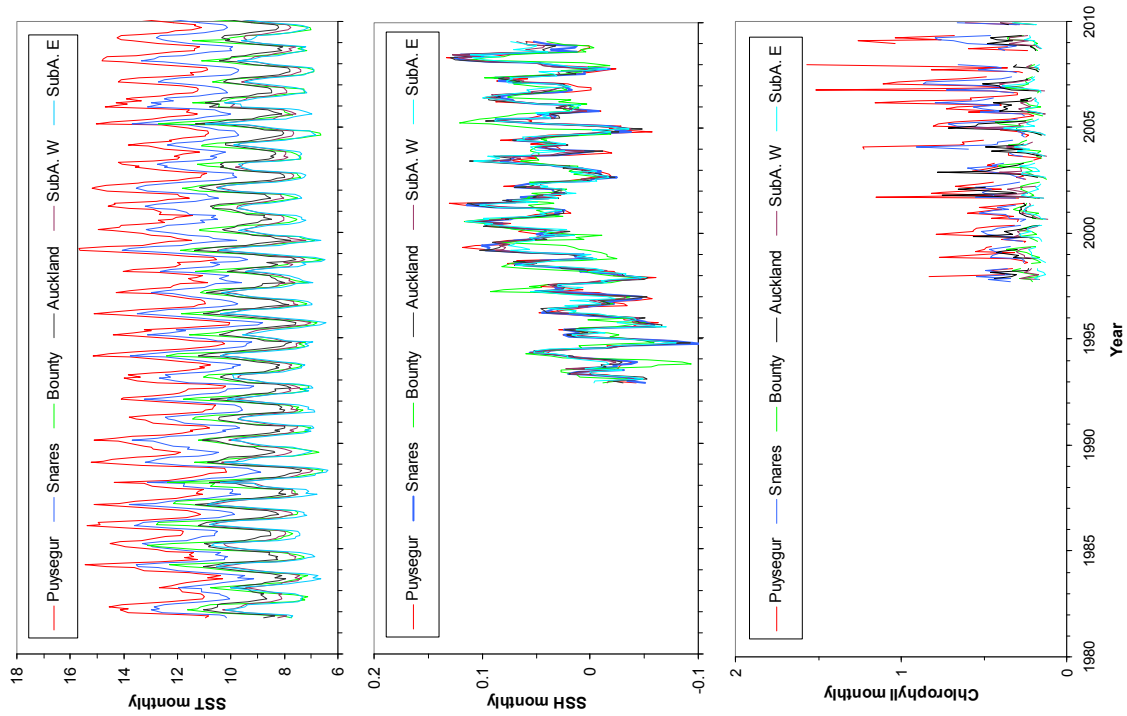
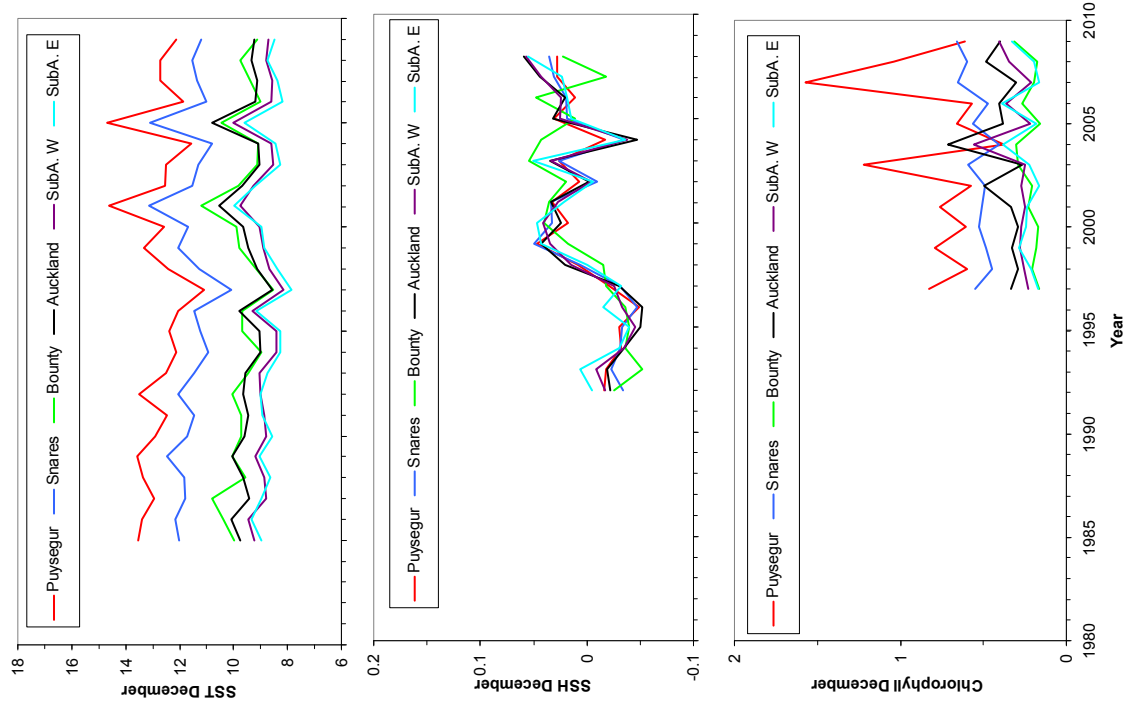


Figure 31: Southland/Sub-Antarctic SST, SSH and Chlorophyll indices, 1985–2010: left panel monthly; right panel January.

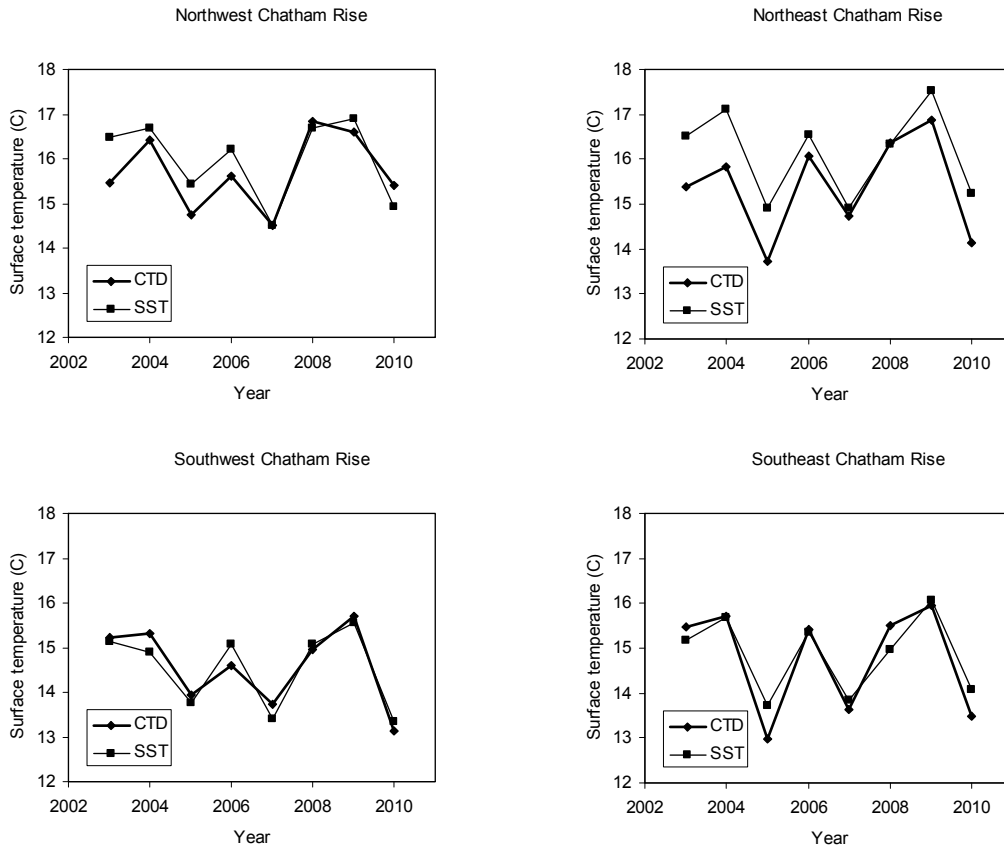


Figure 32: Estimates of surface temperature on the Chatham Rise by sub-area derived from CTD data at 5 m depth during trawl surveys (CTD) and satellite-derived estimates of SST during January (SST).

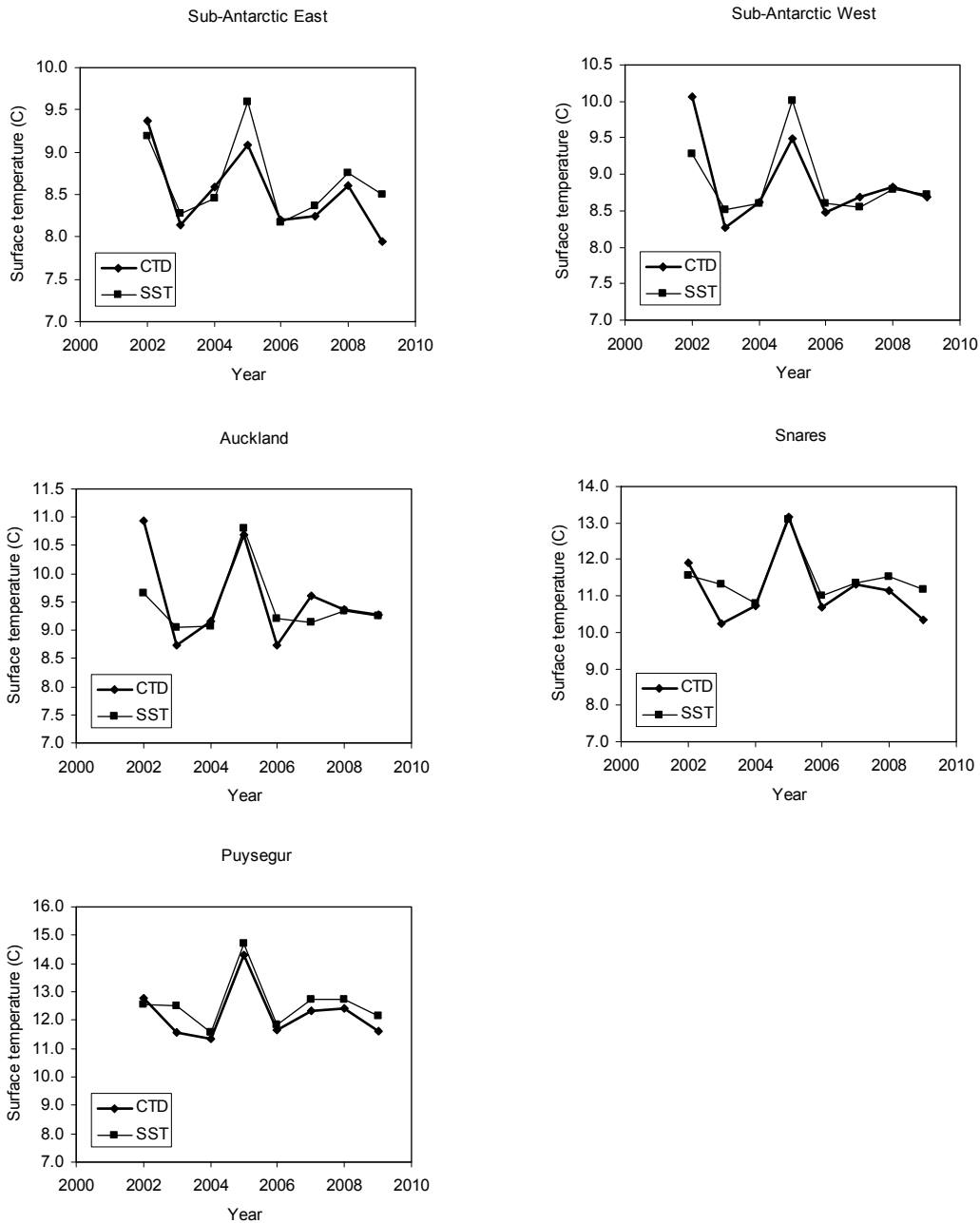


Figure 33: Estimates of surface temperature on the Sub-Antarctic by sub-area derived from CTD data at 5 m depth during trawl surveys (CTD) and satellite-derived estimates of SST during December (SST).

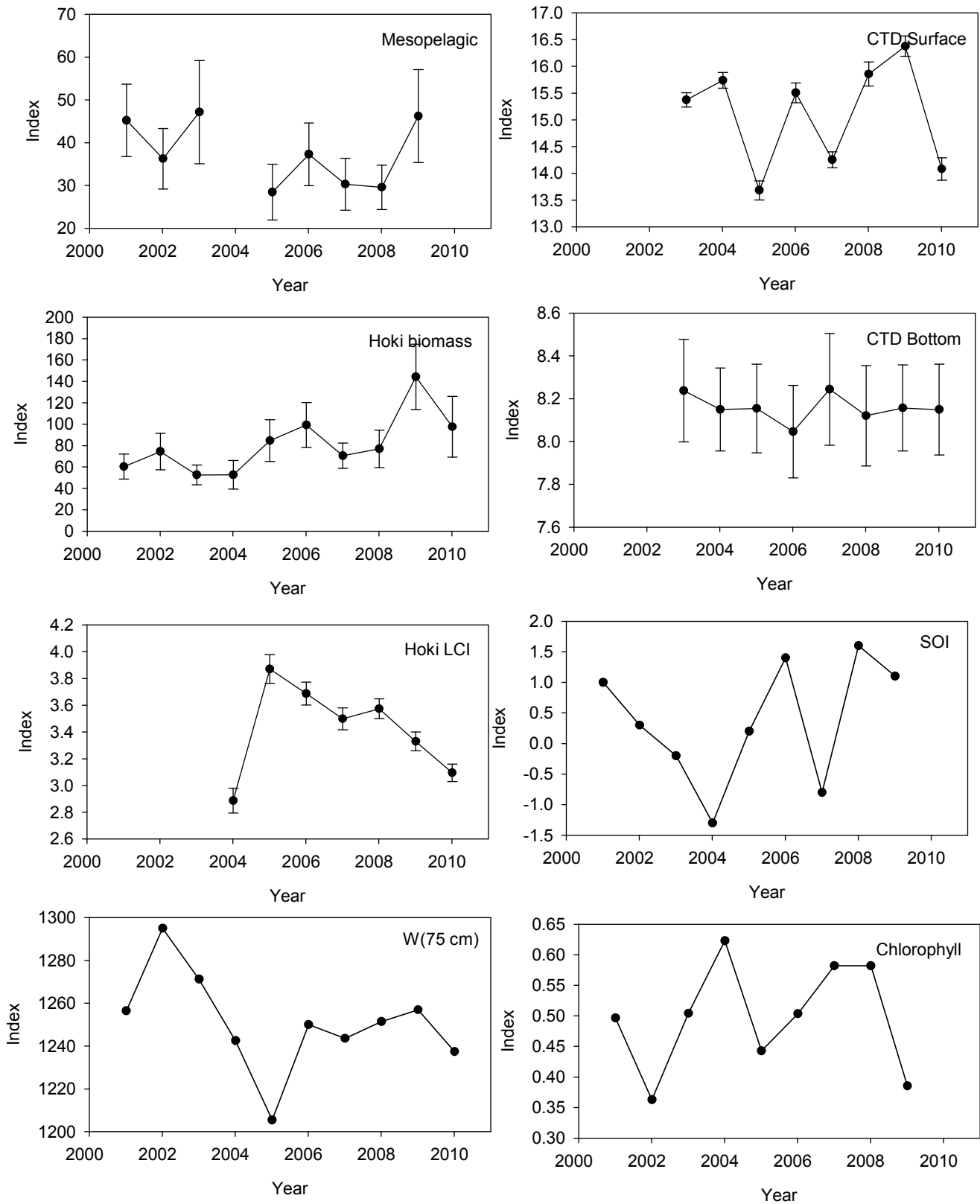


Figure 34: Comparison of mesopelagic acoustic index, hoki abundance and condition and selected environmental variables for the entire Chatham Rise.

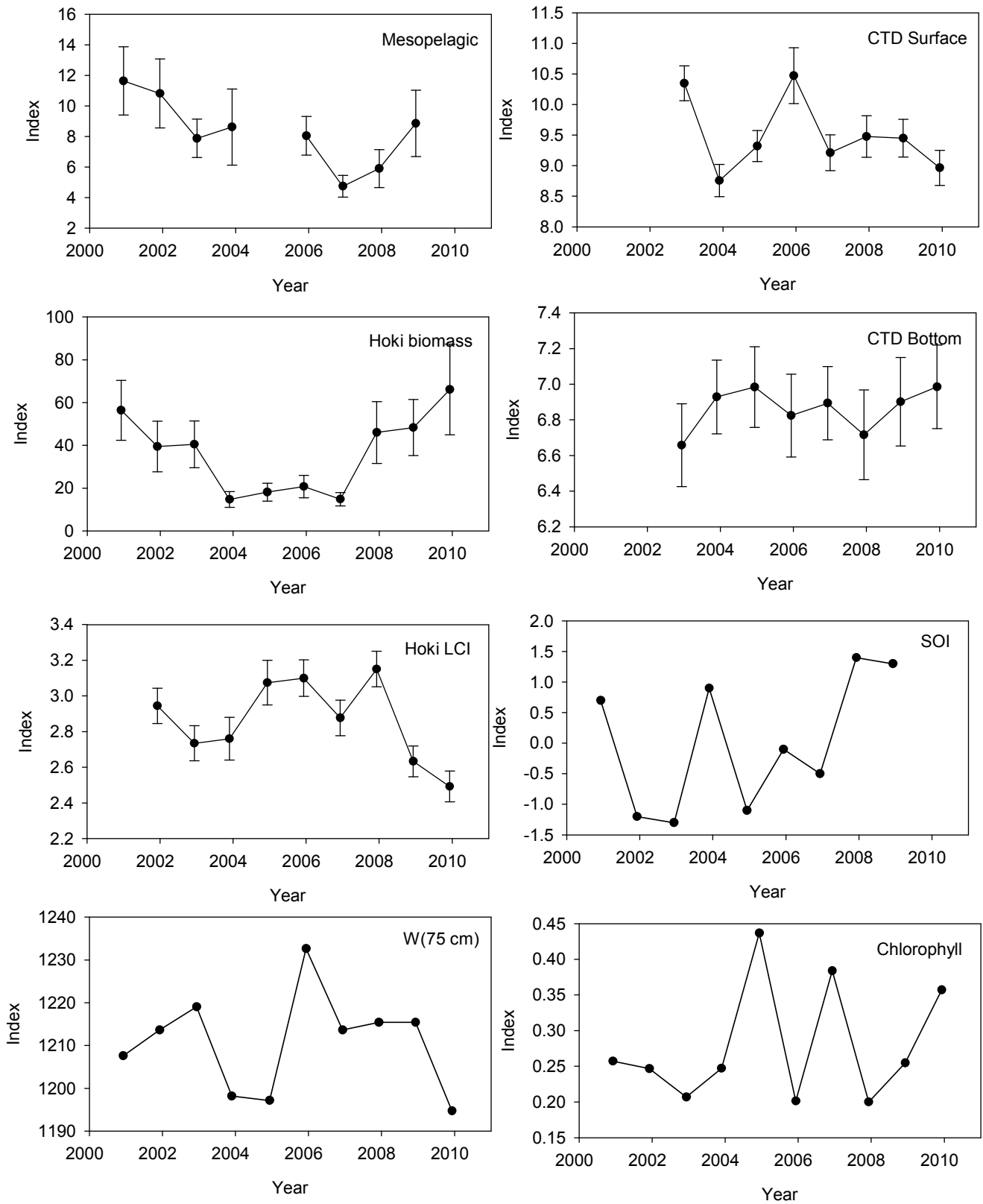
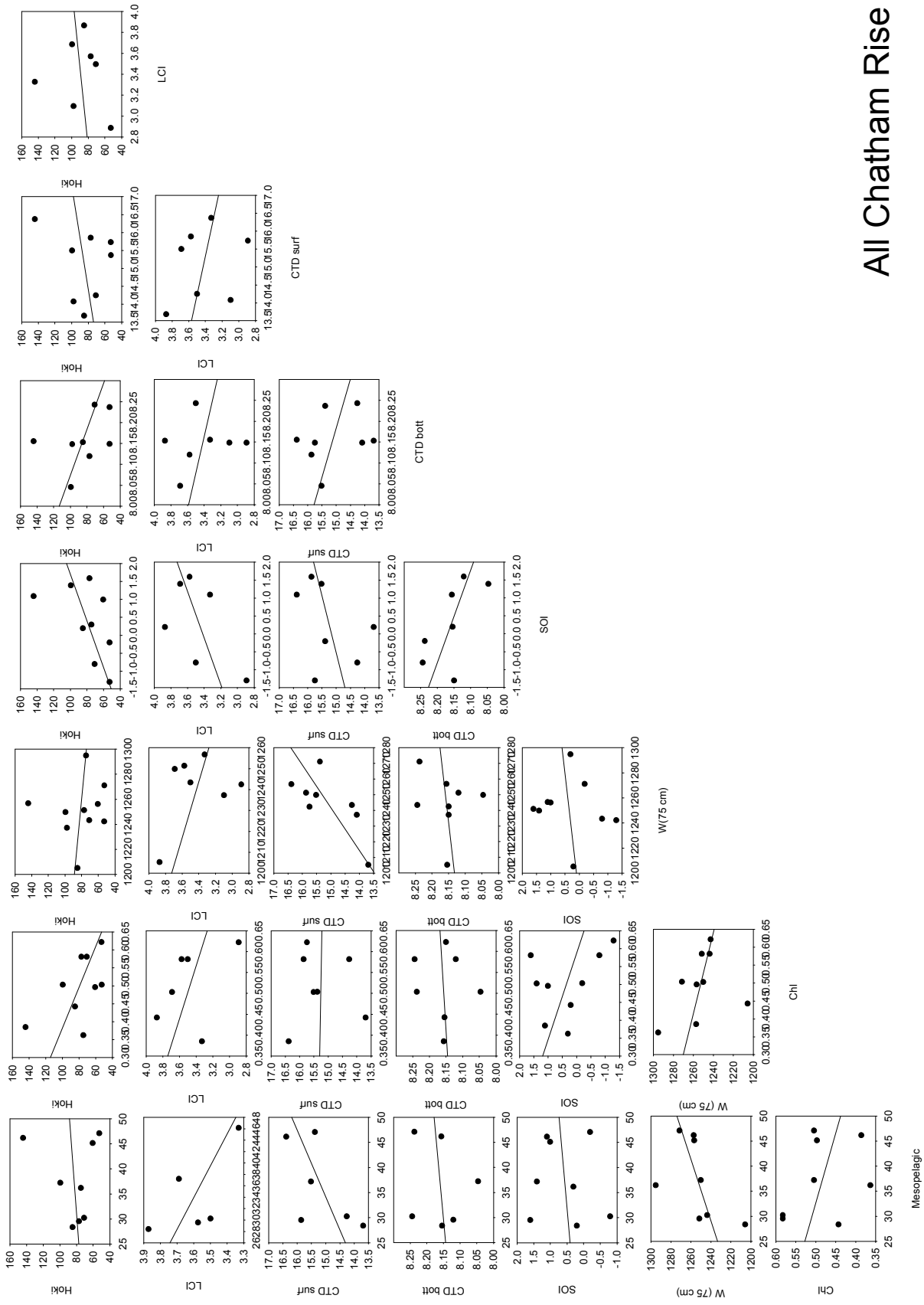
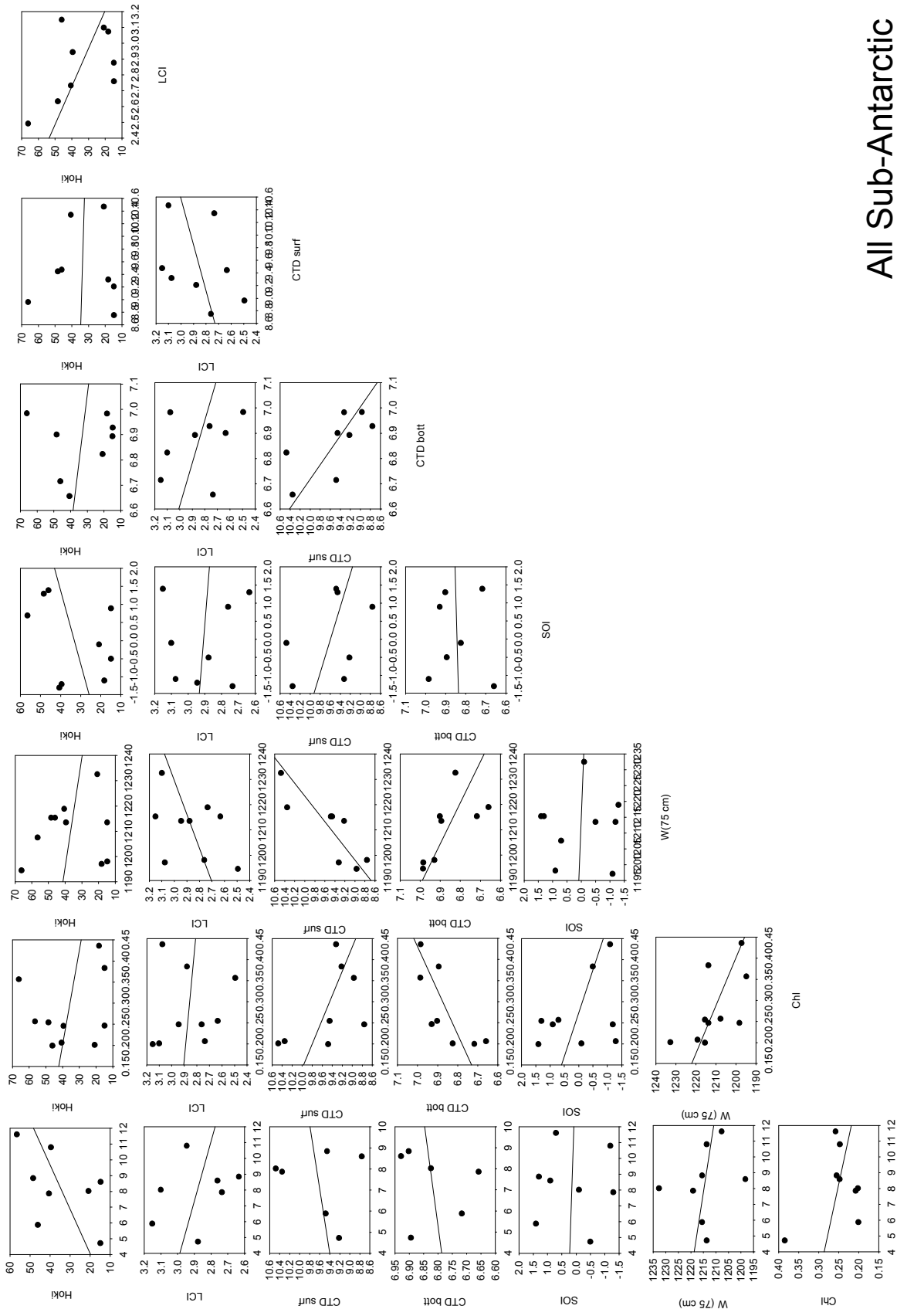


Figure 35: Comparison of mesopelagic acoustic index, hoki abundance and condition and selected environmental variables for the entire Sub-Antarctic.



All Chatham Rise

Figure 36: Pairwise dot-plot comparison of mesopelagic acoustic index, hoki abundance and condition and selected environmental variables for the entire Chatham Rise. Lines show fitted simple linear regression.



All Sub-Antarctic

Figure 37: Pairwise dot-plot comparison of mesopelagic acoustic index, hoki abundance and condition and selected environmental variables for the entire Sub-Antarctic. Lines show fitted simple linear regression.

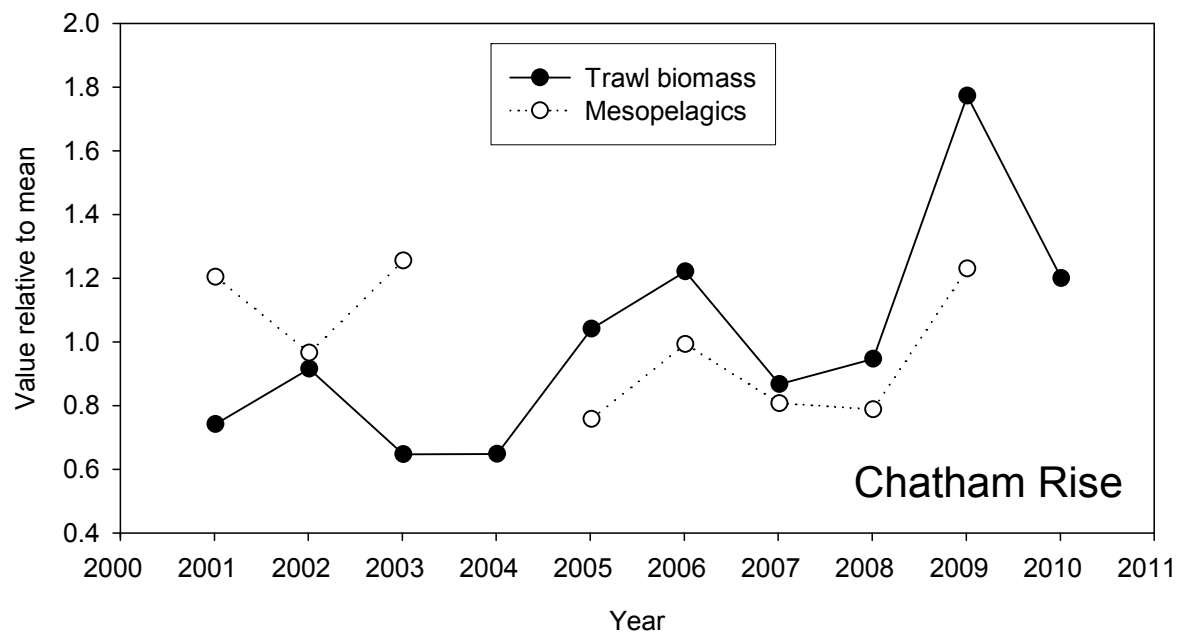
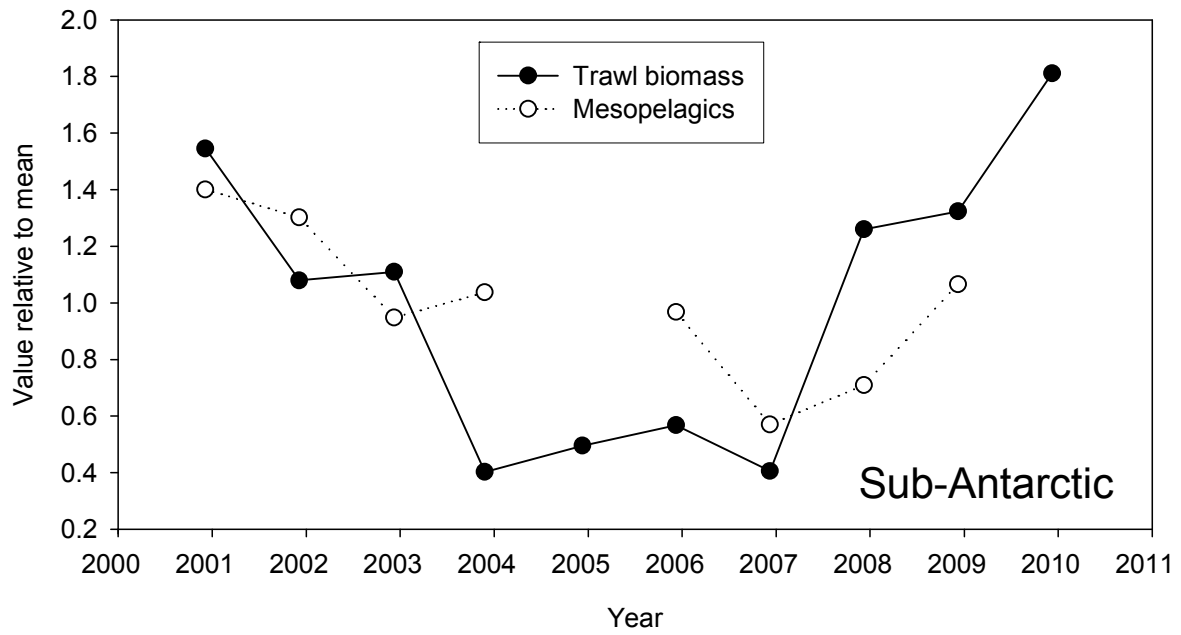


Figure 38: Comparison of scaled estimates (relative to mean) of mesopelagic fish abundance from acoustics and hoki biomass from trawls on the Sub-Antarctic and Chatham Rise.

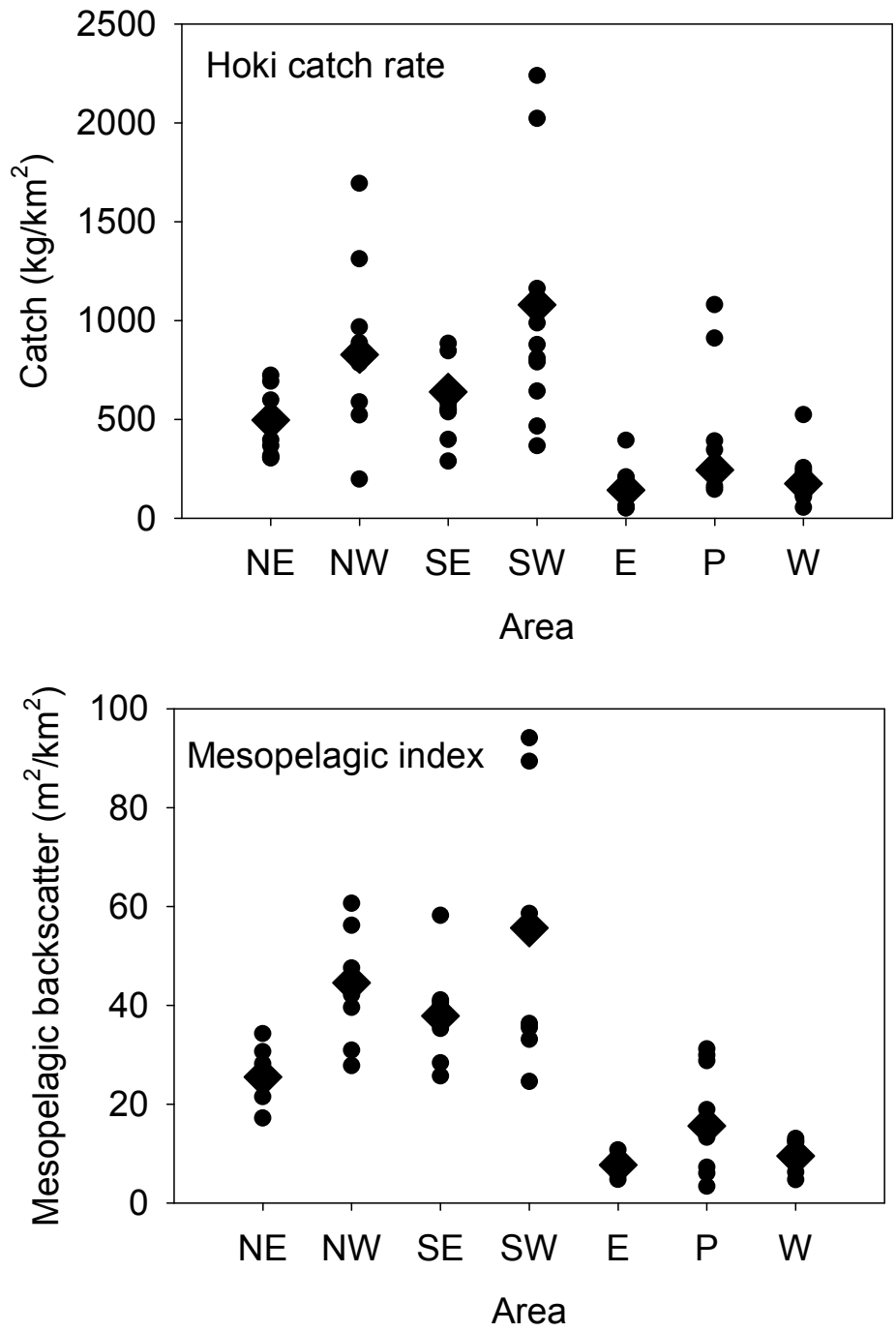


Figure 39: Comparison of estimates of mesopelagic fish abundance from acoustics and catch rates of hoki from trawls by sub-area on the Sub-Antarctic and Chatham Rise. Circles show estimates for each stratum in individual years. Large diamonds are the average stratum estimate across all years.

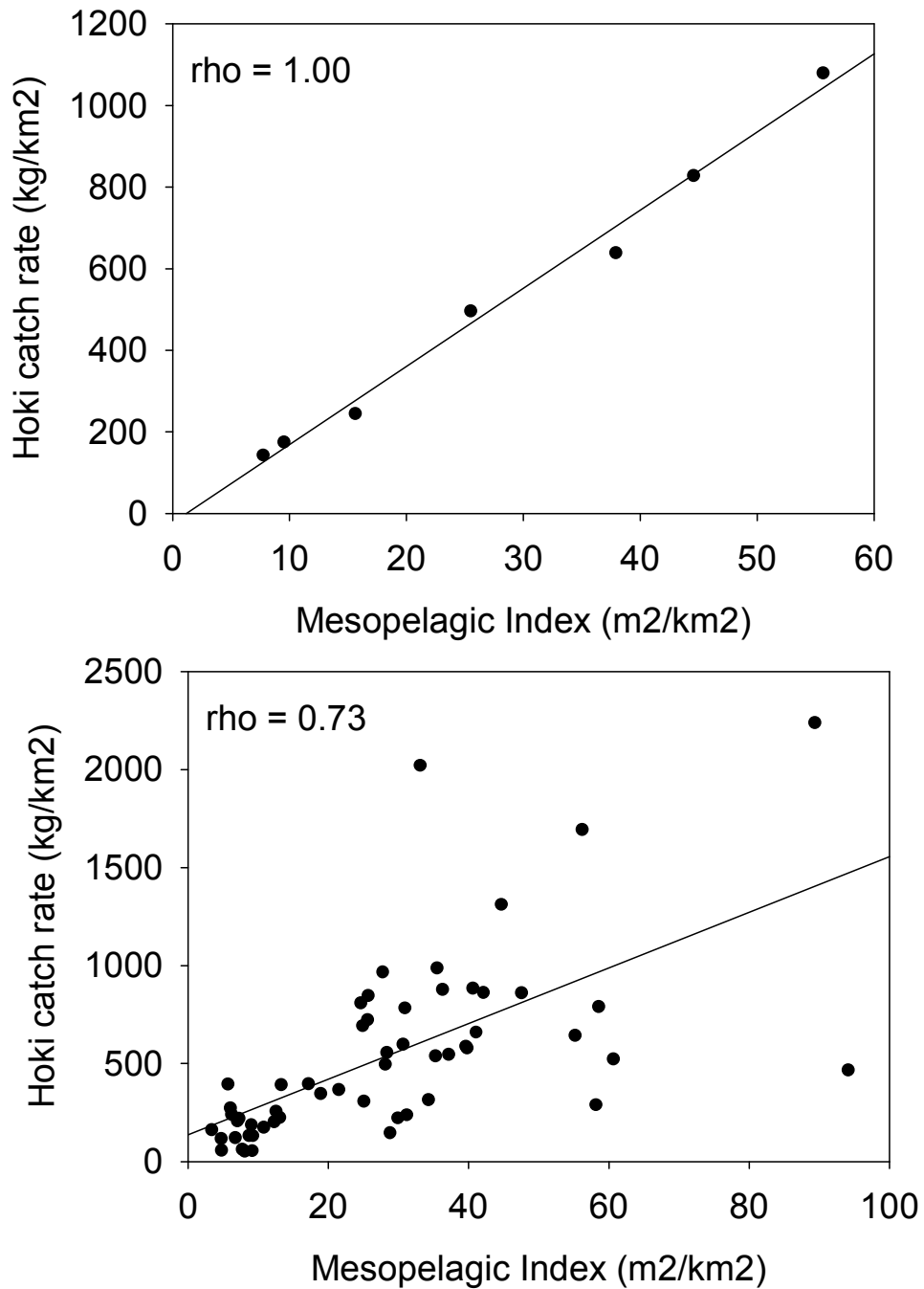


Figure 40: Correlation of estimates of mesopelagic fish abundance from acoustics and catch rates of hoki from trawls by sub-area on the Sub-Antarctic and Chatham Rise. Upper panel is the average stratum estimate across all years. Lower panel is correlation between annual estimates. Lines show best-fit linear regression, rho is the Spearman's rank correlation coefficient.

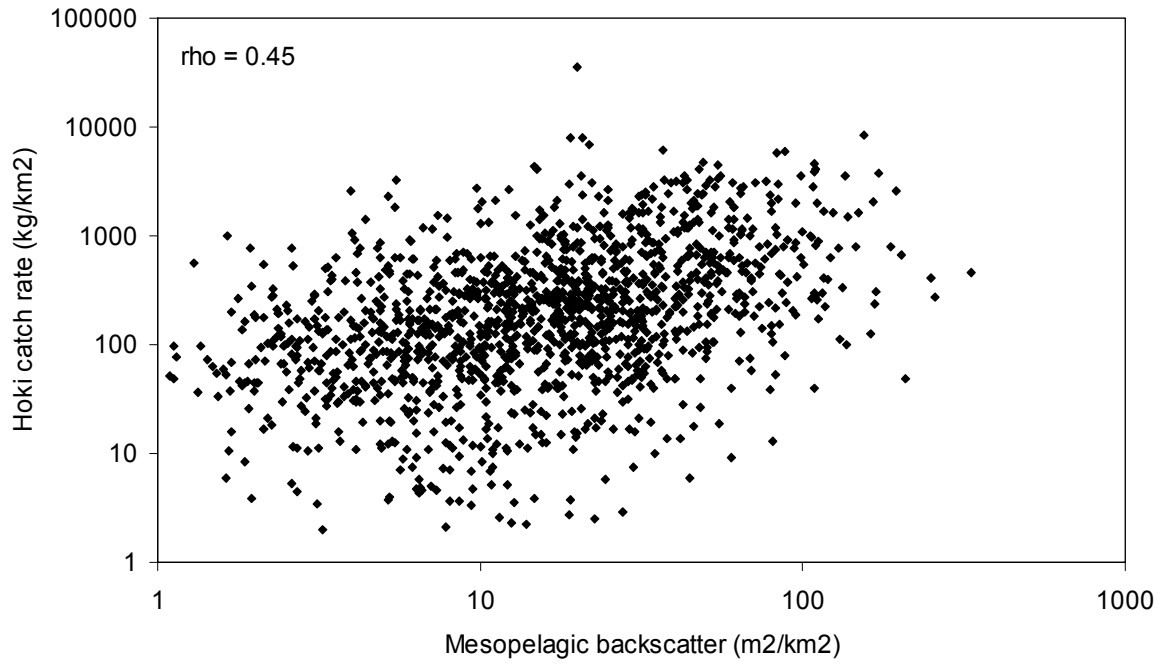


Figure 41: Correlation of estimates of mesopelagic fish abundance from acoustics and catch rates of hoki from trawls from all station data on the Sub-Antarctic and Chatham Rise. Rho is the Spearman's rank correlation coefficient.

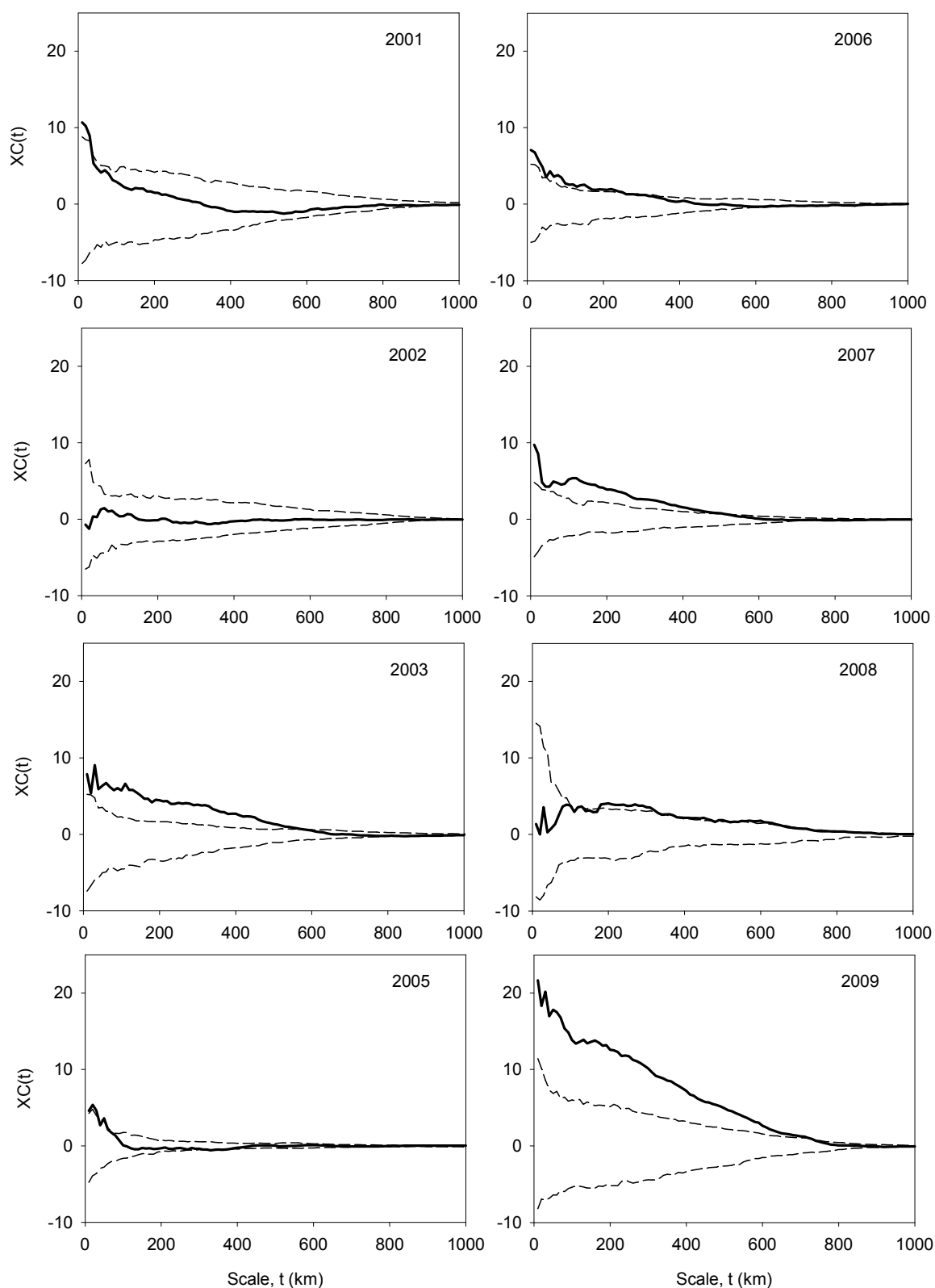


Figure 42: Potential contact between hoki and mesopelagic prey on the Chatham Rise. The statistic $XC(t)$ is a measure of the average acoustic density of mesopelagic fish within a circle of radius t from an individual hoki. Dotted lines are 5 and 95% confidence intervals for a random arrangement of hoki. Where measured $XC(t)$ (solid line) was greater than the upper confidence bound, there was significant positive association.

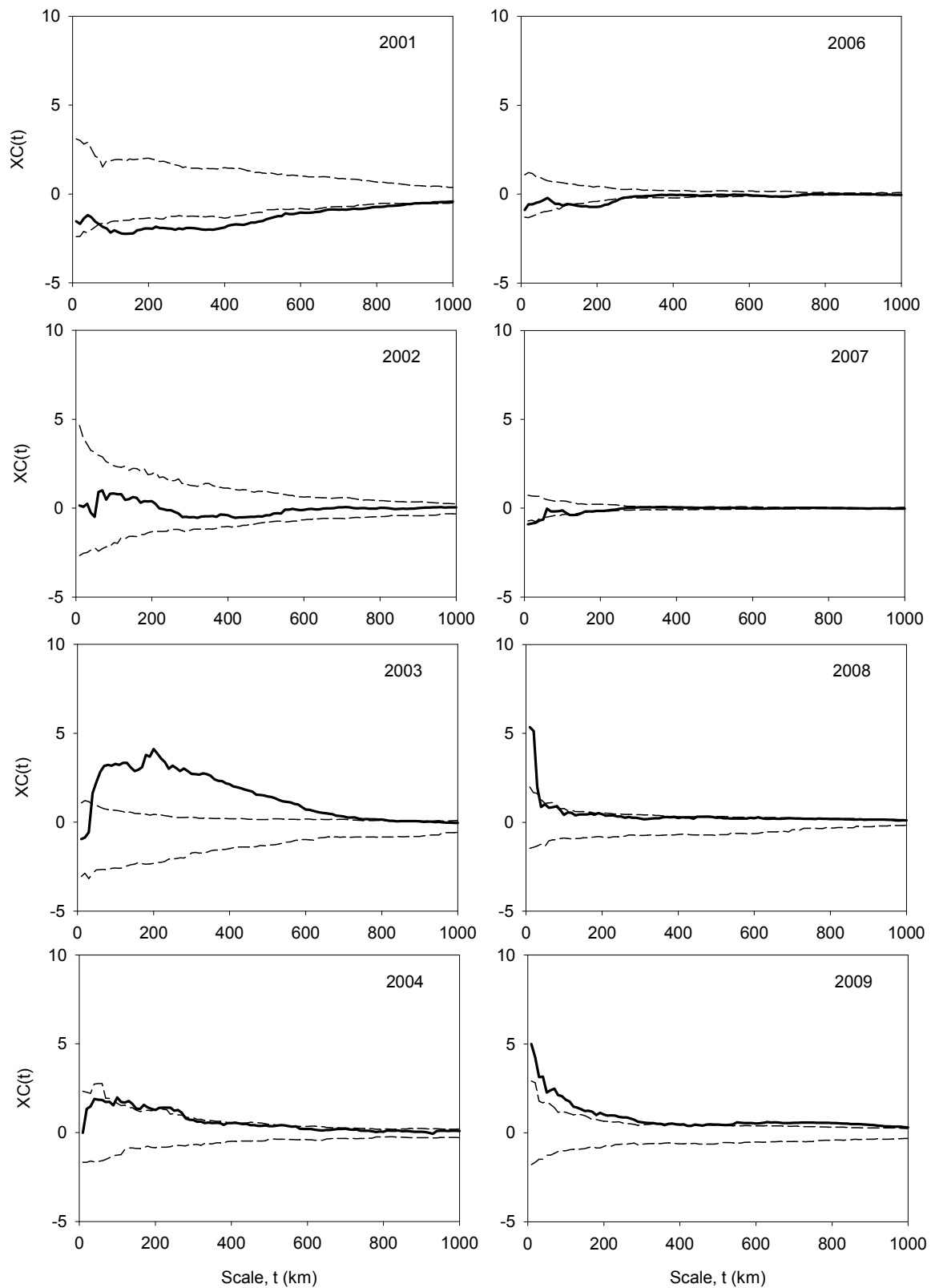


Figure 43: Potential contact between hoki and mesopelagic prey in the Sub-Antarctic. The statistic $XC(t)$ is a measure of the average acoustic density of mesopelagic fish within a circle of radius t from an individual hoki. Dotted lines are 5 and 95% confidence intervals for a random arrangement of hoki. Where measured $XC(t)$ (solid line) was greater than the upper confidence bound, there was significant positive association.

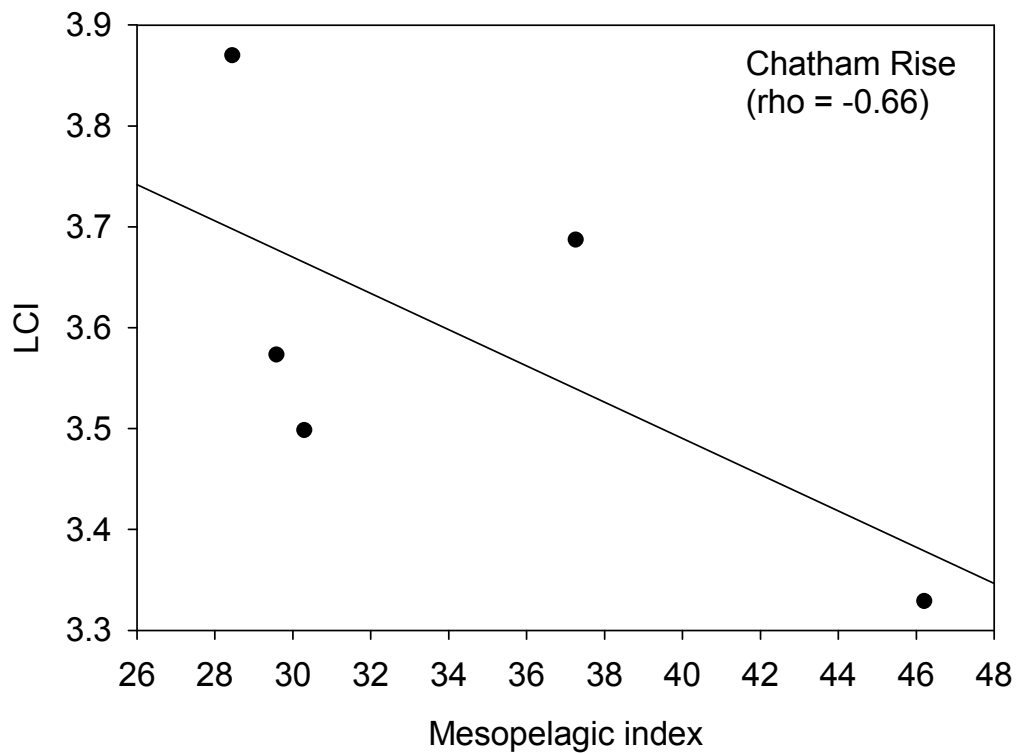
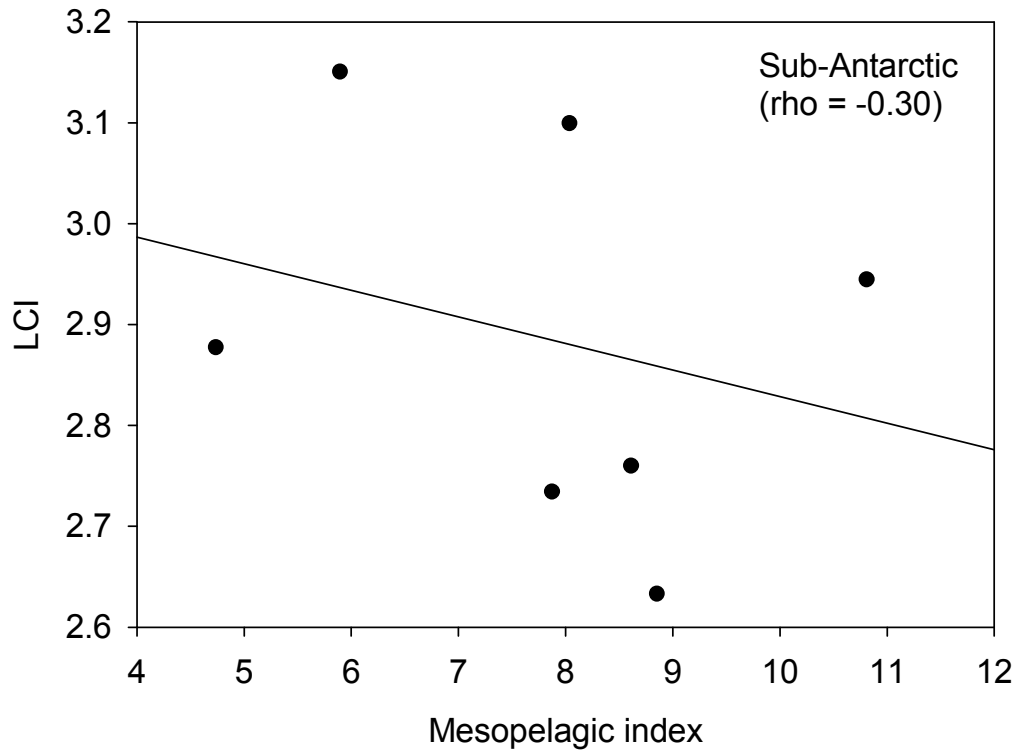


Figure 44: Correlation between annual estimates of mesopelagic fish abundance from acoustics and hoki liver condition on the Sub-Antarctic and Chatham Rise. Lines show best-fit linear regression, rho is the Spearman's rank correlation coefficient.

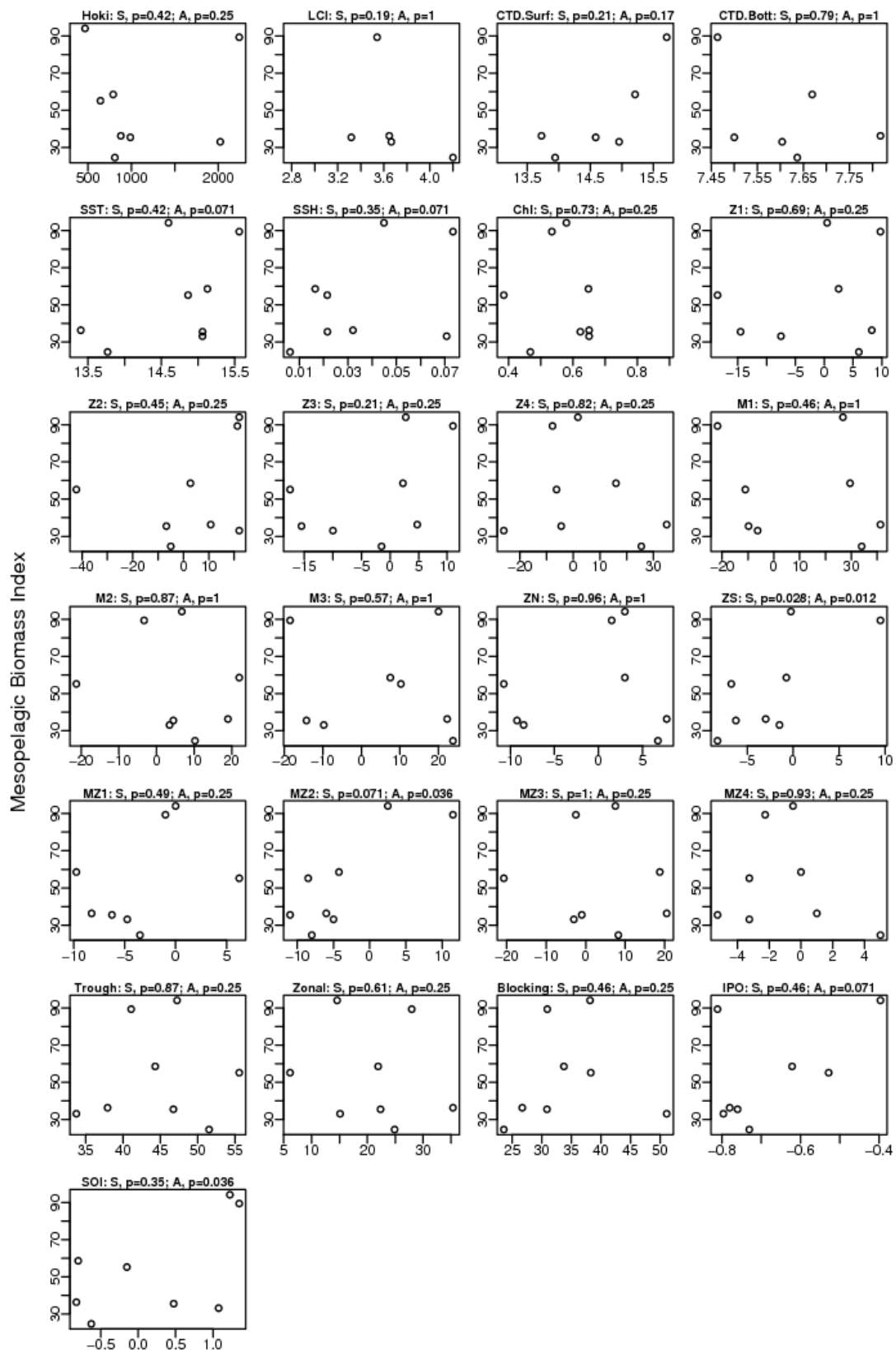


Figure 45: Southwest Chatham Rise mesopelagic biomass index (y-axis) plotted against various environmental and biotic indices, with no annual time lag. Each panel title shows the name of the environmental or biotic index, and the probabilities estimated from the Spearman's rank correlation test (S), and association test (A).

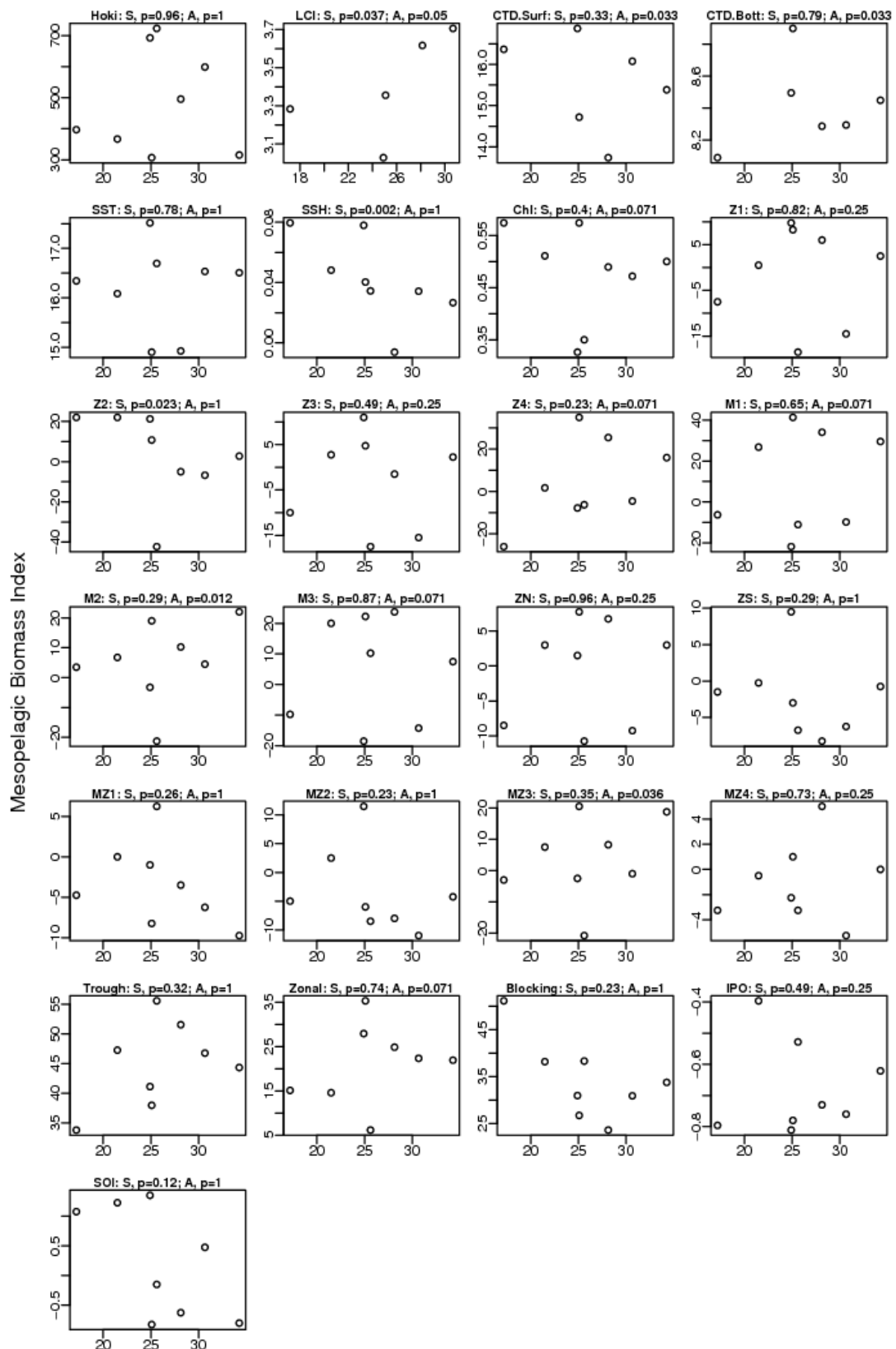


Figure 46: Northeast Chatham Rise mesopelagic biomass index (y-axis) plotted against various environmental and biotic indices, with no annual time lag. Each panel title shows the name of the environmental or biotic index, and the probabilities estimated from the Spearman's rank correlation test (S), and association test (A).

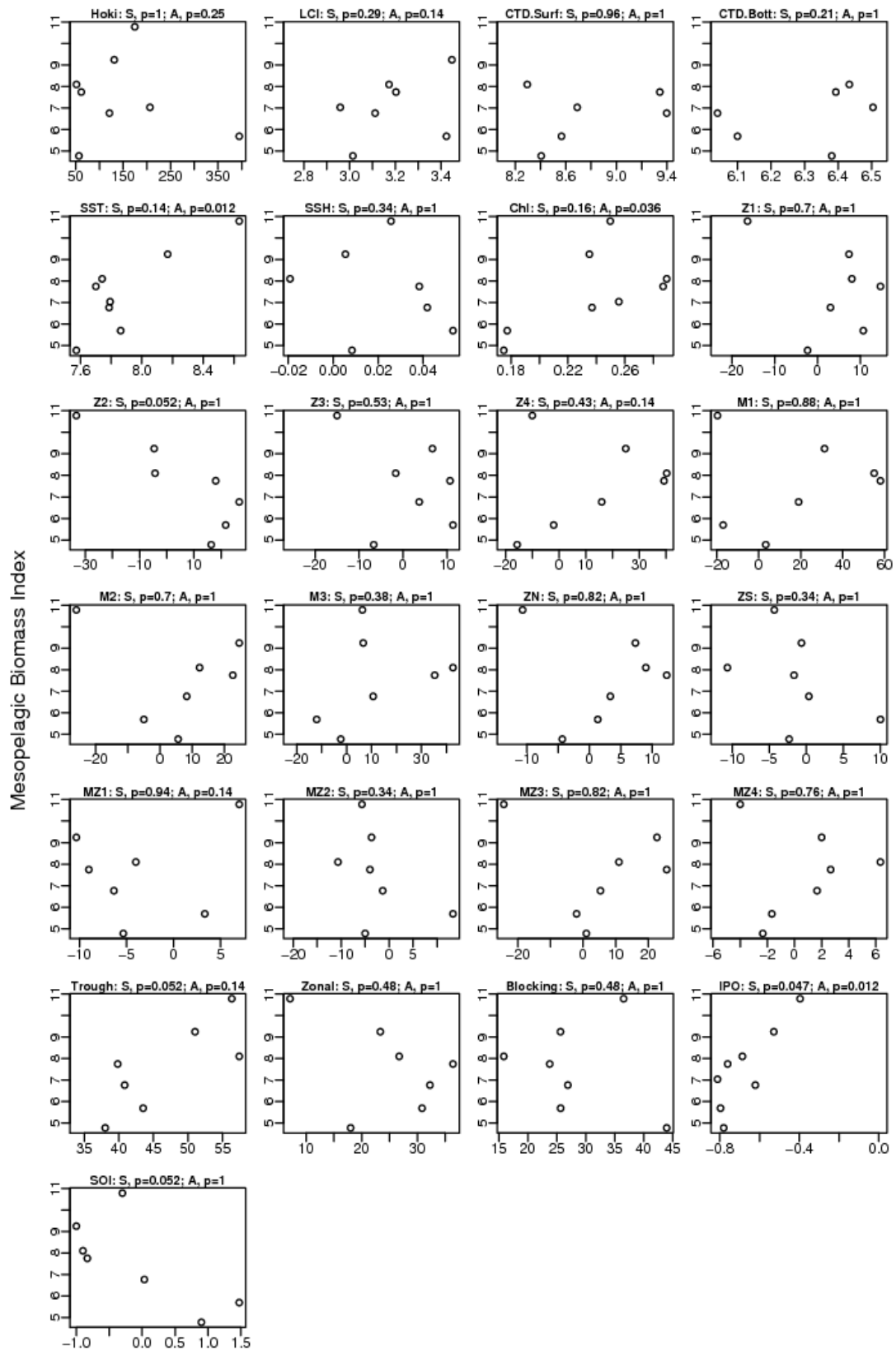


Figure 47: East Sub-Antarctic mesopelagic biomass index (y-axis) plotted against various environmental and biotic indices, with no annual time lag. Each panel title shows the name of the environmental or biotic index, and the probabilities estimated from the Spearman's rank correlation test (S), and association test (A).

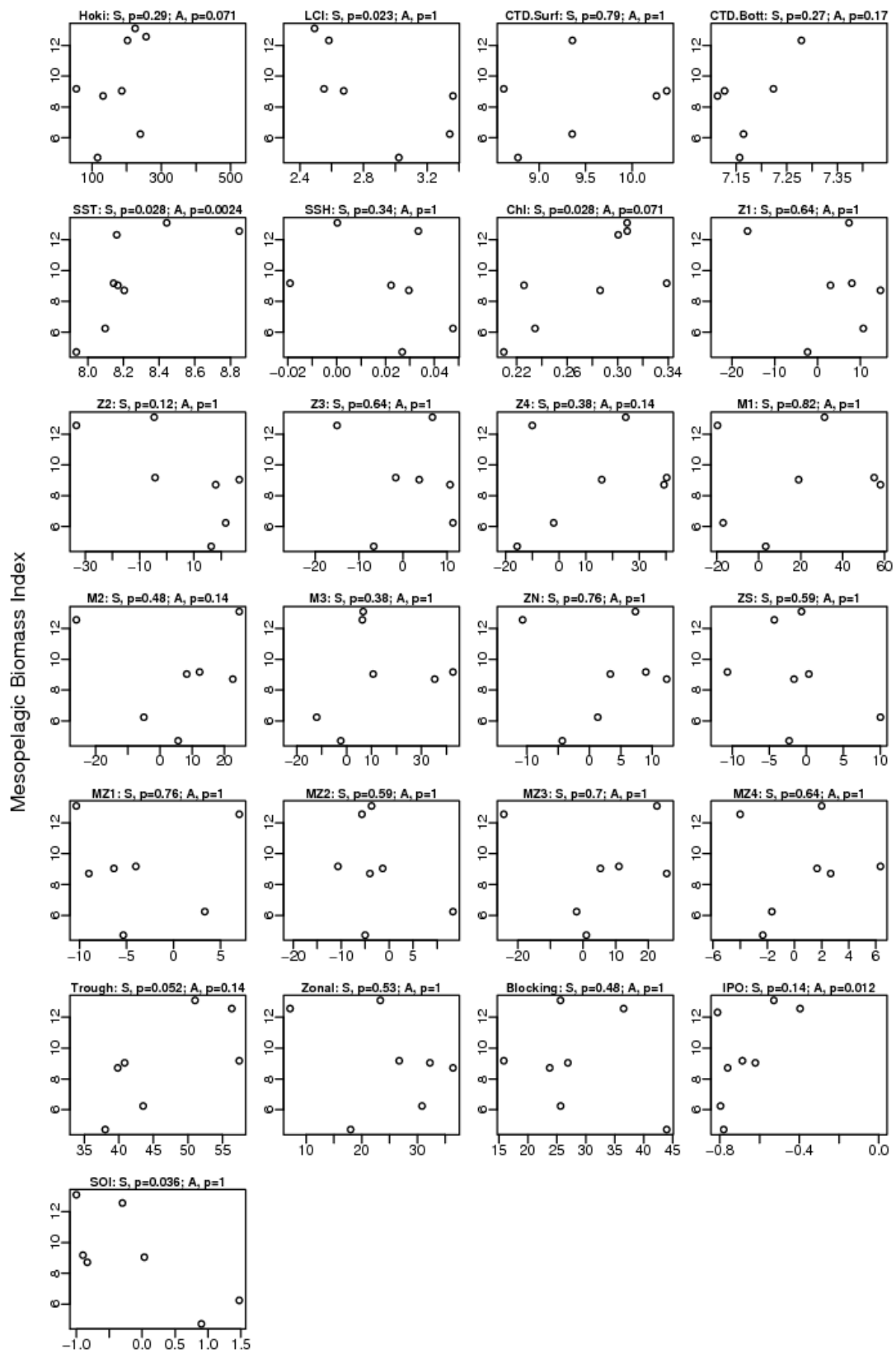


Figure 48: West Sub-Antarctic mesopelagic biomass index (y-axis) plotted against various environmental and biotic indices, with no annual time lag. Each panel shows the name of the environmental or biotic index, and the probabilities estimated from the Spearman's rank correlation test (S), and association test (A).

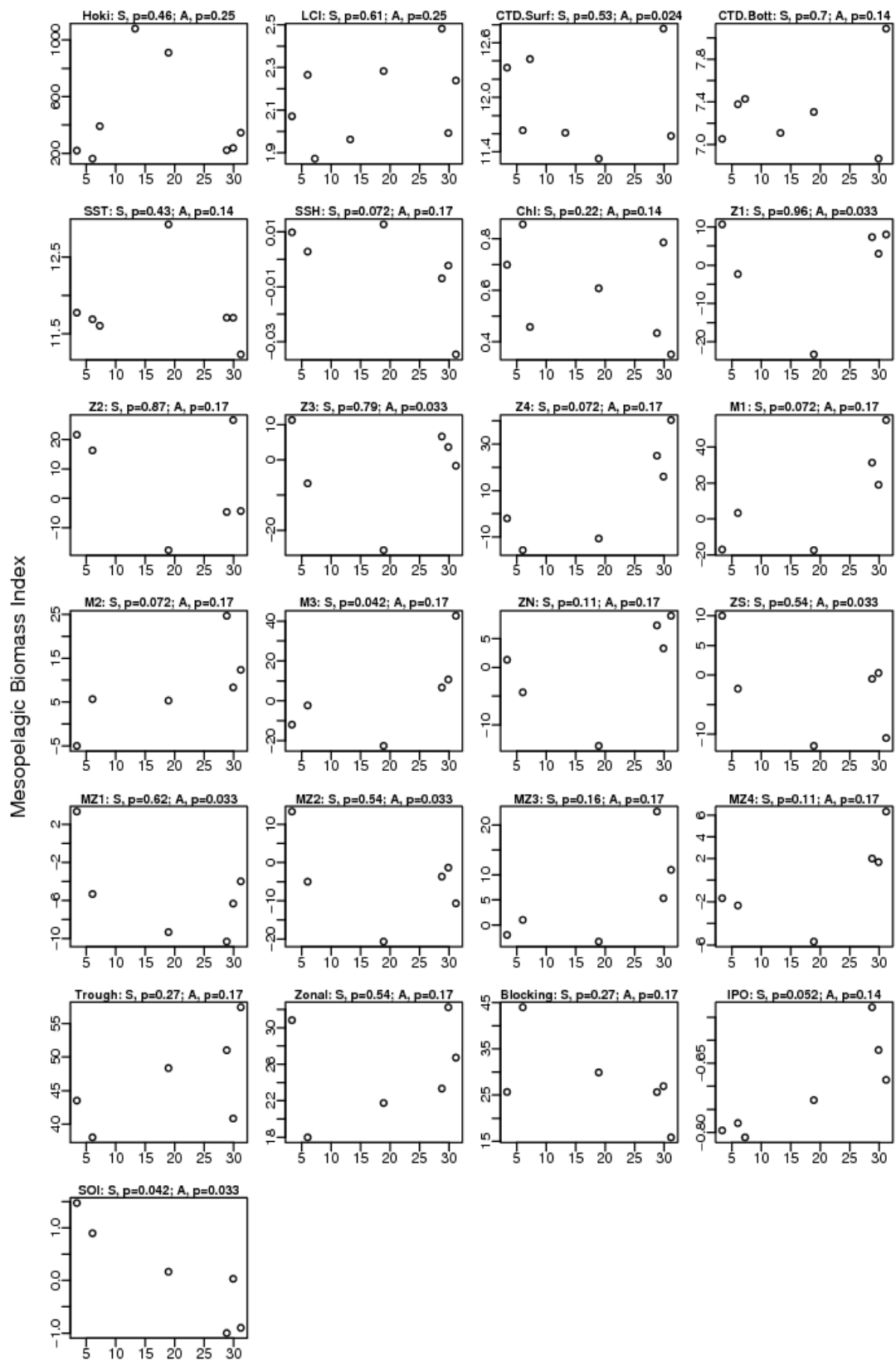


Figure 49: Puysegur Sub-Antarctic mesopelagic biomass index (y-axis) plotted against various environmental and biotic indices, with a one year time lag. Each panel title shows the name of the environmental or biotic index, and the probabilities estimated from the Spearman's rank correlation test (S), and association test (A).

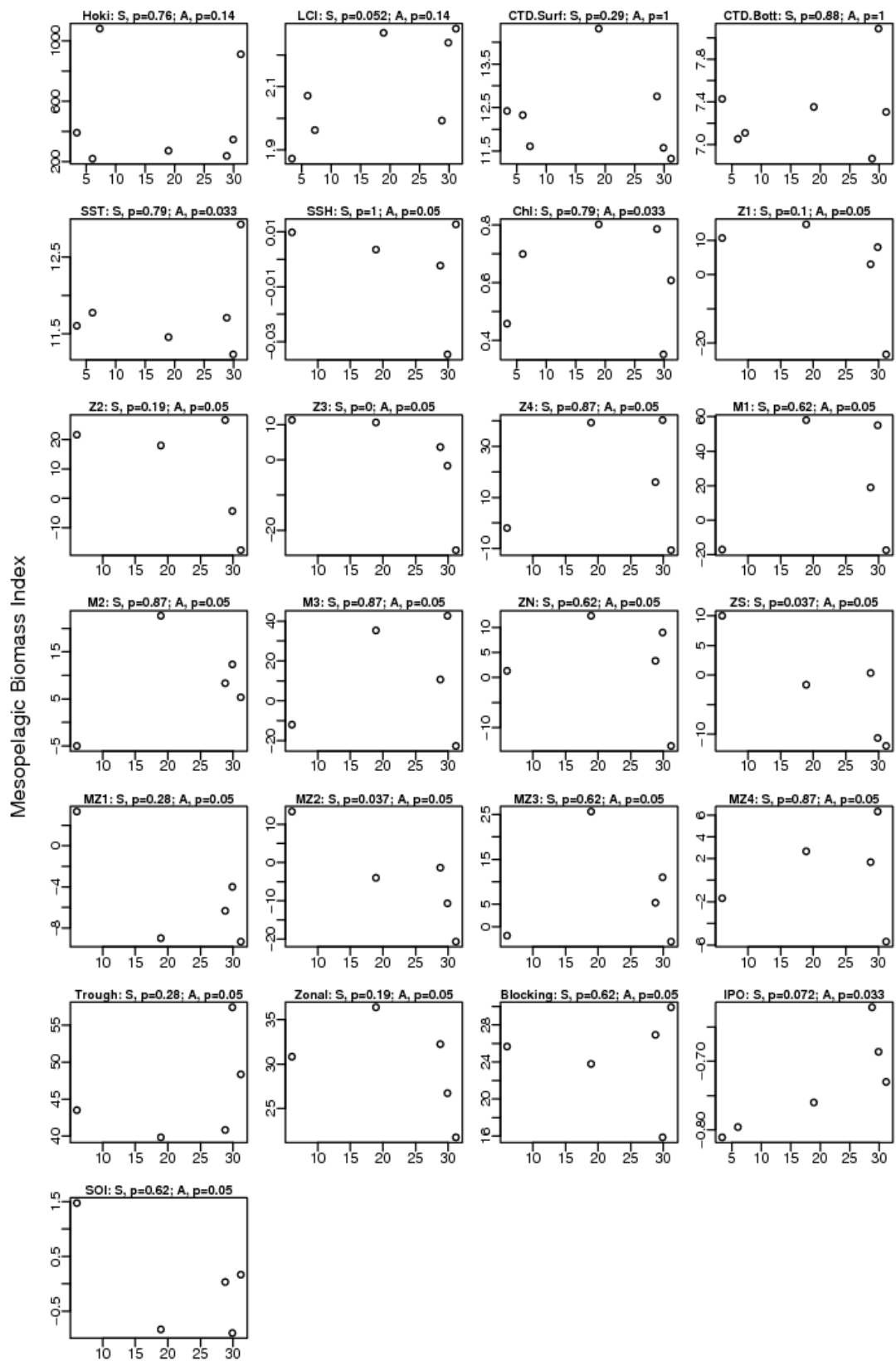


Figure 50: Puysegur Sub-Antarctic mesopelagic biomass index (y-axis) plotted against various environmental and biotic indices, with a two year time lag. Each panel title shows the name of the environmental or biotic index, and the probabilities estimated from the Spearman's rank correlation test (S), and association test (A).

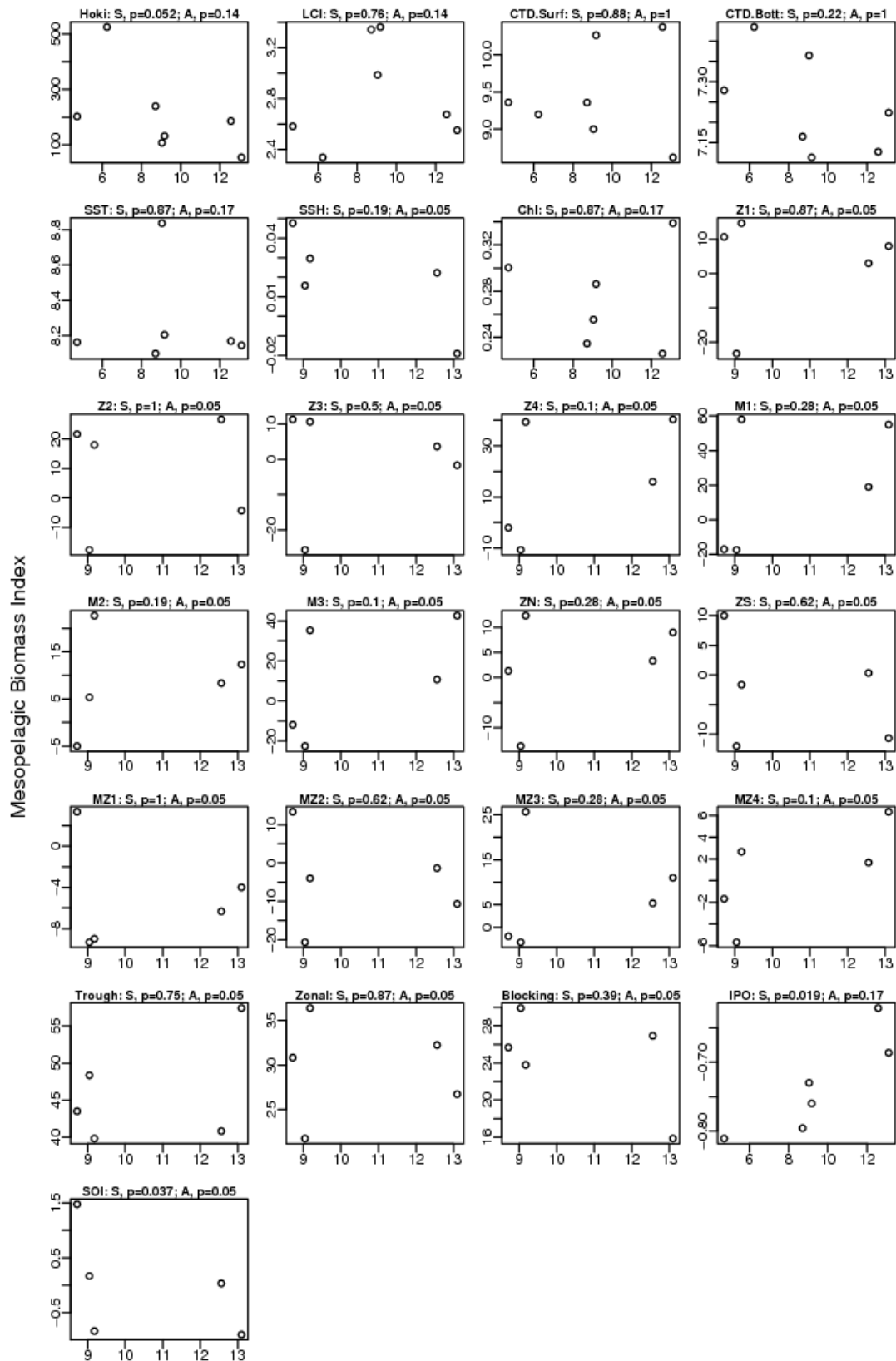


Figure 51: West Sub-Antarctic mesopelagic biomass index (y-axis) plotted against various environmental and biotic indices, with a two year time lag. Each panel shows the name of the environmental or biotic index, and the probabilities estimated from the Spearman's rank correlation test (S), and association test (A).

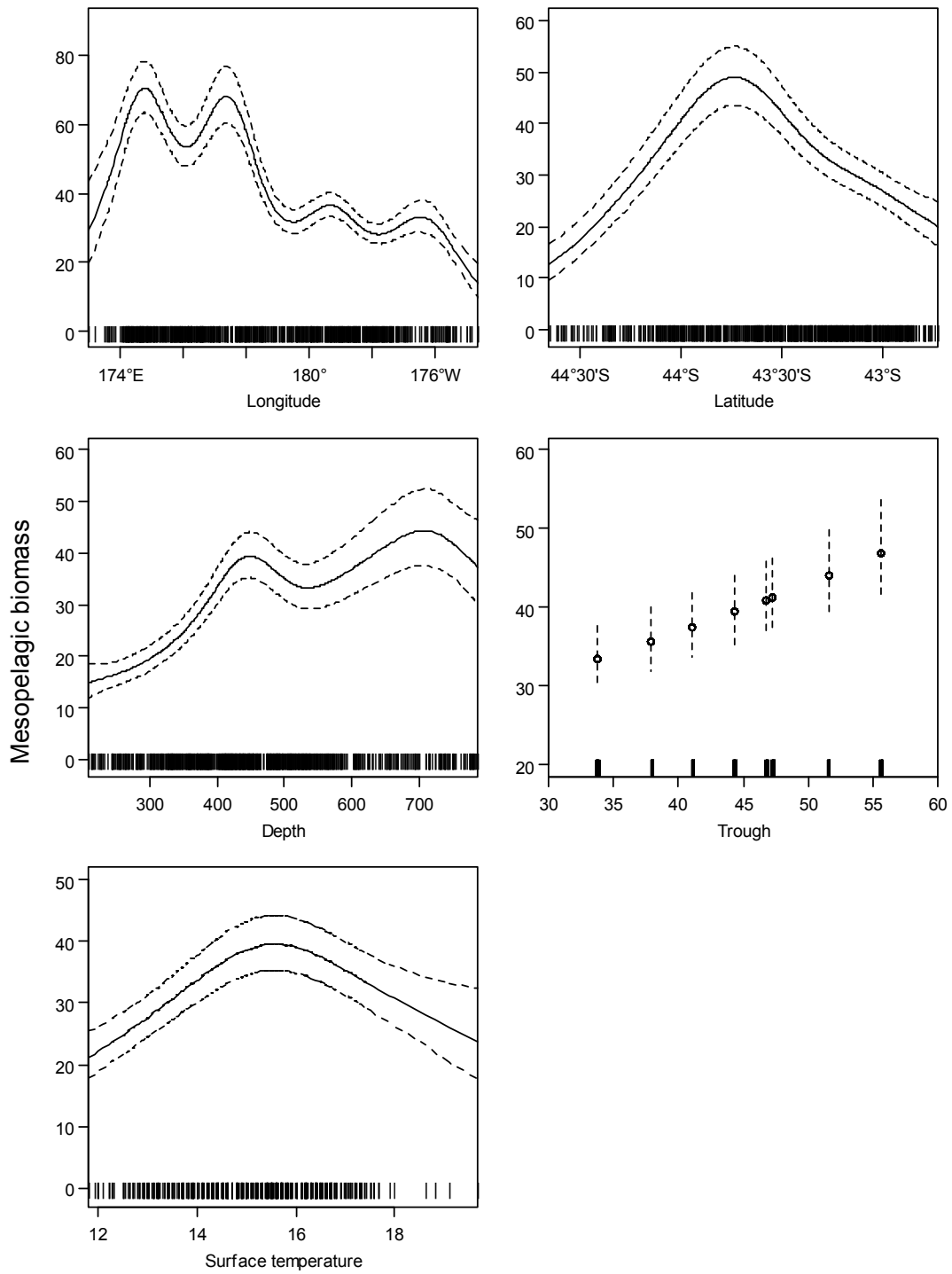


Figure 52: Predicted effects of selected variables on mesopelagic biomass from the final Generalised Additive Model for the Chatham Rise. Solid lines or points indicate the mean predicted effect, and broken lines the 95% confidence intervals. Each effect is plotted after setting all other predictors to their median values. The distribution of data is shown just above the x-axis (the “data rug”).

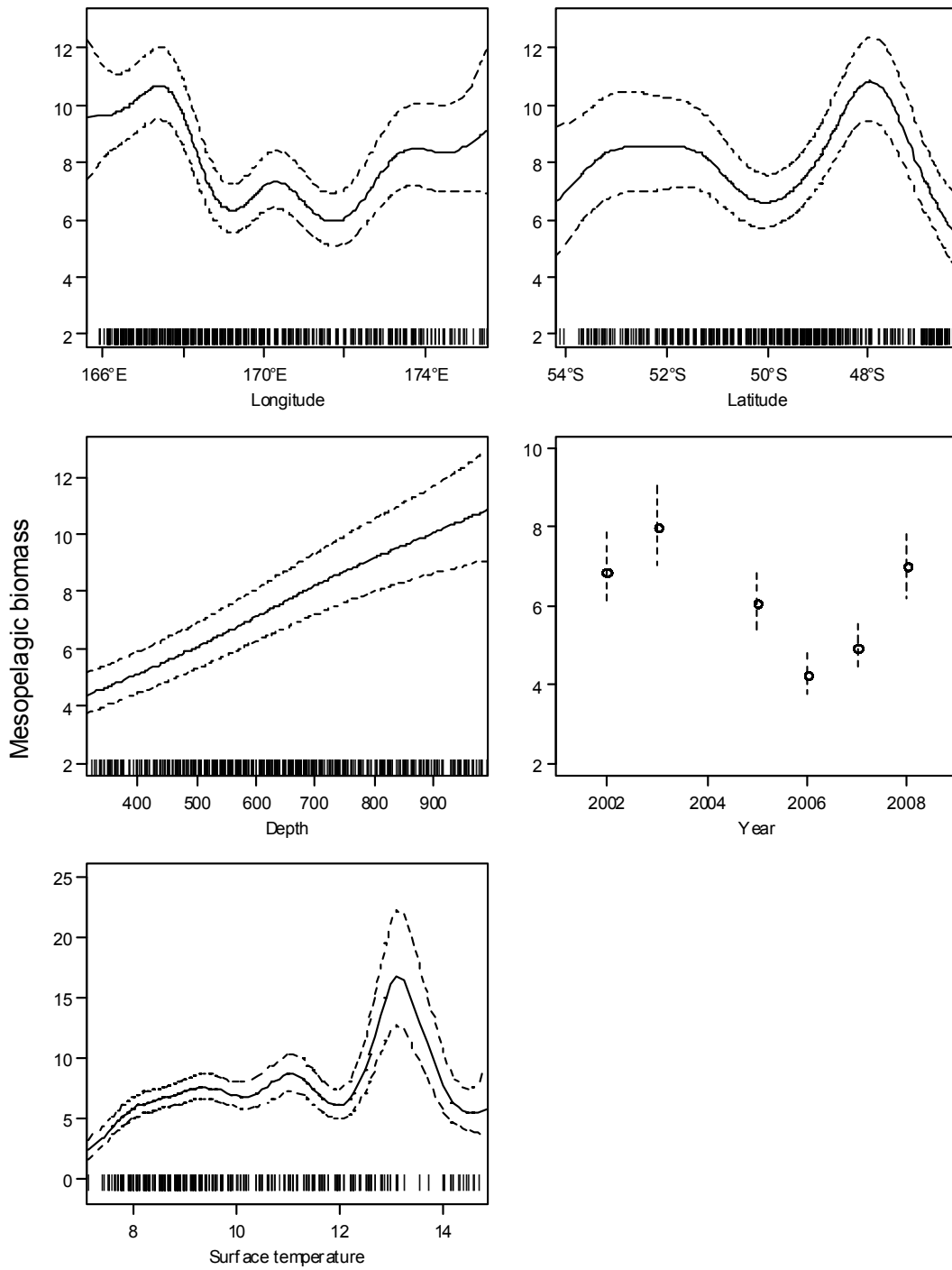


Figure 53: Predicted effects of selected variables on mesopelagic biomass from the final Generalised Additive Model for the Sub-Antarctic. Solid lines or points indicate the mean predicted effect, and broken lines the 95% confidence intervals. Each effect is plotted after setting all other predictors to their median values. The distribution of data is shown just above the x-axis (the “data rug”).